A-RAF kinase functions in ARF6 regulated endocytic membrane traffic

---

Die Rolle der A-RAF-Kinase in ARF6 reguliertem endocytotischem Membrantransport

Doctoral thesis for submission to a doctoral degree
at the Graduate School of Life Sciences,
Julius Maximilian University Würzburg,
Section Infection and Immunity

submitted by

Elena Nekhoroshkova

from

Urdshar, Kazakhstan

Würzburg, 2009

Submitted on: ……………………………………………………………….

Office stamp

Members of the *Promotionskomitee*:

Chairperson:	Prof. Dr. J. Schultz
Primary Supervisor:	Prof. Dr. U. R. Rapp
Supervisor (second):	Prof. Dr. A. Müller
Supervisor (third):	Prof. Dr. R. Hedrich

Day of Rigorosum: ………………………………………………….

Certificates were handed-out on: ………………………………..

"You are never given a wish without also being given the power to make it true.

You may have to work for it, however."

Richard Bach

I dedicate this work to my son Dmitry

Summary

Extracellular signals are translated and amplified via cascades of serially switched protein kinases, MAP kinases (MAPKs). One of the MAP pathways, the classical RAS/RAF/MEK/ERK pathway, transduces signals from receptor tyrosine kinases and plays a central role in regulation of cell proliferation. RAF kinases (A-, B- and C-RAF) function atop of this cascade and convert signals emanating from conformational change of RAS GTPases into their kinase activity, which in turn phosphorylates their immediate substrate, MEK. Disregulated kinase activity of RAF can result in tumor formation, as documented for many types of cancer, predominantly melanomas and thyroid carcinomas (B-RAF).

A-RAF is the least characterized RAF, possibly due to its low intrinsic kinase activity and comparatively mild phenotype of *A-RAF* knockout mice. Nevertheless, the unique phenotype of *a-raf* [-/-] mice, showed predominantly neurological abnormalities such as cerebellum disorders, suggesting that A-RAF participates in a specific process not complemented by activities of B- and C-RAF.

Here we describe the role of A-RAF in membrane trafficking and identify its function in a specific step of endocytosis. This work led to the discovery of a C-terminally truncated version of A-RAF, AR149 that strongly interfered with cell growth and polarization in yeast and with endocytosis and actin polymerization in mammalian cells. As this work was in progress two splicing isoforms of A-RAF, termed DA-RAF1 and DA-RAF2 were described that act as natural inhibitors of RAS-ERK signaling during myogenic differentiation (Yokoyama et al., 2007). DA-RAF2 contains the first 153 aa of A-RAF and thus is nearly identical with AR149. AR149 localized specifically to the recycling endosomal compartments as confirmed by colocalization and coimmunoprecipitation with ARF6. Expression of AR149 interferes with recycling of endocytosed transferrin (Tfn) and with actin polymerization. The endocytic compartment, where internalized Tfn is trapped, was identified as ARF6- and RAB11- positive endocytic vesicles. We conclude that the inhibition of Tfn trafficking in the absence of A-RAF or under overexpression of AR149 occurs between tubular- and TGN- associated recycling endosomal compartments. siRNA-mediated depletion of endogenous A-RAF or inhibition of MEK by U0126 mimic the AR149 overexpression phenotype, supporting a role of A-RAF regulated ERK signalling at endosomes that is controlled by AR149 and targets ARF6.

Our data additionally suggest EFA6 as a partner of A-RAF during activation of ARF6. The novel findings on the A-RAF localization and the interaction with ARF6 have led to a new model of A-RAF function were A-RAF via activation of ARF6 controls the recycling of endocytic vesicles.Endocytosis and rapid recycling of synaptic vesicles is critically important for the physiological function of neurons. The finding, that A-RAF regulates endocytic recycling open a new perspective for investigation of the role of A-RAF in the nervous system.

Zusammenfassung

Extrazelluläre Signale werden über eine Serie von nacheinander geschalteten Proteinkinasen, den MAP-Kinasen (MAPK) weitergeleitet und multipliziert. Einer der MAPK-Signalwege, der RAS/RAF/MEK/ERK-Signaltransduktionsweg, leitet Signale von Tyrosinkinaserezeptoren weiter und spielt eine zentrale Rolle in der Regulation der Zellproliferation. RAF Kinasen (A-, B-, und C-RAF) stehen am Anfang der Kaskade. Sie wandeln die signalbedingte strukturellen Änderungen der RAS-GTPase in ihre Kinaseaktivität um und phosphorylieren ihr direktes Substrat, MEK. Eine Störung in der Regulation der Kinaseaktivität des RAF-Proteins kann zur Tumorbildung führen, wie es bei vielen Krebsarten, vor allem Melanom und Schilddrüsenkarzinom (B-RAF), dokumentiert ist.

A-RAF ist die bislang am wenigsten charakterisierte RAF-Kinase, möglicherweise aufgrund sihrer nidrigen intrinsischen Kinaseaktivität. Weiterhin weist die A-RAF defficiente Maus einen relativ milden hauptsächlich neuronalen Phänotyp auf, der sich unter anderem auch in einer Fehlfunktion des Cerebellums manifestiert. Dieser einzigartige Phänotyp weist darauf hin, dass eine Reihe zellulärer Prozesse spezifisch durch A-RAF und nicht durch aktiveren B- und C-RAF vermitellt wird.

Im Rahmen dieser Doktorarbeit wurde die Rolle des A-RAF-Proteins im intrazellulären Membrantransport analysiert und eine spezifische A-RAF Funktion by endozytotischen Prozessen identifiziert. Diese Arbeit führte zur Entdeckung einer C-terminal verkürtzten Form von A-RAF, AR149, welche das Wachstum und die Polarisation von Hefezellen beeinträchtigt. In Säugetierzellen wirkt AR149 störend auf die Endozytose und die Aktinpolymerisation. Während des Entstehungsprozesses dieser Studie, wurden parallel zwei Spleißisoformen des A-RAF-Proteins, DA-RAF1 und 2, publiziert, die als natürliche Inhibitoren des RAS-RAF-MEK-ERK-Signalwegs in der myogenen Differenzierung agieren (Yokoyama et al., 2007). DA-RAF2 beinhaltet die ersten 153 Aminosäuren des A-RAF Proteines und ist damit fast identisch mit AR149. Eigene Kolokalisierung- und Koimmunopräzipitationsexperimente mit ARF6 weisen darauf hin, dass AR149 spezifisch in ARF6-positiven Recycling-Endosomen lokalisiert ist. Expression des AR149 Proteins bechindert das Recycling von endozytiertem Transferrin und die Aktin Polimerisation. Die endosomalen Kompartimente in denen internalisiertes Transferrin gefangen vor liegt, konntenals ARF6- und RAB11-positive endozytotische Vesikeln charakterisiert werden. Diese Ergebnisse lassen auf eine durch A-RAF Überexpression bzw. durch die Abwesenheit an A-RAF vermittelte Blokade des intrazellulären Transferrintransportes zwischen den tubulären- und Trans-Golgi-Netzwerk-assoziirten endosomalen Recycling-Kompartimenten schließen. Inhibierung der endogenen A-RAF-Expression durch siRNA oder Hemmung der MEK-Aktivität durch U0126 haben den selben Effekt wie AR149.

Auf der Basis dieser Ergebnisse wird ein neues Modell für die Rolle der A-RAF regulierten ERK Signallwirkung auf Endosomen vorgestellt, bei dem das Zielprotein die ARF6 GTPase durch

AR149/DA-RAF2 negativ reguliert wird. Daruber hinaus deuten unsere Daten darauf hin, dass EFA6, ein GEF-Faktor von ARF6, als Kooperationspartner von A-RAF bei der ARF6-Aktivierung fungiert.

Endocytose und das schnelle Recycling von synaptischen Vesikeln ist von besonderer Bedeutung für die Funktion von Neuronen. Aus dem Befund, dass A-RAF ein Regulator des endocytotischen Recyclings ist ergibt sich dacher eine neue Perspektieve für die Untersuchung der A-RAF Funktion im Nervensystem.

List of contents

1.   Introduction

1.1   The RAF protein family

1.1.1 General characteristics of RAF proteins

RAF protein kinases were originally identified as viral oncogenes (Jansen et al., 1984; Rapp et al., 1983) encoded in murine and avian retroviruses. RAF proteins are serine/threonine kinases (Mark and Rapp, 1984; Moelling et al., 1984) that mediate transduction of extracellular mitogenic signals from activated Ras GTPases at the plasma membrane to a MAP kinase module (RAF-MEK-ERK), the mitogenic cascade (reviewed in (Daum et al., 1994)). This process leads to signal amplification and diversification via phosphorylation of dozens of different cytoplasmic and nuclear substrates by activated ERK. As a result, complex physiological responses to growth factor stimulation take place at multiple cellular levels (Fig1-1).
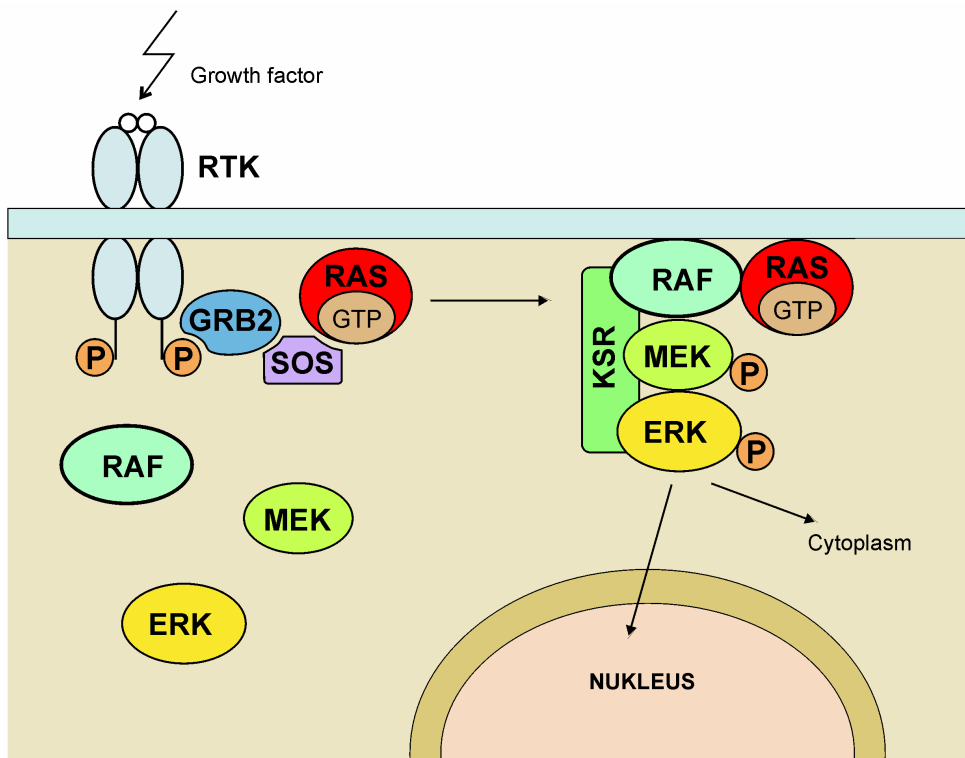
Figure 1-1. *The mitogen pathway.*

Phylogenetically, the appearance of RAF kinases has been linked to the evolution of multicellular organisms. The growing complexity of metazoans is accompanied by the appearance of isoforms and functional specialization of RAF kinases. Arthropod genomes contain only a single *RAF* gene, whereas vertebrates have refined RAF signalling and employ three isoforms that target ERK signalling to different subcellular compartments (Rapp et al., 2006). From the three human RAF isoforms A-, B- and C-RAF, B-RAF is the clothest related one to other eukaryotic RAFs. This leads to the conclusion that B-RAF from evolutionary point of view is the most ancient isoform.

1.1.2 B-RAF characterization

The **B-*raf* gene** is located on chromosome 7p34 and encodes proteins in the molecular weight range between 69 and 100 kDa, which are generated by alternative splising. At least 10 B-RAF isoforms were found in adult mouse tissues (Barnier et al., 1995). The B-RAF isoforms are differently distributed in the tissues, for example isoforms encoded by exon 10 are specifically expressed in neural tissues. In general B-RAF was detected at highest levels in neural tissue (especially in midbrain, dorsal spinal crod and neuroretina) and at high level in ovaries and testis, whereas expression in kidney, spleen, thymus, liver and heart was lower, ranging from intermediate expression level to barely detectable in muscle.

B-RAF knock out mice show overall growth retardation and die in mid-gestation (between E10.5 and E12.5) due to vascular defects caused by massive apoptosis of epithelial cells and some neurological abnormalities such as disturbed growth and differentiation of the neuroepitelium (Wojnowski et al., 1997). Later work with the different combinations of C- and B-RAF knock out mutants shows that B- and C-RAF may cooperate in the activation of MAP kinase (Wojnowski et al., 2000).

Sensory neurons and motoneurons from the B-RAF deficient mice do not survive in primary cell culture upon neurotrophic factors stimulation, possibly due to the upregulation of IAPs (Wiese et al., 1999; Wiese et al., 2001). However, recent work shows that A-RAF expression under the *b-raf* promoter rescues B-RAF-deficient embryos from endothelial apoptosis and allows them to survive until after mid-gestation. A fraction of these late-stage embryos survived to adulthood. Histological analysis demonstrated that A-RAF can substitute for B-RAF in mediating growth factor-dependent survival. However, A-RAF is unable to restore neuron migration and dendrite formation (Camarero et al., 2006).

Biochemically, B-RAF is the most active kinase. Mutations within the B-*raf* gene were found to be assotiated with human cancer (Davies et al., 2002). Specifically somatic mutations in B-RAF are associated with 60% of malignant melanomas and occur with moderate to high frequency in colorectal (Rajagopalan et al., 2002), ovarian (Singer et al., 2003), and papillary thyroid carcinomas (Brose et al., 2002; Cohen et al., 2003).

1.1.3 C-RAF characterization

The **C-*raf* gene** is located on chromosome 3p25 and encodes a 75 kDa protein. Till now, no C-RAF splicing isoforms have been identified. Earlier studies on the expression pattern of RAF showed that the C-RAF transcript was ubiquitously expressed in mouse, with highest level in striated muscle, cerebellum and fetal brain. (Barnier et al., 1995)

C-RAF knock out mice, like B-RAF deficient mice, show general growth retardation and also die in mid-gestation. In contrast to B-RAF, a different spectrum of tissues are affected encompassing lungs, skin and liver. In an inbred background, mice with abrogated C-RAF expression die between E10.5 and E12.5, while in an outbred background they survive until P0, but die within hours after birth, because their lungs fail to inflate (Mikula et al., 2001; Wojnowski et al., 1998). C-RAF-/- fetal livers were hypocellular, contained numerous apoptotic cells. Similarly, the appoptotic index in primary fibroblast and haematopoietic cell cultures was increased (Mikula et al., 2001).

These data indicate an essential role of C-RAF in counteracting apoptosis. This is further supported by more recent work, which identified new substrates of C-RAF such as XIAP, a potent inhibitor of apoptosis (Dogan et al., 2008; Tian et al., 2006) and eukaryotic elongation factor 1A (eEF-1a) (Lamberti et al., 2007). In both cases C-RAF activity mediated stabilisation of these proteins and induced their prosurvival activity.

Interestingly, C-RAF was found to be selectively bound with mitochondria, one of the main platforms for apoptosis regulation. In this context C-RAF found to have an influence on mitochondrial shape and cellular distribution (Galmiche et al., 2008). Recently it was also shown that C-RAF controlls mitochondrial Ca $^{2+}$ homeostasis through counteracting of ROS production (Kuznetsov et al., 2008).

C-RAF was found to be amplified in different lung cancer cell lines and its expression level is a critical parameter in lung tumor development (Kerkhoff et al., 2000).

1.1.4 A-RAF characterization

The **A-*raf* gene** is located on the X chromosome at position Xp11.2 and encode a 68 kDa protein. Recently two A-RAF splicing isoforms were described, DA-Raf1 and DA-Raf2, which are generated by alternative splicing of the A-*raf* pre-mRNA (Yokoyama et al., 2007). The amino acid sequences of DA-Raf2 (17 kDa) and DA-Raf1 (23 kDa) correspond to the first N-terminal 154 and 186 amino acids of A-RAF respectively, which contain the CR1 but lack the CR2 and the CR3 domains, the regions within RAF which sequences are conserved between RAF isoforms.

The human A-*raf* promoter region is unique as it contains three potential glucocorticoid response elements GRE-1, GRE-2, GRE-3 (Lee et al., 1996). GRE-2 and GRE-3 motifs were shown to interact with the glucocorticoid receptor DNA binding domain (DBD) in vitro. The fact that CRE1,2,3 are conserved sequences in the A-RAF promoters of rat, mouse and human suggests A-RAF exerts specific functions that are distinct from B- and C-RAF.

With this high expression levels of A-*raf* were observed in steroid-hormone-responsive tissues such as epididymis and ovary (Storm et al., 1990). The expression was found to be hormone-

dependent (Winer and Wolgemuth, 1995). The later research of A-RAF tissue distribution at mRNA and protein levels supported and refined this view. It was found that the distribution of full length A-RAF mRNA shows the highest level in urogenital tissue, lower levels were observed in thymus, spleen, pancreas, lung and cerebellum, expression was barely detectable in cerebral cortex and skeletal muscle. This information was refined by X-Gal staining of A-RAF through generation of transgenic mice expressing the *β-gal* reporter gene controlled by the A-*raf* promoter. Intriguingly, in the cerebellum A-RAF was found to be located only in the cell body of Purkinje cells, but not in the molecular or granular layers (Luckett et al., 2000).

In contrary to A-RAF full length protein expression, both splicing isoforms; DA-RAF1,2, were highly expressed in brain, heart and skeletal muscle and less expressed in urogenital tissue, liver and spleen (Yokoyama et al., 2007).

The **A-RAF knock out mice** phenotype was milder compared to that of B- and C-RAF. The animals survived until adulthood (Pritchard et al., 1996). Again background dependent differences were observed. On a predominantly C57 Bl/6 genetic background, A-RAF deficient mice developed neurological and intestinal abnormalities and died between 7 and 21 days post-partum. They were in general smaller and showed progressive wasting, despite normal feeding, suggesting that they either had a metabolic defect in sufficient absorbation of nutrients, wich may reflect the involvement of A-RAF in M2PK regulation (Mazurek et al., 2007). A-RAF deficient animals bread on 129/OLA background survived to adulthood, are fertile, do not display obvious intestinal abnormalities, but have a subset of neurological defects.

The urogenital tract, spleen and thymus, which express high level of A-*Raf* mRNA (Storm et al., 1990), showed only generalized reduction in size, but normal morphology and architecture.

The main intestinal defect obserwed in A-*raf*-deficient mice was the megacolon. This was similar to aganglionic megacolon (Hirschsprung disease), which is associated with the absence of enteric ganglia and results in intestinal blockade (reviewed in (Amiel et al., 2008)). Although no morphological changes were detected in tissue architecture and distribution of enteric neurons in colon of A-*raf*–deficient animals, it was proposed that in this case function of enteric neurons could be affected without histopathological manifestation. It is conceivable that A-RAF has a crucial role in function of enteric neurons, so that lost of A-RAF mimics the phenotype of absence of enteric ganglia.

The neurological abnormalities are constricted to classical cerebellum disorders: abnormal movement (ataxia) and affected proprioception, continuous tremor and a rigidity of their musculature. However, despite intensive investigations, none histological abnormalities were observed in the cerebellum of A-RAF deficient mice. This data, together with localisation of A-

RAF to Purkinje cells (see above), clearly suggested that A-RAF may be crucial for normal function of Purkinje cells without affecting their survival (Pritchard et al., 1996).

In summary the phenotype of the A-RAF knock out mouse demonstrated the involvement of A-RAF in metabolic processes and neuronal cell functions.

1.1.5 Structure of RAF proteins

The three RAF isoforms share common structural features comprising three conserved regions, CR1, CR2, CR3. The N-terminal CR1 encompasses the RAS binding domain (RBD) and the cysteine-rich domain (CRD), CR2 contains a conserved 14-3-3 binding motif and the C-terminally located CR3 encodes a kinase domain (Fig.1-2).

The RAF kinase can functionally be divided into two parts: the regulatory part (CR1+CR2) and the kinase domain (CR3). The N-terminal part contains predominantly negatively regulating phosphorylation sites. It mediates the initiation of activation steps via RBD. CRD domain presents lipid binding domain which determines different localization of RAF isoforms to specific lipid membranes. Through negatively regulated 14-3-3 phosphorylation site in CR2-domain the RAF conformation in signalling complex is determined.

Deletion of CR1+CR2 leads to a constitutively active kinase, also reported to as RAF-BXB (Bruder et al., 1993). B-RAF-BXB is the only RAF molecule that has sofar been crystallized (Wan et al., 2004). Its atomic structure shows a bilobal architecture: consisting of a N- and C-lobe. The N-lobe contains an N-region, P-loop and the glycin-rich ATP-binding site, whereas the C-lobe contains the substrate binding site and the so called activation segment. These two lobes build a deep hydrophobic pocket. Conformational changes of this pocket determine the activation state of the kinase.
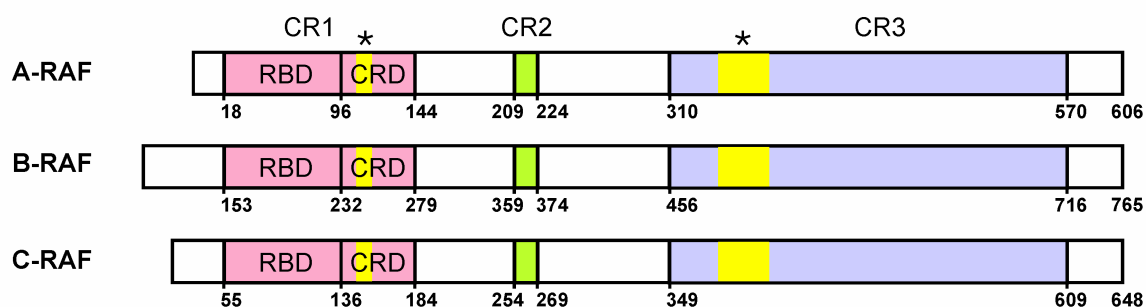
Figure 1-2. *Schematic diagram of domain structure of RAF proteins*
Lipid binding domains are indicated by yellow boxes.

1.2 Regulation of RAF kinase activity

1.2.1 Activation of RAF kinases by the RAS family of small GTPases

The RAS protein family comprises a group of structurally and functionally conserved small GTP-binding proteins, such as H-RAS, K-RAS, R-RAS, RAL, RAP and RHEB (reviewed in (Hancock, 2003; Kinbara et al., 2003)). RAS proteins are small GTPases that operate as molecular switches linking exstracellular stimuli to diverse biological outcomes such as cell growth, proliferation and differentiation.

Ras proteins cycle between GTP-bound and GDP-bound forms. The kinetics of GTP hydrolysis and GDP dissociation are catalysed by two classes of auxiliary proteins: GAPs (GTPase-activating proteins) and GEFs (guanidine-nucleotide exchange factors), respectively. GEFs promote the release of bound GDP and the capture of a new GTP molecule, which activates RAS-family proteins. GAPs stimulate the low intrinsic GTPase activity, resulting in de-activation of RAS proteins.The receptor interface for effectors is provided by so called switch regions (switch I, switch II and the P-loop) within RAS proteins. The P-loop encompasses the nucleotide binding site and coordinates the phosphate binding, whereas the switch I and II regions form mobile effector binding surface RAS proteins (H-, N- and K-RAS) have two structural domains: the highly conserved amino-terminal catalytic domain (1-165 aa) and a carboxy-terminal sequence (165-188/9), called hypervariable region (HVR). The HVR contains two anchor elements common for RAS proteins: the CAAX motif and a second motif which comprises a single palmitoylation site (C181) in N-RAS, two palmitoylation sites (C181, C184) in H-RAS and a polybasic domain of six contiguous lysine residues in K-RAS. These motifs function as a platform for posttranslational modifications which are critical for RAS protein trafficking and their isoform specific membrane microdomain localization.

The activation of RAS starts with binding of ligands (growth factors) to their receptor tyrosine kinase (RTK) at the plasma membrane (Fig.1-1). This event recruits Son-of-sevenless (Sos) protein, a RAS GEF, to the plasma membrane. In succession a complex with the adaptor proteins growth-factor receptor bound protein 2 (Grb2) and SRC-homology-2 domain containing (SHC). Sos, promotes the capture of a new GTP molecule to RAS at the plasma membrane. This switches RAS to its "on" conformation. In this open active form RAS binds to the RAS-binding domain (RBD) of RAF and forms a secondary interaction surface with the cysteine-rich domain (CRD) located in CR1 (Wittinghofer and Nassar, 1996). RAF is recruited to the plasma membrane and initiates several phosphorylation events within the RAF kinase domain.

The human RAS isoforms bind to the RBD with different affinity (Weber et al., 2000). A recent study showed that C-RAF only binds farnesylated (membrane bound) H-RAS, whereas B-RAF binds with similar affinity to both farnesylated and non-farnesylated forms. It has been concluded, that B-RAF does not necessarily need to be recruited to the membrane for RAS binding, because its

extended N-terminus causes more open protein conformation, than that of C-RAF (Fischer et al., 2007).

RAS signalling may not be restricted to the plasma membrane, but also may occur at endomembranes, such as Golgi apparatus and endoplasmic reticulum (Chiu et al., 2002) (Rocks et al., 2005). Indeed there is strong evidence that RAS transits through the endosomal compartment in its active state (Burke et al., 2001; Jiang and Sorkin, 2002; Rizzo et al., 2001).

1.2.2 RAF regulation by phosphorylation

Phosphorylation of RAF kinases is a very important part of signal transduction processes, because it regulates not only their activation state, but also their docking to several interaction partners which in turn impacts the sub-cellular localisation of RAF proteins.

The best investigated RAF isoform with regard to phosphorylation is C-RAF. In general, the N-terminus of RAF comprises inhibitory phosphorylation sites, while the C-terminus – horbors activatory sites. Three phosphorylation sites have been identified At the N-terminal region   of C-RAF:

i)   **S43** - seems to sterically hinder C-RAF binding to RAS (Wu et al., 1993);

ii)   **S233 -** forms the core of the third 14-3-3-binding site (Dumaz and Marais, 2003);

iii)   **S259** - internal 14-3-3 binding site, common for all three RAF isoforms (Dumaz and Marais, 2003; Ory et al., 2003).

These three phosphorylation sites contribute to C-RAF inhibition by PKA (Dumaz and Marais, 2003), S259 can be also phosphorylated by AKT/PKB (Zimmermann and Moelling, 1999).

iv)   **T268** - represent the residue homologous to T372 in B-RAF, an autophosphorylation site (Morrison et al., 1993);

v)   **S289, S296, S301** - are sites for ERK-mediated inhibitory feedback phosphorylation (Balan et al., 2006; Dougherty et al., 2005; Hekman et al., 2005). These sites are also present in B-RAF. For A-RAF new ERK feedback phosphorylation sites (**T253/S257/S259**) were identified in the so called IH-segment, which may, in contrast to B-and C-RAF, positively regulate A-RAF activity (Baljuls et al., 2008).

The C-terminus of RAF includes the kinase domain. Most of the phosphorylation sites in this region are activating:

i)   **S621** - C-terminall 14-3-3 binding site, is essential for activation by stimulatory factors (Mischak et al., 1996; Yip-Schneider et al., 2000);

ii)   **S338** - is located in N-region. Its phosphorylation is required for C-RAF activation (Diaz et al., 1997). This site is probably targeted by PAK 1, PAK2 kinase (King et al., 2001) and phosphatidylinositol 3-kinase (PI3-kinase) (Sun et al., 2000). In B-RAF the

homologous site **S446** is constitutively phosphorylated and therefore possible responsible for high basal B-RAF activity (Hekman et al., 2002).

iii) **Y340/341** - phosphorylation are necessary for C-RAF activation (Marais et al., 1995; Marais et al., 1997). These sites are targeted by SRC-family kinases in cooperation with S338 phosphorylation by PAK (King et al., 2001); homologous sites are present in A-RAF. This site are substituted by phosphomimetic aspartates in B-RAF, that lead to constitutive phosphorylation of **S446**. The analogous site in A-RAF, S299, was not considered as regulatory site. Recent work by Baljuls et al. (2007) showed, that the unique Y296 in A-RAF is the major determinant of the low activating potency of A-RAF.

1.2.3 Regulation of RAF signalling by scaffold proteins

14-3-3 - adaptor proteins participate in the regulation of a number of crucial processes: metabolism, signal transduction, protein trafficking, cell cycle control etc. (reviewed in (Aitken, 2002; Dougherty and Morrison, 2004)). Seven mammalian isoforms of 14-3-3 proteins have been identified so far. The association of 14-3-3 with client proteins occurs through defined high affinity peptide motifs, two of which (RSX**pS**XP and RXXX**pS**XP) are recognized by all 14-3-3 isoforms. Morrison et al. identified three basal phosphorylation sites in C-RAF: the serine residues at positions 43, 259 and 621 (Morrison et al., 1993). Two of these sites (serine 259 and 621) are involved in binding of 14-3-3 proteins to C-RAF. Phosphorylation of serine 621 seems to be essential for C-RAF activation, since the mutation of serine 621 to alanine resulted in a RAF protein that could no longer be activated by growth factor stimulation (Hekman et al., 2004; Tzivion et al., 1998). In contrast, exchange of serine 259 by alanine or aspartic acid resulted in enhancement of kinase activity, indicating that phosphorylation of serine 259 is inhibitory (Zimmermann and Moelling, 1999). Furthermore, the binding of 14-3-3 proteins to the C-terminal conserved site has been found to be differentially and dynamically regulated (Hekman et al., 2004).

KSR - kinase suppressor of RAS - has a high homology to RAF proteins, but its kinase domain has mutations in key residues that are essential for catalytic activity in other protein kinases. Only one work showed that KSR has kinase activity and works not only as a scaffold protein (Kolesnick and Xing, 2004). As a scaffold for mitogen signalling, KSR binds directly to RAF, MEK, ERK and other scaffolds (CNK, 14-3-3) thereby tethering these components together and ensuring a fast and selective response (reviewed in (Kolch, 2005)).

CNK - conector enchancer of KSR - was identified as an enhancer of a dominant negative phenotype caused by the isolated KSR kinase domain. CNK has no catalytic motifs, but

contains several protein interaction domains, contributing to its function as a multivalent adaptor protein (Kolch, 2005).

Prohibitin - an ubiquitously expressed protein functions in cell cycle and apoptosis regulation. Recent work shows that prohibitin targets C-RAF to the cell membrane through direct interaction (Rajalingam et al., 2005).

Hsp90 - heat shock protein 90 - an ubiquitous chaperone has an important role in assisting and maintaining the folding of many signaling proteins including C-RAF. Drugs, such as geldanamycin and derivatives, that prevent the interaction of Hsp90 with client proteins, lead among others to the ubiquitination and degradation of C-RAF (Blagosklonny, 2002).

MP1 - MEK partner 1 - is a widely expressed small scaffold protein that aids MEK1 binding to ERK1 and enhances their activity. MP1 forms a tight heterodimer with p14, a protein that targets MP1 and its binding partners to late endosomes. (Schaeffer et al., 1998; Teis et al., 2002).

1.2.4 Heterodimerisation of RAFs

The study of oncogenic mutations of B-RAF in cancer cells reviewed that: three out of 22 analyzed B-RAF mutants had reduced kinase activity *in vitro*, but lead to increased ERK activity *in vivo*. Subsequent analysis showed that the mutants with impaired kinase activity stimulate MEK by stimulating endogenous C-RAF activity, possibly via an allosteric or transphosphorylation mechanism. RAS induces wild type B-and C-RAF complex formation. In the case of above mentioned B-RAF mutants, the heterodimerization occurs in the cytosol independently of RAS, leading to oncogenic transformation (Wan et al., 2004).

1.2.5 Lipids, membranes and RAF activation.

The Singer-Nicholson fluid mosaic concept postulated the biomembranes as the luid structures in which lipids and integral proteins are arranged in a mosaic manner. Recent work added new insight to this concept. It could be shown, that lipids exist in several phases in bilayer's model system: gel, liquid ordered and liquid disordered states, depending a fluidity (reviewed in (Brown and London, 1998)). The different components of biological membranes, such as lipids and proteins, coexist, interact with and influence each other.

Lipid rafts - were originally defined biochemically as detergent-resistant membrane (DRM) fractions, later named rafts. Rafts are proposed to be highly dynamic, submicroscopic assemblies that float freely within the liquid disordered bilayer in the cell membrane. Sphingolipids and cholesterol play a crucial role in the assembly of these domains (Simons and Vaz, 2004). Clustering of separate rafts exposes proteins to a new membrane environment. Rafts are shown to be enriched

in specific enzymes, such as kinases, phosphotases, palmitoylases and depalmitoylases (Simons and Toomre, 2000).

The cell surface invaginations called caveolae are formed from lipid rafts by polymerisation of caveolins - hairpin-like palmitoylated integral membrane proteins that tightly bind cholesterol (Smart et al., 1999). Caveolae formation is actually the initial step of one type of endocytosis, called caveolae-dependend endocytosis.

Mitogenic signal transduction is sensitive to depletion of caveolins. H-RAS is palmitoylated and therefore, unlike K-RAS, targeted raft microdomains. Release of H-RAS·GTP from rafts is necessary for efficient activation of RAF (Prior et al., 2001; Roy et al., 1999).

Phosphatidylserine (PS) **-** is a major phospholipic component of all biological membranes. Like other phospholipids, PS contains a diglyceride, a phosphate group, and a simple organic molecule, in this case serine. PS act as principal physiological co-factor for protein kinase C (PKC) activation. It works in cojunction with diacylglycerol and phorbol ester (Hannun et al., 1986) through binding to the cysteine-rich domain of PKC (Mosior et al., 1996). The CR1 region of C-RAF kinase contains a zinc-coordinating motif, which is the binding site for PS. The cluster of amino acids R143, K144, and K148 appeared to be critical for interaction with PS, which binds predominantly via electrostatic interactions, driven by a cluster of basic amino acid residues (Improta-Brears et al., 1999; Mott et al., 1996).

Phosphatidic acid (PA) - is the acidic form of phosphatidate, a common phospholipid which is a major constituent of cell membranes. PA is the smallest of the phospholipids. Activated phospholipase D (PLD) catalyses the hydrolysis of phosphatidylcholine to generate PA.

Due to its physical properties PA can influence membrane curvature and therefore participates in both: cell und vesicle fusion. Moreover, PA acts as a signalling lipid, recruiting cytosolic proteins to appropriate membranes. MAP kinase pathway stimulation by insulin is dependent on PLD activation and leading to the PA mediated C-RAF translocation to the plasma membrane (Rizzo et al., 1999) (Rizzo et al., 2000). C-RAF contains a PA-binding site (398-401aa), which is strongly conserved in all three RAF isoforms. Mutational analysis of this domain showed that the residues R398, K 399, and R401 are crucial for C-RAF binding to PA (Ghosh et al., 2003). These binding sites are necessary for C-RAF function. PA did, however, not activate C-RAF *in vitro* or *in vivo*. The primary function of PA is therefore to enhance the recruitment of C-RAF to the plasma membrane where other factors, such as RAS, lead to its activation.

Thus RAF kinases are located in different lipid microdomains due to specific binding to membrane lipids. This specification seems vary between the three RAF isoforms and is changed upon activation/deactivation steps (Hekman et al., 2002).

Phosphatidylinositol-4,5-bisphosphate (PtdIns(4,5)P$_2$) - is a minor phospholipid which contains an inositol ring, phosphorylated on position 4 and 5, which is aligned with phosphatidate. PtdIns(4,5)P$_2$, a precursor of inositol-1,4,5-triphosphate (IP$_3$) and diacylglycerol (DAG), comprises ~1% of the total phospholipids in the eukariotic plasma membrane. Hydrolysis of PtdIns(4,5)P$_2$ by phospholipase C (PLC) to the second messengers, IP$_3$ and DAG, is a general and well defined response of cells to membrane receptor stimulation. It is now recognised that PtdIns(4,5)P$_2$ are signalling molecules by themselves and can, by binding to unique phosphoinositide-binding sites, affect the activity and subcellular localization of many proteins, including several actin regulatory proteins, wide range of ion channels and phospholipase D (PLD) (reviewed in (Huang, 2007; Oude Weernink et al., 2007)).

The micro-localisation of PtdIns(4,5)P$_2$ in membrane is currently under discussion. Two concepts suggest that PtdIns(4,5)P$_2$ is either localized to lipid rafts (Pike and Casey, 1996) or has specific PtdIns(4,5)P$_2$ clustering (van Rheenen et al., 2005).

The cellular distribution of PtdIns(4,5)P$_2$ can be visualised via its high-affinity interaction with the pleckstrin homology (PH) domain of PLCδ tagged with green fluorescent protein (GFP-PLCδ(PH)) (Falasca et al., 1998). Using GFP-PLCδ(PH) it was shown that PtdIns(4,5)P$_2$ localizes to plasma membrane (PM) and to recycling tubular compartment in HeLa cells (Robertson et al., 2006) and to highly dynamic, actin rich regions of PM (Tall et al., 2000)

The synthesis of PtdIns(4,5)P$_2$ by phosphoinositide 5-kinase (PIP5K) isoforms is tightly regulated by small GTP-ases. Although ARFs GTP-ases have been shown to stimulate PIP5K activity *in vitro*, in cells it is ARF6 that localizes with PIP5K at the PM (Honda et al., 1999).

In regard to RAF proteins and PtdIns(4,5)P$_2$, there is only one published study of all three RAF isoforms binding to phospholipids *in vitro* (Johnson et al., 2005). From these experiments it can be concluded that A-RAF, but not C- und B-RAF, binds specifically to PtdIns(4,5)P$_2$ and that crucial binding domain is located to the N-terminus of A-RAF.

1.2.6 Downstream targets of RAFs

The RAF kinases act as MAP kinase kinase kinases (MAPKKK), activating MEK (MAPKK), which in turn activates the MAP kinase ERK (Kyriakis et al., 1992).

MEK (mitogen activated kinase kinase) has two isoforms MEK1 and MEK2, which are phosphorylated by RAFs on two serine residues S218, S222 of their activation segment – LID<u>S</u>MAN<u>S</u>. Mutation of these residues to glutamic acid resulted in constitutive active kinase – LID<u>E</u>MAN<u>E</u>. MEK phosphorylates its target, ERK, on two residues: T183 and a Y185 on its regulation segment (Payne et al., 1991; Robbins et al., 1993).

ERK (extracellular signal-regulated kinase) in mammals has two isoforms ERK1 (44 kD) and ERK2 (42 kD). ERK1/2 has a lot of different substrates, such as transcription factors: Elk1, c-fos and c-jun (reviewed in (Yoon and Seger, 2006)).

Concerning this work, there is a significant evidence, that ERK1/2 is able to phosphorylate a GEF factor for RhoA, GEF-H1, enhance its activity and thus contribute to the activation of RhoA (Fujishiro et al., 2008)

1.3 Endocytosis

1.3.1 Classification and structural units of endocytosis

Endocytosis is a cellular process involving the PM, by which macromolecules, membranes and particles are internalized. There are four main types of endocytosis:

i) caveolar endocytosis;

ii) clatrin-mediated endocytosis (CME);

iii) macropinocytosis;

iv) clathrin and caveolin-independend endocytosis

v) phagocytosis.

The endocytic pathways differ with regards to the size of endocytotic vesicle, the nature of the cargo (ligands, receptors or lipids) and the mechanism of vesicle formation.

Dynamin is an atypically large and modular GTP-ase with domains that support PtdIns(4,5)P$_2$ binding, self-assembly and interaction with other endocytic components. It works as a master regulator of membrane internalization at the cell surface, partially as mechanochemical enzyme to drive membrane vesiculation (Conner and Schmid, 2003).

Clathrin coat is a three-legged structure, called triskelion, formed by three clathrin heavy chains. Each chain is tightly associated with a clathrin light chain which helps to deform the overlying plasma membrane into a coated pit. CME involves the concentration of high-affinity transmembrane receptors and their bound ligands in 'coated pits' on the plasma membrane. The coated pits are formed by the assembly of cytosolic coat proteins, the main assembly unit being clathrin. Coated pits invaginate and pinch off to form endocytic vesicles, that are encapsulated by a polygonal clathrin coat and carry concentrated receptor–ligand complexes into the cell. CME is crucial for intercellular communication during tissue and organ development. It furthere has an important role throughout the life of organism, as it modulates signal transduction by both controlling the levels of surface signalling receptors. It also mediates the rapid clearance and down regulation of activated signalling receptors.

The formation of coated pit requires association with the assembly proteins (AP): AP180 and AP2. The AP180 spontaneously binds to PtdIns(4,5)P$_2$ and clathrin, and may help to tether clathrin to the membrane. Therefore, AP180 is unique to the clathrin-dependent internalization pathway.

Transferrin is known to be specifically internalised via the clathrin-dependent pathway, and therefore can be employed as a marker for the clathrin–dependent endocytic compartments.

The clathrin-mediated internalization of voltage-gated calcium channels in neurons helps to control the strength and duration of synaptic transmission, and might have a role in learning and memory. Finally, CME is required for efficient recycling of synaptic vesicle membrane proteins after neurotransmission (reviewed in (Conner and Schmid, 2003)).

Caveolae are small uncoated invaginations in the plasma membrane of strikingly regular size. They represent one type of cholesterol-rich domains, so called rafts, with resident caveolin 1. Their unique lipid composition provides a physical basis for specific sorting of membrane proteins (Nichols, 2003). The budding mechanism of caveolae has not been determined. It is, however, becoming clear that uptake by such a clathrin-independent mechanism can lead to delivery to caveolin-1-containing endosomes, termed caveosomes (Pelkmans and Helenius, 2002).

Caveolar budding might be regulated by reversible phosphorylation. Caveolin 1 is phosphorylated on at least one tyrosin residue (Y14) in response to a variety of stimuli, such as insulin (Nichols, 2003). Moreover, caveolin 1 interact with different signalling receptors (Liu et al., 2002). These data demonstrate the role of caveolin-dependent endocytosis in trafficking of signalling molecules.

1.3.2 Endocytic pathway

Once internalized, the membrane and content of the resulting endosome can undergo different fates such as movement to late endosomes and lysosomes for degradation, or recycling back to the PM (reviewed in (Gruenberg, 2001; Nichols, 2003; Soldati and Schliwa, 2006)).

Endocytosis is highly dynamic process. Definitions of endocytic compartments are poorly standardized. Here we used definitions given in (Gruenberg, 2001). The first entry point for internalized membrane is the so called **early endosome**, where the first step of sorting possibly happens. Some proteins are considered as organelle markers due to their restricted distribution, such as small GTP-ases of the Rab and ARF family (Fig.1-3).
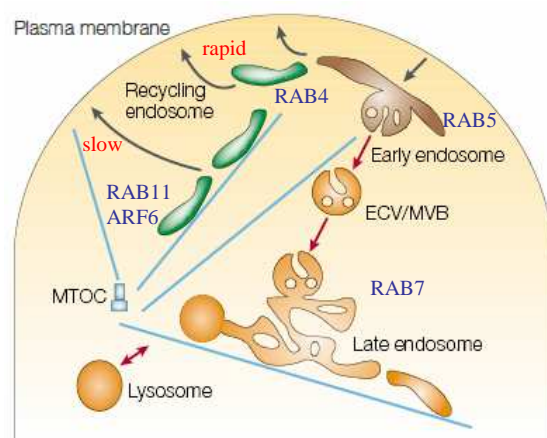
Figure 1-3. *Endocytic pathway (Gruenberg, 2001) , modified*

In early endosomes, for example, Rab5 protein builds a specific effector platform, which regulates membrane fusion, budding and interaction with cytoskeletal components.

Recently, it was shown that early endosoms have a highly complex organization which consist of cisternal regions, from which thin tubes and large vesicles emanate (Gruenberg, 2001).

The next step in the endosome maturation are the so called **endosomal carrier vesicles/ multivesicular bodies** (ECV/MVBs), which are large endosomal structures with a limiting membrane and internal invaginations.

The **late endosomes** have a similar multivesicular structure and represent the last state where sorting to recycling endosomes can occur. Otherwise proteins are targeted to final degradation within lysosomes. Rab7-GTPase and lysobisphosphatidic acid (LBPA) are good standardized as modulators and markers of late endosomes.

Lysosomes - are cell lytic organelles. Ion pumps in their membranes provide an acidic pH within lumen, which is required for acidic hydrolases.

Two different types of **recycling pathway** can be descriebed (Sorkin and Von Zastrow, 2002) (Fig. 1-3):

1. Rapid or direct recycling is modulated through Rab4 GTPase and branches off at the level of early endosome with a kinetic halftime (t½) of about 2 min.

2. Slow or indirect recycling (t½ = 10-30 min) which is processed through the endosomal recycling compartment (ERC) and is regulated by Rab11and ARF6 GTP-ases. This branches off at the level of sorting and late endosomes.

The endosomal recycling compartment (ERC) is a collection of tubular organelles with a diameter of about 60 nm which are associated with microtubules. Depending on cell type, the ERC tubules are mostly condensed around the microtubule-organizing centre or are distributed throughout the cytoplasm (reviewed in (Maxfield and McGraw, 2004)).

1.3.3 Cytoskeletal-based motility.

The geometry of the cytoskeleton appears to allow two types of endosome movement in mammalian cells: **short**, non-directed movement depending on actin filaments and **long**, directed movement depending on microtubules. However, participation of the cytoskeleton architecture in endocytosis varies greatly among different cell types, for example in polarized cells, such as epithelial cells and neurons, and non-polarized cells (see below) (Murray and Wolkoff, 2003).

1.3.3.1 Microtubule-dependent endocytosis

Microtubules are dynamic protein filaments, which stretch across the cells from the "minus end" at the microtubule-organizing centre in the peri-centriolar area to the "plus end" at the cell

periphery. They provide a mechanical basis for chromosome sorting, cell polarity, organelle localisation and endocytic trafficking. Direct observation of endocytosis by live cell microscopy show that endocytic processing occurs in association with microtubules. Transport of vesicles from the early to late endosome state is dependent on microtubules and microtubules can promote fusion and fission of endocytic vesicles. Some of the so called "microtubule plus–end tracking proteins" or TIPs, regulate microtubule growth dynamics. They seem to be able to link endosomes to microtubule and participate in minus-end directed endocytosis (Wu et al., 2006).

1.3.3.2 Actin-dependent endocytosis

Filamentous actin drives muscle contraction, cytokinesis and extension of the plasma membrane. It can form well-organized intracellular networks (Smythe and Ayscough, 2006). The actin filaments can be in general extended in two different forms: short filaments, also called cortical actin and long filaments, so called stress fibers. The long-distance endocytic transport along actin filaments can occur in some cell types, such as neurons due to short stretches of bundled, unipolar filaments, attached with each other along the stress fiber axis. But in general, the most important place for actin-dependent endocytosis is cortical, periplasmic area, where actin forms short polarity bundles (Murray and Wolkoff, 2003).

Moreover, cortical actin reorganization is an important step during membrane invagination and internalization and can also participate in endocytic processing events of clathrin-mediated uptake.

1.3.3.3 Motor proteins

In human the motor protein family includes about 100 members divided into 3 classes: kinesins, dyneins and myosins. A common functional characteristic of motor proteins in endocytosis is the ability to bind the vesicular cargo and transport it along cytoskeletal filaments (microtubule or actin) through ATP hydrolysis (is reviewed in (McGrath, 2005; Vale, 2003)).

Kinesins bind microtubules and hydrolyze ATP to produce movement mostly toward the plus-ends. Structural kinesins exist as an elongated dimers with an ATP-hydrolyzing motor domain on the N-terminus followed by a coiled-coil region, were the dimmers interact with each other. The C-terminal, light chain binding tail region, exirts cargo-binding function.

Dyneins are large microtubule motor proteins. They largely differ from kinesins and myosins. Dyneins are characterised by a "pinwheel with arms" structure with centrally located motor domains. Rotation of the motor domains causes movment of the microtubule-bound arm in a 15-nm "power stroke". The cytoplasmic dynein drives a huge array of organelle transport and is often involved in endocytic trafficking, which originates from the cell surface and terminates at perinuclear lysosomes.

The coordination of bidirectional movement is achieved by repeated binding of dyneins or kinesins to **dynactin**, a protein, linking both dyneins and kinesins to organelles and stimulating their movement (Dell, 2003). The capability of organelles to switch from forward to reverse movement and back is linked to the presence and coordination of different motors on the same organelle. The best-studied model system, and one that functions as a paradigm for other transport phenomena, is the melanosome in vertebrate cells (Soldati and Schliwa, 2006).

Myosins structurally resemble kinesins, but have actin-based motor activity. The large variety of myosins are dividet into two subclasses:

1) the class II – (muscle contraction class) which polymerize to form long structures with actin such as sarcomere (muscle contraction) and contractile ring (cytokinesis);

2) the class V – (vesicle driving class) which move cargo along actin filaments mostly towards the barbed-ends. Some members, like myosin VI, move towards pointed-ends of F-actin, analogous to kinesins.

1.3.4 The role of the ARF6 GTPase in endocytosis

ARF proteins were originally identified as targets of cholera toxin - a bacterial protein catalysing ADP-ribosylation of G-proteins (Kahn and Gilman, 1986). They have later been shown to regulate membrane trafficking pathways (reviewed in (D'Souza-Schorey and Chavrier, 2006)). ARF6 GTPase is a member of the class III ADP-ribosylation factor (ARF) family. As such it belongs to the RAS superfamily of small GTPases. Like Ras GTPase, ARF6 cycles between the active GTP-bound and the inactive GDP-bound conformation, which is mediated by specific GEFs and GAPs respectively (see above).

The GTP and GDP bound states determine the localization of AFR6 to different membranes. Thus, the GTP-bound form of ARF6 and its activated mutant ARF6_Q67L are located to the plasma membrane, whereas in the GDP-bound state ARF6, like its dominant negative mutant ARF6_T27N, localizes to the intracellular membrane compartment - the recycling endosomes (D'Souza-Schorey et al., 1995; Radhakrishna and Donaldson, 1997), Fig.1-4.

Sence localization is changed during the activation-deactivation cycle of ARF6 it works like a shuttle between the plasma membrane and the so called tubulo-vesicular recycling endosomes. ARF6 exerts different effector mechanisms during membrane trafficking, the most important being phospholipids methabolism. ARF6 has been shown to activate phosphatidylinositol 4-phosphate 5-kinase (PIP5K) (Honda et al., 1999; Krauss et al., 2003) as well as phospholipase D (PLD) (Brown et al., 1993; Cockcroft et al., 1994). At the same time, the product of PLD activity, PA, is a cofactor in the activation of PIP5K (Martin, 2001). Therefore, the synergistic effect of ARF6 on PIP5K and PLD activity can lead to a large increase of the PtdIns(4,5)P_2 level at the cell periphery.

The best studied function of ARF6 is its participation in different levels of endocytosis (reviewed in (D'Souza-Schorey and Chavrier, 2006; Donaldson, 2003).

1.3.4.1 ARF6 facilitates membrane internalization

In its activated state ARF6 localizes to the plasma membrane. Hydrolysis of ARF6 bound GTP facilitates clathrin-depependent and clathrin-independent internalisation of its ligands. This process is regulated by GAPs, which catalyze hydrolysis of ARF6·GTP and facilitate vesicle trafficking from the plasma membrane to the recycling compartment.

It has been shown in polarized epithelial cells that ARF6 binds to the plasma membrane and recruits the nucleoside diphosphate kinase, NM23-H1, which provides a source of GTP for dynamin-dependent vesicle fission (Palacios et al., 2002). Furthermore, ARF6 is involved in clathrin-mediated endocytosis by direct recruitment of the adaptor protein 2 (AP2), which links the clathrin coat with the cargo proteins, to the plasma membrane (Paleotti et al., 2005). ARF6 activation has also been linked to the dissociation of arrestin molecules from the G-coupled receptors to facilitate clathrin-mediated receptor internalisation (Claing et al., 2001; Mukherjee et al., 2000).

ARF6 was shown to assotiate with the caveolae-enriched membrane fraction and the inhibition of its activity results in inhibition of signalling in response to vascular endothelial growth factor (Ikeda et al., 2005) and oncogenic RAS (Xu et al., 2003).

ARF6 has been shown to be involved in unique clathrin- and caveolin-independent internalization of a number of ligands (Donaldson, 2003).
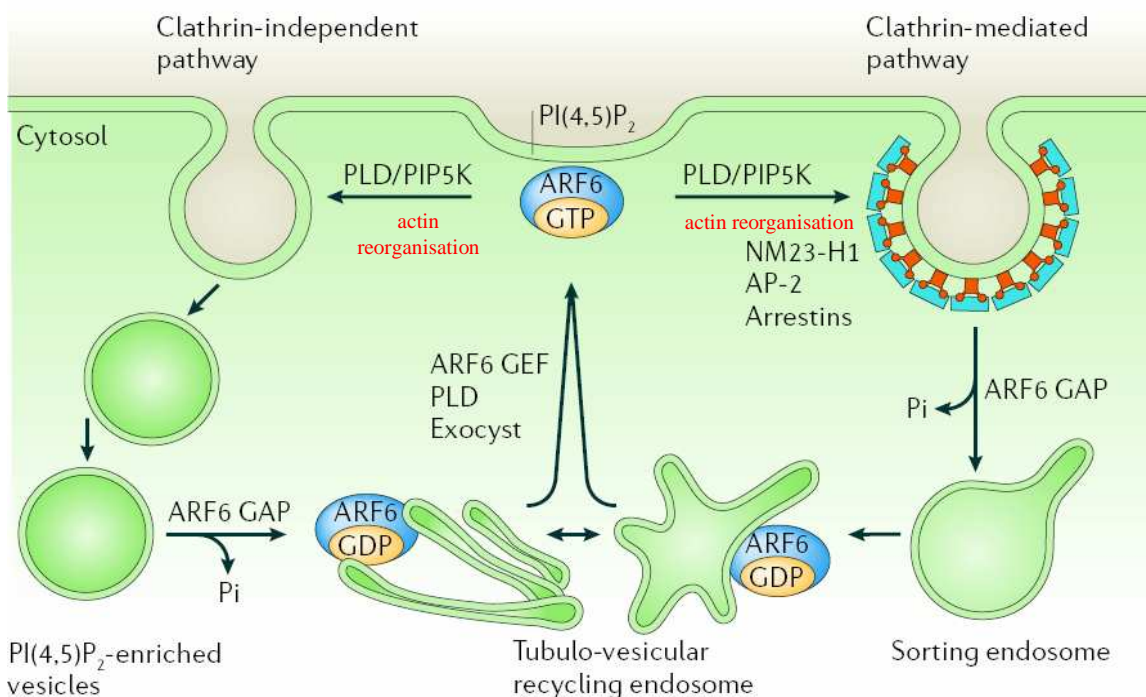
Figure 1-4. *ARF6 regulates clathrin-dependent and clathrin-independent endocytic pathways (D'Souza-Schorey et al, 2006), modified*

1.3.4.2 ARF6 is required for endosome recycling

The first evidence for ARF6 participation in endocytic recycling was demonstrated in CHO cells by overexpression of a dominant negative mutant, ARF6_T27N. Overexpression of ARF6_T27N affected the recycling of the transferrin receptor (Tfn-R) (D'Souza-Schorey et al., 1995). In HeLa cells the endosomal recycling compartment is very extended and can be visualized by GFP-PLCδ(PH) which indicates PtdIns(4,5)P_2-rich compartments. ARF6 colocalizes with PIP5K on these intracellular membranes (Brown et al., 2001). ARF6-labelled recycling endosomes form a tubular network which radiates from the pericentriolar area to the cell periphery. ARF6 can be colocalized with the RAB11 GTP-ase and a number of internalized molecules such as transferrin, β1-integrin and MHC class I, but not with early endosome marker RAB5 (Powelka et al., 2004). Functional assays showed that ARF6 activity affects recycling of transferrin, MHC class I, IL2 receptor α-subunit and glycosylphosphatidylinositol (GPI)-anchored proteins (D'Souza-Schorey and Chavrier, 2006). ARF6 function in the trafficking of intracellular vesicles to the plasma membrane requires the ARF6 activation through the exchange of bound GDP with GTP. This exchange is facilitated by ARF6 GEF proteins. The best characterized ARF6 specific GEF is the **exchange factor for ARF6 (EFA6)**, which contains Sec7 and PH domains typical for this protein family. Overexpression of EFA6 induces a redistribution of Tfn-Rs from the perinuclear endosomal compartment to the plasma membrane and the membrane ruffles (Franco et al., 1999).

1.3.4.3 ARF6 regulates actin polymerisation and membrane remodelling

ARF6 - regulated actin remodelling is required for the formation of pseudopods and membrane ruffles, neurite outgrowth, cell spreading, cell migration and phagocytosis (reviewed in (D'Souza-Schorey and Chavrier, 2006; Donaldson, 2003)). All these effects occur through the activation of RAC1 GTP-ase and/or lipid metabolism.

The mechanism of ARF6-mediated RAC1 activation is not fully understood. It was shown that ARF6 causes redistribution of endosome-localized RAC1 to the cell surface. One of possible mechanism of RAC1 regulation would be the activation of some GEFs for RAC1, such as DOCK-ELMO complex (Santy et al., 2005) or release of TIAM1 by recruitment of their downregulator, NM23-H 1(Palacios et al., 2002). The other RAC1 regulation way is the binding of ARF6 to POR1, a partner for RAC1 (D'Souza-Schorey et al., 1997).

ARF6 can also modulate the actin cytoskeleton via activation of PIP5K and PLD which leads to accumulation of PtdIns(4,5)P_2. It has been shown that PtdIns(4,5)P_2 can stimulate actin polymerization through addition of actin monomers at the rapidly growing end (+) of actin polymers on the different way. One mechanism involves actin nucleation and filament branching by Arp2/Arp3 complex, activated by WASP family proteins, which besides other ligands can be

activated by PtdIns(4,5)P$_2$. The second mechanism is PtdIns(4,5)P$_2$-induced dissociation of capping proteins from the pre-existing (+) end, such as gersolin family. The third one is PtdIns(4,5)P$_2$-mediated inhibition of cofilin/actin-depolimerizing factor (ADF) and as followed, a decrease of the number of actin nuclei.

Actin stress fibers and cortical actin networks attach to the plasma membrane via a number of proteins including vinculin, talin, and ezrin/radixin/moesin (ERM) to consolidate the cytoskeletal/membrane linkage and to increase the adhesion to substrates. Most of these proteins are activated to bind actin or are directed to link actin to the transmembrane receptors by PtdIns(4,5)P$_2$ (reviewed in (Yin and Janmey, 2003)).

1.3.4.4 Role of ARF6 in nervous system

Through its participation in actin cytoskeleton dynamics and membrane trafficking ARF6 plays important role in the most important processes in neuronal development, synaptic transmission effects and synaptic plasticity (reviewed in (Jaworski, 2007)). In the focus of this work it is important, that active ARF6 was shown to enhance neurotransmitter release (Ashery et al., 1999) and to facilitate AP2/clathrin recruitment to the synaptic vesicles (Krauss et al., 2003). Intriguingly, the tissue distribution of A-RAF and EFA6C, one of GEF isoform for ARF6, in the adult mouse brain is restricted to the Purkinje cells, whereas ARF6 is widely expressed in the cerebellum (Luckett et al., 2000; Matsuya et al., 2005).

1.4 *Saccharomyces cerevisiae*

1.4.1 Mitogenic cascade from yeast to man
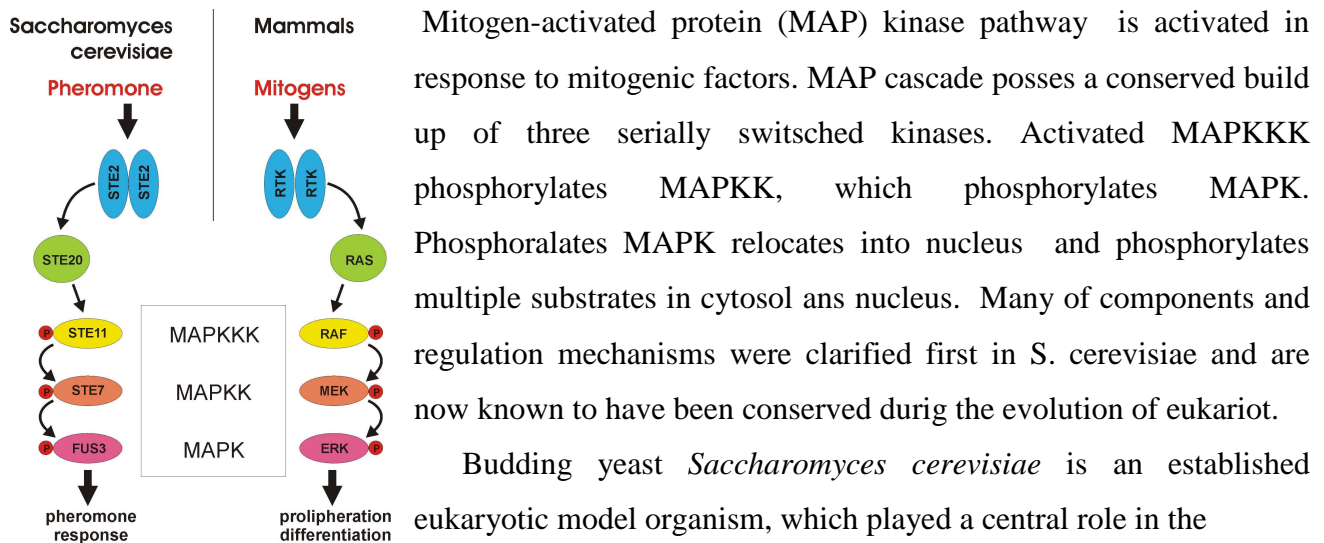
Figure 1-8. *MAPK cascades are conserved during evolution.*

Mitogen-activated protein (MAP) kinase pathway is activated in response to mitogenic factors. MAP cascade posses a conserved build up of three serially switsched kinases. Activated MAPKKK phosphorylates MAPKK, which phosphorylates MAPK. Phosphoralates MAPK relocates into nucleus and phosphorylates multiple substrates in cytosol ans nucleus. Many of components and regulation mechanisms were clarified first in S. cerevisiae and are now known to have been conserved durig the evolution of eukariot.

Budding yeast *Saccharomyces cerevisiae* is an established eukaryotic model organism, which played a central role in the elucidation of basic cellular processes such as cell division (Nurse, 1985), intracellular trafficking (Novick et al., 1980) and signal transduction (Madhani and Fink, 1998). In spite of the presence of two redundant RAS genes and at least 6 MAPK cascades (van Drogen and Peter, 2001), no RAF kinases are present in the *S. cerevisiae* genome. Yeast RAS proteins signal through the cAMP pathway (Broek et al., 1985). One of the MAPK pathways in *S. cerevisiae,* response to pheromone, consist STE11, STE7 and FUS3, which are equivalent to RAF, MEK and ERK respectively. Yeast pheromone response pathway governs cellular response to mating pheromone, human RAS-ERK pathway respond to extracellular mitogens (Fig.1-8).

RAF isoforms are highly promiscuous in their interactions and are known to form heterodimers in mammalian cells. Heterodimerization was shown to be a prerequisite for transactivation of RAF isoforms(Rapp et al., 2006). On this background, a system allowing the investigation of a single RAF isoform function is highly desirable.

1.4.2 Regulation of actin polymerization and endocytosis in yeast

In yeast, the actin cytoskeleton comprises two types of structure: actin patches, containing F-actin, that localize to the cell cortex, and actin cables, which are distributed throughout the cytoplasm. Regulation of cortical actin patches assembly and their rearrangement in response to internal and external signals is regulated through actin-binding proteins, many of which have functional homologues in higher eukaryotic cells. Actin polymerization is essential for cell polarization, cytokinesis and endocytosis. Many of the endocytic proteins, such as AP-2, Hip1/Sla2p, epsin/ Ent1p/Ent2p, have binding sites for PtdIns(4,5)P$_2$. However, the standart marker of PtdIns(4,5)P$_2$,

PLCδ-PH domain, when expressed as GFP fusion in yeast, labelled the yeast plasma membrane uniformly instead of showing a patch-like localization that would be characteristic of endocytic proteins. Recent studies identified a new PtdIns(4,5)P$_2$ binding domain, the AP180 N-terminal homology (ANTH) domain, which could detect PtdIns(4,5)P$_2$ on endocytic sites (Sun et al., 2007).

In yeast PtdIns(4,5)P$_2$ plays a key role in actin assembly and endocytosis (Stefan et al., 2005; Sun et al., 2005). Moreover, the yeast homolog of mammalian ARF6, Arf3p was shown in an earlier studies to regulate cortical actin formation but not endosytosis of a fluid-phase marker (Huang et al., 2003). Recent data indicates, that Arf3p localizes at sites of endocytosis and is necessary for wild-type levels of PtdIns(4,5)P$_2$ at the plasma membrane (Smaczynska-de Rooij et al., 2008).

In conclusion, involvement of PtdIns(4,5)P$_2$ in actin recruitment and vesicle formation are likely to be conserved across eukaryotic evolution.

2. Materials

2.1 Escherichia coli strains

Strain	Genotype	Source
DH5αF'	F-superE44 ΔlacU169 (φ80 lacZΔM15) hsdR17(rK-,mK+) recA1 endA1 gyrA96 thi-1 relA	Bethesda Res. Lab. (BRL)
BL21 (DE3)	F⁻ *ompT gal [dcm] [lon] hsdS_B* (r_b⁻ m_b⁻ ; an *E. coli*B strain) with DE3, a λ prophage carrying T7 RNA polymerase gene	Novagen

2.2 Yeast strains

Strain	Genotype	Source
BJ5459	**MATa** *ura3 leu2 his3 lys2 pep4*::HIS3 *prb1D1.6R kan1*	Yeast Genetic Stock Center, UC Berkeley, USA
cl3-ABYS-86	**MATα** *ura3-5 leu2-3 112 his3 pra1-1 prb1-1 prc1-1 cps1-3 can*^R	D. H. Wolf (University of Stuttgart, Germany)
cl3-ABYS-86 Δbmh2	**MATα** *ura3-5 leu2-3 112 his3 pra1-1 prb1-1 prc1-1 cps1-3 can*^R *bmh2::kan1*	Stefan Albert, University of Würzburg, Germany

2.3 Escherichia coli plasmids

Vector	Description	Source
pGEX-TT	for expression of GST fusion proteins in E. coli contains the polylinker from pEG-KT	Stefan Albert, University of Würzburg, Germany
pGEX-TT-AR149	for production of GST-	E. Nekhoroshkova

	AR149 in E. coli	
pGST-GGA3	for production of GST-GGA3 in E. coli	Margaret Chou, University of Pennsylvania, USA

2.4 *Saccharomyces cerevisiae* plasmids

pEG-KT	2µ; *URA3*; GAL UAS-*CYC3* driven production of GST fusion proteins in yeast	Mitchell et al., (1993)
pEG-KT-A-RAF	for production of GST-A-RAF in *S. cerevisiae*	E. Nekhoroshkova
pEG-KT-B-RAF	for production of GST-B-RAF in *S. cerevisiae*	Stefan Albert, University of Würzburg, Germany
pEG-KT-C-RAF	for production of GST-C-RAF in *S. cerevisiae*	Stefan Albert, University of Würzburg, Germany
pYES-2	2µ; URA3, GAL1 promotor	Invitrogen
pYES-2-B-RAF	for production of His-tagged B-RAF in *S. cerevisiae*	E. Nekhoroshkova
pYES-2-B-RAF_S364A	for production of His - tagged B-RAF 14-3-3 binding mutant in *S. cerevisiae*	E. Nekhoroshkova
pYES-2-B-RAF_S728A	for production of His - tagged B-RAF 14-3-3 binding mutant in *S. cerevisiae*	Stefan Albert, University of Würzburg, Germany
pYES-2-B-RAF_S364A, S728A	for production of His - tagged B-RAF 14-3-3 binding double mutant in *S. cerevisiae*	Stefan Albert, University of Würzburg, Germany
pUG36	2µ; URA3, MET25-P promoter for expression of GFP-tagged proteins in *S. cerevisiae*	J.H. Hegemann at al., (1996)
pUG36-B-RAF	for expression of GFP-tagged B-RAF in *S. cerevisiae*	E. Nekhoroshkova
pUG36-C-RAF	for expression of GFP-tagged C-RAF in *S. cerevisiae*	E. Nekhoroshkova

pUG36-C-RAF-C4	for expression of GFP-tagged C-RAF deletion mutant in *S. cerevisiae*	E. Nekhoroshkova
pUG36-A-RAF	for expression of GFP-tagged A-RAF in *S. cerevisiae*	E. Nekhoroshkova
pUG36-AR149	for expression of GFP-tagged A-RAF deletion mutant in *S. cerevisiae*	E. Nekhoroshkova
pUG36-A-RAF_1-230	for expression of GFP-tagged A-RAF deletion mutant in *S. cerevisiae*	E. Nekhoroshkova
pUG36-A-RAF_1-312	for expression of GFP-tagged A-RAF deletion mutant in *S. cerevisiae*	E. Nekhoroshkova
pUG36-A-RAF_1-388	for expression of GFP-tagged A-RAF deletion mutant in *S. cerevisiae*	E. Nekhoroshkova
pUG36-A-RAF_88-606	for expression of GFP-tagged A-RAF deletion mutant in *S. cerevisiae*	E. Nekhoroshkova
pUG36-A-RAF_142-606	for expression of GFP-tagged A-RAF deletion mutant in *S. cerevisiae*	E. Nekhoroshkova
pUG36-A-RAF_205-606	for expression of GFP-tagged A-RAF deletion mutant in *S. cerevisiae*	E. Nekhoroshkova
pUG36-A-RAF_306-606	for expression of GFP-tagged A-RAF deletion mutant in *S. cerevisiae*	E. Nekhoroshkova
pUG36-A-RAF_1-96	for expression of GFP-tagged A-RAF deletion mutant in *S. cerevisiae*	E. Nekhoroshkova
pUG36-A-RAF_18-96	for expression of GFP-tagged A-RAF deletion mutant	E. Nekhoroshkova

	in *S. cerevisiae*	
pUG36-AR149_R52L	for expression of GFP-tagged A-RAF deletion mutant with Ras-binding site mutation in *S. cerevisiae*	E. Nekhoroshkova
pUG36-A-RAF_R52L	for expression of GFP-tagged A-RAF Ras-binding site mutant in *S. cerevisiae*	E. Nekhoroshkova
pUG36-A-RAF_ R103A,K104A	for expression of GFP-tagged A-RAF phosphatidylserine binding site mutant in *S. cerevisiae*	E. Nekhoroshkova
pUG36-A-RAF_ R359A,K360A	for expression of GFP-tagged A-RAF phosphatidic acid - binding site mutant in *S. cerevisiae*	E. Nekhoroshkova

2.5 Mammalian expression vectors

pcDNA3	CMV-promotor, for expression of proteins in mammalian cells	Invitrogen
pcDNA3-Myc-A-RAF	for expression of Myc-tagged A-RAF in mammalian cells	Angela Baljuls, University of Würzburg, Germany
pcDNA3-Myc-A-RAF_DD	for expression of Myc-tagged A-RAF dominant active mutant in mammalian cells	Angela Baljuls, University of Würzburg, Germany
pEGFP-N1-ARF6	for expression of GFP-tagged ARF6 protein in mammalian cells	Antoine Galmiche, University of Würzburg, Germany
pEGFP-N1-ARF6_Q67L	for expression of GFP-tagged ARF6 dominant active mutant in mammalian cells	E. Nekhoroshkova
pEGFP-N1-ARF6_T27N	for expression of GFP-tagged ARF6 dominant negative	E. Nekhoroshkova

	mutant in mammalian cells	
pLNCX-HA-ARF6	for expression of HA-tagged ARF6 protein in mammalian cells	Margaret Chou, University of Pennsylvania, USA
pLNCX-HA-ARF6_Q67L	for expression of HA-tagged ARF6 dominant active mutant in mammalian cells	Margaret Chou, University of Pennsylvania, USA
pLNCX-HA-ARF6_T27N	for expression of HA-tagged ARF6 dominant negative mutant in mammalian cells	Margaret Chou, University of Pennsylvania, USA
pFLAG-EFA6	for expression of FLAG-tagged EFA6 protein in mammalian cells	Margaret Chou, University of Pennsylvania, USA
pEGFP-C1	CMV-promotor, for expression of GFP-tagged proteins in mammalian cells	Invitrogen
pEGFP-C1-C-RAF	for expression of GFP-tagged C-RAF in mammalian cells	Andreas Fischer, University of Würzburg, Germany
pEGFP-C1-C-RAF-C4	for expression of GFP-tagged C-RAF deletion mutant in mammalian cells	E. Nekhoroshkova
pEGFP-C1-A-RAF	for expression of GFP-tagged A-RAF in mammalian cells	Angela Baljuls, University of Würzburg, Germany
pEGFP-C1-AR149	for expression of GFP-tagged A-RAF deletion mutant in mammalian cells	E. Nekhoroshkova
pEGFP-C1-A-RAF_205-606	for expression of GFP-tagged A-RAF deletion mutant in mammalian cells	E. Nekhoroshkova
pEGFP-C1-A-RAF_R52L	for expression of GFP-tagged A-RAF Ras-binding site mutant in mammalian cells	E. Nekhoroshkova

2.6   Oligonucleotides

Oligonucleotides used in this work were custom-synthesized by Metabion (Martinsrid, Germany)

2.6.1 Oligonucleotides for PCR amplification of *A-RAF* gene
and its truncations.

A-RAF_for	5'- CGC ACT AGT ATG GAG CCA CCA CGG GG-3'
AR149_for	5'- CGA GGA TCC ATG GAG CCA CCA CGG-3'
AR149_rev	5'- CGA AGC TTC TAG GTA GTG ATG TCA ACA CAG-3'
AR149 (6*His) rev	5' – CGA AGC TTC TAA TGA TGA TGA TGA TGA TGG GTA CTC ATG TCA ACA CAG-3'
A-RAF 1-230_for	5'- CGA AGC TTC TAG TTG GAG TCC ATG GGG G-3'
A-RAF 1-312_rev	5'- GCG AAG CTT CTA CAG CTG CAC CTC ACT G-3'
A-RAF 1-388_rev	5'- CG AAG CTT CTA GCC CTC ACA CCA CTG TG-3'
A-RAF 88-606_for	5'-GCG ACT AGT ATG GTC GAG GTC CTT GAA GAT-3'
A-RAF 142-606_for	5'- GCG ACT AGT ATG ACA GTC TGT GTT GAC ATG AG-3'
A-RAF 205-606_for	5'- CTC CCG GGA TGG CCC CCC TAC AGC GCA TC-3'
A-RAF 306-606_for	5'- CTC CCG GGA TGC CAC CCA GTG AGG TGC AG-3'
A-RAF 606_rev	5'- CGA AGC TTC TAA GGC ACA AGG CGG G-3'
A-RAF-RBD_for	5'- CGC AAG CTT CAT ATG GTG GGC ACC GTC AAA G-3'
A-RAF_RBD_rev	5'- GCG CTC GAG CTA CAG CGG GAC ATC TTC-3'

2.6.2 Oligonucleotides for mutagenesis

A-RAF_ R52L_for	5'- GAC AAG GCC CTG AAG GTG CTG GGT CTA AAT CAG GAC TGC-3'
A-RAF_R52L_rev	5'- GCA GTC CTG ATT TAG ACC CAG CAC CTT CAG GGC CTT GTC – 3'
A-RAF_R103A, K104A_for	5'- C ATG CAC AAT TTT GTA GCG GCG ACC TTC TTC AGC CTG-3'
ARAF_R103A, K104A_rev	5'- CAG GCT GAA GAA GGT CGC CGC TAC AAA ATT GTG CAT G-3'
ARAF_R359A, K360A_for	5'- GAG ATG CAG GTG CTC GCG GCG ACG CGA CAT GTC AAC-3'
ARAF_R359A, K360A_rev	5'- GTT GAC ATG TCG CGT CGC CGC GAG CAC CTG CAT CTC-3'

ARF6(Q67L)_for	5'- GGA TGT GGG CGG CCT AGA CAA GAT CCG GCC-3'
ARF6(Q67L)_rev	5'- GGC CGG ATC TTG TCT AGG CCG CCC ACA TCC-3'
ARF6(T27N)_for	5'- GGA CGC GGC CGG CAA GAA CAC AAT CCT GTA CAA G -3'
ARF6(T27N)_rev	5'- CTT GTA CAG GAT TGT GTT CTT GCC GGC CGC GTC C-3'

2.7 Antibodies

2.7.1 Primary antibodies

Name	Application	Sourse
rabbit anti-Emp47p	Western Blot, 1:1000	D.Gallwitz Lab, MPI, Göttingen
rabbit anti-Kar2p	Western Blot, 1:3000	D.Gallwitz Lab, MPI, Göttingen
rabbit anti-CPYp	Western Blot, 1:5000	D.Gallwitz Lab, MPI, Göttingen
rabbit anti-Kar2p	Western Blot, 1:5000	D.Gallwitz Lab, MPI, Göttingen
rabbit anti-Rer1p	Western Blot, 1:1000	D.Gallwitz Lab, MPI, Göttingen
mouse anti-GFP (B2)	Western blot 1:1000 Immunoprecipitation 1:100	Santa Cruz Biotechnology, USA
rabbit anti-14-3-3 β (K19)	Western blot 1:1000	Santa Cruz Biotechnology, USA
rabbit anti-A-RAF (C20)	Western blot 1:1000 Immunocytochemie 1:50	Santa Cruz Biotechnology, USA
rabbit anti-B-RAF (C19)	Western blot 1:1000	Santa Cruz Biotechnology, USA
rabbit anti-C-RAF (C12)	Western blot 1:1000	Santa Cruz Biotechnology, USA
mouse anti-β-tubulin MAB3408	Immunocytochemie 1:50	Chemicon International, USA
mouse anti-c-Myc (9E10)	Western blot 1:1000 Immunoprecipitation 1:100	Santa Cruz Biotechnology, USA

mouse anti-C-RAF pS621 (6B4)	Western blot 1:1000	*nano*Tools, Germany
mouse anti-C-RAF pS259	Western blot 1:1000	Cell Signalling, USA
mouse anti-ERK2 (C14)	Western blot 1:1000	Santa Cruz Biotechnology, USA
mouse anti-pERK - p44/42 MAPK (Tyr202/Tyr204) E10	Western blot 1:1000	Cell Signalling, USA
mouse anti-HA (HA.C5)	Western blot 1:1000 Immunoprecipitation 1:100	Santa Cruz Biotechnology, USA
mouse anti-His Tag (4D11)	Western blot 1:1000	Upstate, USA
rabbit anti-GST (A5800)	Western blot 1:100000	Invitrogen, USA

2.7.2 Secondary antibodies

ECL™ anti-mouse Horseradish Peroxidase linked whole antibody; from sheep; NA931V	Western blot 1:5000	Amersham, UK
ECL™ anti-mouse Horseradish Peroxidase linked whole antibody; from donkey; NA934V	Western blot 1:5000	Amersham, UK
anti-mouse FITC-conjugated donkey antibody	Immunocytochemie 1:100	Jackson ImmunoResearch Laboratories, UK
anti-rabbit FITC-conjugated donkey antibody	Immunocytochemie 1:100	Jackson ImmunoResearch Laboratories, UK
anti-mouse CY5-conjugated donkey antibody	Immunocytochemie 1:100	Jackson ImmunoResearch Laboratories, UK
anti-rabbit CY5-conjugated donkey antibody	Immunocytochemie 1:100	Jackson ImmunoResearch Laboratories, UK
anti-rabbit TRITC	Immunocytochemie 1:100	Jackson ImmunoResearch Laboratories, UK
anti-mouse TRITC	Immunocytochemie 1:100	Jackson ImmunoResearch Laboratories, UK

2.8 Chemical reagents and general materials

Reagent	Purchased from
1 kb DNA ladder	Fermentas
Acrylamide (30%)/Bisacrylamide (0,8%)	Roth
Adenosin-5'Triphosphate (ATP)	Sigma
Agarose	Roth
Ammonium Acetate	Sigma
Ammonium peroxydisulfate (APS)	Sigma
Ampicillin	Sigma
AntifoamA	Sigma
Aprotinin	Roth
Bacto-Agar	DIFCO
Bovine serum albumin (BSA)	Sigma
Bradford-reagent	Sigma
Bromphenolblue	Sigma
β-Mercaptoethanol	MERK
Calciumchloride (CaCl$_2$)	Sigma
Chloroform	Roth
Dimethylsulfoxide (DMSO)	Sigma
Dithiothreitol (DTT)	Sigma
dNTP	Fermentas
Ethylenediaminetetraacetic acid-disodium salt (EDTA)	Sigma
EGTA	Sigma
Ethanol	AppliChem
Ethidiumbromide	Sigma
Glutathion-sepharose	Amersham
Glycerol	Roth
Hydrochloride (HCl)	Roth
IGEPAL (NP-40)	Fluka
Isoropyl-1-thio-ß-D-thiogalactopyranoside (IPTG)	Roth
Isopropanol	Applichem
Leupeptin	Sigma
L-Arginine	Sigma
L-Lysine	Sigma

L-Methionine	Sigma
L-Phenylalanine	Sigma
L-Threonine	Sigma
L-Tryptophan	Sigma
Magnesiumchloride	Sigma
Phenol	Roth
Phenol/Chloroform (TE saturated)	Sigma
PIPES	Sigma
PMSF	Fluka
Ponceau S	Sigma
Potassium acetate (KAc)	Roth
Potassiumchloride (KCl)	Roth
Potassiumdihydrophosphate (KH$_2$PO4)	Merck
Protein A-agarose	Roche
Protein G-agarose	Roche
Protein ladder	Fermentas
SDS ultra pure	Roth
Sodium citrate	Merck
Sodiumdihydrophosphate (NaH$_2$PO4)	AppliChem
Sodiumhydrophosphate (NaHPO4)	AppliChem
Sodiumhydroxide (NaOH)	Sigma
Sodium orthovanadate	Sigma
TEMED	Sigma
Tris-(hydroxymethyl)-aminomethane (Tris)	Roth
Triton-X100	Sigma
Tyrosine	Sigma
Uracil	Sigma
Whatman 3MM Paper	Schleicher & Schüll
X-ray film	Hartenstein
Yeast extract	DIFCO

2.9 Enzymes

Items	*Source*
Calf Intestinal Phosphatase (CIAP)	Fermentas
Bio Therm DNA polymerase	Gene Craft
DNA-Polymerase I, (Klenow-Fragment)	Fermentas
Deep Vent DNA polymerase	NEB
Pfu DNA polymerase	Stratagene
Pfu Turbo DNA Polymerase	Stratagene
RNaseA	Roche
T4 Ligase	Fermentas
Resriction Endonucleases	Fermentas, NEB

2.10   Kits

Items	*Source*
ECL Western blotting detection reagents	Amersham
QIAEX II Gel Extraction Kit	Qiagen
QIAGEN Plasmid Kit (Mini, Midi)	Qiagen
QIAquick PCR purification Kit	Qiagen
mi - plasmid miniprep Kit	Metabion
mi – gel extraction Kit	Metabion

2.11   Cell culture

2.11.1 Cell lines

HeLa   - epithelial-like cell line from human cervix carcinoma

ATCC [America Type Culture Collection] CCL-2

COS 7   - simian cell line from african green monkey kidney,

fibroblast-like cells growing as monolayers.

ATCC CRL-1651

NIH3T3   - fibroblast cell line from mouse Swiss NIH embryo,

immortalise, contact inhibited, DMEM 10% FCS

ATCC CRL-1711

2.11.2 Cell culture materials

Items	Source
DMEM	Invitrogen
EGF	Cell Systems
FCS	PanBiotech
HBSS	Invitrogen
L-Glutamine	Invitrogen
Penicillin-Streptomycin	Invitrogen
Trypsin-EDTA	PanBioteh

2.12   Instruments

Hardware	Manufacturer
Bacterial incubator	Heraeus B 6200
Cell culture incubator	Heraeus Instrument
Cell culture microscope	Leica
Cell culture hood	Gelaire Flow Laboratories
Cover glasses	Hartenstein
Developing machine	CP100, Agfa
Electrophoresis power supply	Bio-Rad
Electrophoresis unit, small	Bio-Rad Mini-Protean II
Fluorescence microscope	DMIRBE, Leica
Freezer (-20ºC)	Liebherr
Freezer (-80ºC)	ULT, Thermo Scientific
Heat block	Liebisch, Type 2099-DA
Horizontal electrophoresis gel	MWG Biotech
Magnetic stirrer	IKA Labortechnik
Mega centrifuge	J-6B, Beckman;
	J2-HS, Beckman;
	Megafuge 1.0 R, Heraeus;
	RC 5B plus, Sorval
Microscope Slides, Super Frost® Plus	Menzel-Gläzer
Mini centrifuge	5417R, Eppendorf
pH meter	inolab720, WTW
PCR machine	primus 96 advance, peqlab
Power supplier	BioRad
Refrigerated incubator shaker	innova 4330, New Brunswick Scientific
Refrigerator	Premium, Liebherr
Spectrophotometer	Ultraspec 3000, Pharmacia Biotech
Thermomixer comfort	Eppendorf
Ultracentrifuge	Optima L-80 XP, Beckman Coulter
Ultraviolet Crosslinker	UVC500 Hoefer Scientific Instruments
Vortex	Scientific Industries Genie-2
Water bath	GFL 1083, Amersham-Buchler

3. Methods

3.1   Microbiological Methods

3.1.1 Cultivation of Escherichia coli

3.1.1.1 Growth media for Escherichia coli

LB-Medium:	5 g/l	yeast extract
	10 g/l	trypton
	5 g/l	NaCl
	5 ml/l	1 N NaOH

| Additives: | | final concentration: |

Antibiotics:	Ampicillin:	50 µg/ml
	Chloramphenicol	30 µg/ml
	Kanamycin	50 µg/ml
	Tetracycline	15 µg/ml

| IPTG | | 0.1-1 mM |

2xYT-Medium:	10g/l	yeast extract
	16 g/l	trypton
	5 g/l	NaCl
	5 ml/l	1 N NaOH

For plates, 2% (w/v) agar has been added prior to sterilization. Sterilization was performed in an autoclave under the following conditions: 20 min at 121°C. Antibiotics were added after sterilization, to media chilled to approximately 50°C.

All media were stored at 4°C until use.

3.1.1.2   Growth and storage of Escherichia coli cultures

Escherichia coli strains and transformants were inoculated from a fresh agar plate into liquid medium, containing antibiotics when necessary. Luquid cultures were incubated with shaking (180 rpm) at 37°C. Permanent cutures were prepared by mixing 500 µl of logarithmically-growing bacteria with 500 µl of sterile glycerol. Thus prepared, cells were shock-frozen in liquid nitrogen and stored at -70°C.

3.1.2 Cultivation of *Saccharomyces cerevisiae*

3.1.2.1 Growth media for *Saccharomyces cerevisiae*

YEPG-Medium: 10.0 g/l   yeast extract

                     20.0 g/l   pepton (Nr. 190)

                     20.0 g/l   glucose

YEPGal-Medium: 10.0 g/l   yeast extract

                     20.0 g/l   pepton (Nr. 190)

                     20.0 g/l   galactose

PM-Medium: 6.7 g/l   yeast nitrogen base w/o AA

                       5.0 g/l   pepton (Nr. 140)

                     20.0.g/l   glucose or galactose

SD-Medium (Minimal medium):   6.7 g/l   yeast nitrogen base w/o AA

                     20.0 g/l   glucose

SGal-Medium (Minimal medium):6.7 g/l   yeast nitrogen base w/o AA

                     20.0 g/l   galactose

Additives for minimal media:

       Amino acids: 20 mg/l   L-histidine

                     60 mg/l   L-leucine

                     30 mg/l   L-lysine (mono-HCl)

                     40 mg/l   L-tryptophan

       Bases: 40 mg/l   adenine

                     20 mg/l   uracil

       Antibiotics: 200 mg/l   Geneticin 418

For plates, 2% (w/v) agar has been added prior to sterilization. Sterilization was performed in an autoclave for 20 min at 121°C. Antibiotics were added after sterilization, after media were chilled to approximately 50°C.

All media were stored at 4°C until use.

3.1.2.2 Growth and storage of *Saccharomyces cerevisiae* cultures

Plates:

S.cerevisiae was inoculated on corresponding plates from the permanent culture and incubated at 25-30°C. Such plates could be stored for several weeks at 4°C.

Liquid cultures:

50-100 ml of medium containing all requirements for growth and selection of the culture was inoculated from the plate and shaken at 25°C or 30°C untill the optical density at 600 nm (OD_{600}) reached the required value.

For cultivation of greater amounts of *S.cerevisiae*, 100 ml of liquid culture was used for inoculation of 1 liter of medium.

Permanent cultures:

0.5 ml of overnight liquid culture was mixed with equal volume of 50% sterile glycerol and stored frozen at -70°C. These stocks can be used for several years, when stored at the temperature of -70°C.

3.2 Molecular Biological Methods

3.2.1 Isolation of plasmid DNA

3.2.1.1. Analytical and large scale DNA preparation.

For analytical DNA preparation 5 ml E.coli overnight culture + antibiotic were sedimented and followed to DNA preparation according protocol for miniprep kits from QUIAGEN or Metabion. Greater amounts (100-500 µg) for ultra pure plasmid DNA were prepared by using QIAGEN ion exchange columns (midi and maxi). Culture volumes for these preparations were 100-500 ml of LB + antibiotic. Buffers and protocols delivered by manufacturer were employed.

3.2.1.2 Genomic DNA preparation from *Saccharomyces cerevisiae*

DNA was isolated according to Hoffman and Winston (1987) . 2 -4 ml of overnight *S.cerevisiae* culture were centrifuged at 10 000 rpm for 5 minutes. Cell pellets were washed once with STES buffer and resuspended in 40 µl of this buffer. Acid-washed glass beads were added to 80% volume and the test tubes were vortexed for 5 min. 200 µl of TE buffer and 200 µl of phenol were added to the mixture, followed by vortexing for 2 min. After vortexing, test tubes were centrifuged for 5 min at 14 000 rpm. Aqueous phase (upper) was extracted twice with chloroform, then was precipitated with 0.7 volumes of isopropanol, rinsed twice with 70% ethanol and dissolved in 100 µl of TE buffer. genomic DNA was used directly as a template for polymerase chain reaction

STES buffer:

1% (v/v) sodium dodecyl sulfate (SDS)
100 mM NaCl
10 mM Tris.Cl, pH 8.0
1 mM EDTA, pH 8.0

3.2.2 Spectrophotometric determination of the concentration and the purity of DNA solutions

The concentration and the purity of nucleic acids were determined by measuring the absorbance of properly diluted solutions at wave lengths λ=260 nm, and λ=280 nm against the used buffer. Absorbance A_{260}=1 measured under standard conditions (1ml volume and 1 cm cuvette) means the following concentrations:

> 50 µg/ml of double-stranded DNA
>
> 40 µg/ml of RNA or single-stranded DNA
>
> 20 µg/ml of oligonucleotides

Aromatic residues such as amino acids tyrosine, tryptophan, phenylalanine but also phenol absorb at λ=280 nm stronger than DNA. From that, protein and phenol contamination can be estimated by ratio between A_{260} and A_{280} values. $A_{260} : A_{280}$ values < 1.8 (or < 2.0 for RNA) indicate protein or phenol contamination.

3.2.3 Enzymatic treatment of DNA

3.2.3.1 Digestion of double-stranded DNA with restriction endonucleases

Today, about 200 restriction endonucleases are available from different manufacturers. They mostly belong to type II restriction endonucleases that recognize palindromic sequences (with a twofold symmetry axis). The recognition sequences may be four to eight base pairs long and are being cut within or immediately next to the recognition sequence. Dependent on the used enzymes and their cutting sites, sticky (5'-protruding or 3'-protruding single strand DNA) or blunt-ended DNA fragments can be generated.

The used enzyme was added (~1 unit per µg DNA) to the solution containing the DNA to be restricted, the corresponding buffer (delivered by the manufacturer in 10x concentration). Reaction volumes were 15 or 50 µl for analytic and preparative digestions respectively. Reaction mixtures were incubated at recommended temperatures for 1-3 hours.

3.2.3.2   Dephosphorylation of linearized DNA fragments

Removal of 5'-phosphate residues is catalyzed by alkaline phosphatase (Calf Intestinal, CIAP from Boehringer Mannheim). Thus treated vectors loose the possibility to self-ligate, which decreases the background during cloning of DNA fragments.

For dephosphorylation, about 5 µg of linearized DNA was dissolved in 50 µl of 1x CIAP buffer and incubated with 1 unit of alkaline phosphatase for 30 min at 37°C. The enzyme was inactivated by phenol/chloroform extraction or separated away by preparative gel electrophoresis. During dephosphorylation, some bases can be removed from the DNA strand, therefore it is suitable to decrease the enzyme amount or to use shorter incubation times.

CIP buffer (10x concentrated):

500 mM Tris-HCl, pH 8.5

1 mM EDTA

3.2.3.3   "Repairing" of 3'-or 5'-overhangs to generate blunt ends

"Blunting" of cohesive DNA ends was used when incompatible DNA ends were to be ligated.
For this purpose, the Klenow fragment of *E. coli* DNA polymerase I (Klenow and Henningsen, 1970) was used, which fills in 5'-overhangs by its polymerase activity, whereas 3'-overhangs are removed by residual 3'to5'- exonuclease activity. This polymerase is active in any restriction buffer, therefore no buffer change after restriction nuclease digestion was necessary.

To 4-5 µg of DNA digested with restriction endonucleases in 50 µl volume, 1 µl of deoxyribonucleotide stock solution was added. After the addition of 1 to 5 U of the Klenow fragment, the mixture was incubated at 30°C for 15 min. The reaction was stopped by heating to 75°C for 10 minutes. For generation of sticky-blunt ends by selective repair of ends generated by one enzyme, reaction was first cleaved by the first enzyme, and rendered blunt-ended by the Klenow enzyme. The enzyme was inactivated by heating to 75°C for 10 minutes, and the DNA subsequently cleaved by the second enzyme.

Deoxyribonucleotides stock solution (in water):

       2.5. mM dATP

       2.5. mM dGTP

       2.5. mM dCTP

       2.5. mM dTTP

3.2.3.4 Ligation of DNA fragments

Linearized DNA fragments can be connected by formation of phosphodiester bonds between adjacent 5'phosphate and 3' OH residues. T4 DNA ligase catalyses this reaction powered by hydrolysis of one ATP molecule.

The reaction contained about 100 ng of linearized vector DNA and a five to ten fold molar excess of the DNA fragment to be inserted, in the volume of 15µl of 1x ligation buffer (commercial, Fermentas). 1 unit of T4 DNA ligase was added and the reaction was incubated for 1 hour to overnight at RT (blunt ends) or 15°C.

3.2.4 Agarose gel electrophoretic separation of DNA fragments

The agarose gel electrophoresis is a method for separation of large (0.5-25 kbps) DNA fragments. Due to the negative charge of phosphate groups present in the structure, DNA moves towards the positively charged anode in an electric field. The electrophoretic mobility of DNA fragment is proportional to the logarithm of its molecular mass (Helling et al., 1974). The length and the amount of DNA fragments was estimated by comparison of the mobility and fluorescence of the fragment with the molecular mass standard. Molecular mass standards used in this work were from Fermentas. Concentration of agarose was varied from 0.7% to 2%, dependend on the size of the separated DNA fragments.

Agarose gels were prepared by resuspending the required amount of agarose in 1x TAE buffer and boiling in the microwave oven for 3-4 minutes. After a short cooling, the agarose solution was poured into the mold with the comb. After the gel hardened completely, the comb was pulled out, the gel was mounted in the electrophoresis chamber and overlayed with 1xTAE buffer. Samples to be separated were prepared in the loading buffer and loaded into the slots prepared by the comb.

The electrophoresis was carried out at 5V/cm and controlled by the mobillity of the electrophoretic marker dyes. After the electrophoresis the gel was stained with ethidium bromide, which allows the visualization of DNA fragments by fluorescence after illumination with UV transluminator (λ = 302 or 366 nm). Depending upon requirements, the stained gel was either photographed or used for isolation of DNA fragments.

10x gel loading buffer:

20% Ficoll 400

0.1 M EDTA, pH 8

1.0% sodium dodecyl sulfate

0.25% Bromphenol blue

0.25% xylene cyanol

TAE electrophoretic buffer (50x stock solution):

242 g Tris base

57.1 ml glacial acetic acid

37.2 g EDTA disodium salt

H_2O to 1 liter

Ethidium bromide solution:

1 µg/ml ethidium bromide in water

3.2.5 Isolation of DNA fragments from agarose gels

DNA fragments were isolated from the gel pieces containing DNA fragment by QIAquick Gel Extraction Kit from QIAGEN according protocol from manufacturer.

3.2.6 Preparation of competent Escherichia coli

E.coli cells were platted on LB Petri plate without antibiotics and incubate on 37ºC overnight. 250 ml of SOB-medium were inoculated with 10-12 big colonies picked from the plate. The culture was incubated with shaking at 180 rpm to an OD_{600} = 0.4-0.6. Cells were chilled on ice for 10 minutes and then harvested in sterile 500 ml centrifugation bottle. The bottle was centrifuged at 4000 rpm for 10 minutes in a precooled rotor.

Cell pellet was washed in 80 ml ice-cold TB-buffer, chilled on ice for 10 min and harvested.

Pellet was resuspended in 20 ml ice-cold TB buffer with adding from 1.4 ml DMSO (7% end concentration). Cells suspension was incubated on ice for 10 min, 200 µl aliquots were frozen in liquid nitrogen and stored at -80°C.

SOB-medium

2%	Bacto Trypton
0.5%	yeast extract
10 mM	NaCl
2.5 mM	KCl

After autoclaving two filtrated solutions were added to sterilised medium:

10 mM	$MgCl_2$
10 mM	$Mg\,SO_4$

TB-buffer

10 mM	PIPES, pH 6.7- KOH
15 mM	CaCl$_2$
250 mM	KCl
55 mM	MnCl$_2$

was sterilised by filtration.

3.2.7   Transformation of competent Escherichia coli

About 200 µl of frozen competent Escherichia coli cells were thawed on ice. To the cells, 3-4 µl of ligation mixture or 10 ng of plasmid DNA was added. Mixtures were incubated on ice for 5-30 minutes. Heat shock was performed by incubation at 42°C in a water bath for 90 seconds. After the heat shock, 1 ml of LB medium was added to the cells. Incubation for 30-45 minutes allows the expression of plasmid-encoded resistence genes. After that, the cells were pelleted (1 min 10 000 rpm) in a benchtop centrifuge, resuspended in ~50 µl of LB medium and plated on selective plates. The plates were incubated overnight at 37°C.

3.2.8 Amplification of DNA fragments via polymerase chain reaction (PCR)

The polymerase chain reaction is a cyclic process, allowing in each cycle the duplication or the number of the DNA molecules (Mullis and Faloona, 1987). PCR was used in this work for isolation of genes from the yeast genome, site-directed mutagenesis and other modifications.

In the first step of each cycle, double helices of template DNA are denatured by heating to high temperature (94°C). In the second step, the reaction mixture is cooled to 52-60°C, where the two oligonucleotide primers anneal on the template. The polymerization step heats the mixture to the temperature optimal for the DNA polymerase activity (72°C). At this step, the annealed primers are extended by DNA polymerization, the double helix is resynthesized in a template-dependent manner, the number of amplified molecules doubles. All these molecules can be substrates in the subsequent cycles

Multiple repetition of these steps yields to an exponential increase of the amount of the template molecule fragments which are determined by the used oligonucleotide primers.

Typical reaction:

        1 µl of template DNA (~0.5µg of yeast genomic, or 10 ng of plasmid DNA)

        1 µl of oligonucleotide #1 (50 µM)

        1 µl of oligonucleotide #2 (50 µM)

10 µl of 10x reaction buffer + MgCl$_2$ (delivered by manufacturer)

2 µl of desoxynucleotide mix (10 mM each)

84.5 µl of H$_2$O

99.5 µl

The reaction mixture was heated to 94°C for 3 minutes. During this step, 0.5 µl of DNA polymerase (Taq, DeepVent, or their mixture 5:1, depending on the application) was addet to reaction mixture.

Typical cycling:

denaturation	30 sec	94°C
annealing	30 sec	52-60°C
polymerization	x min	72°C (1min/1000 bases)

Cycles described above were repeated 30 times. At the end of the whole reaction, an additional polymerization step, 72°C for 10 min, was applied.

3.2.9 Methods for yeast genetics

3.2.9.1 Transformation of *Saccharomyces cerevisiae*

For yeast transformation a modified method of (Ito et al., 1983) was used. Treatment of yeast cells with alkaline cations leads to increased permeability of the DNA through the cell membrane, so that it is then taken-up by the cell. Cells can be transformed by linear DNA fragments that can subsequently integrate into the genome via homologous recombination (Rothstein, 1983). This is used widely for gene disruption of specific gene.

100 ml of the appropriate yeast strain was grown in complete YEPG medium to OD$_{600}$=0.5-1. The culture was centrifuged for 3 minutes at 2000xg and washed once with LiAc/TE solution. Cell pellets were resuspended in 1 ml of LiAc/TE solution. For transformation, 100 µl aliquot of cell suspension was mixed with an appropriate amount of DNA (<1 µg of plasmid DNA, 5-10 µg of linear DNA fragment for gene disruption or integration). After 5 minutes at RT, 280 µl of of 50% PEG4000 solution was added and the tube was incubated for 45 minutes at 30°C. Heat shock was performed by incubating at 42°C for 5 minutes. Cells were pelleted by centrifugation for 2 minutes

at 3000 rpm in a benchtop centrifuge, the supernatant was aspirated and discarded. The cell pellet was washed once with sterile H_2O and resuspended in 200 µl of sterile H_2O.

Cells were plated on appropriate selective plates and incubated at 30°C for several days.

LiAc/TE solution:

      0.1M Li-acetate

      10mM Tris.HCl pH 7.5

      1mM EDTA

      Sterilized by autoclaving

50% PEG4000 solution:

      50% (w/v) PEG4000 in H_2O

      Sterilized by autoclaving

3.2.9.2   Measurement of yeast growth curves

The required amount of yeast cells in the logarithmic phase of growth were washed with sterile water and used for inoculation of 100-200 ml of the appropriate medium to reach an optical density OD_{600} ~ 0.01. A new cell culture was inoculated at the appropriate temperature and the optical density was determined at regular time points. At an $OD_{600} > 0.8$, the culture was diluted with the same medium so that the measured OD_{600} value was lower than 0.8.

3.3 Biochemical Methods

3.3.1 Determination of protein concentration according to Bradford (1976)

The method is based on the observation that the protein dye Coomasie brillant blue G250 shifts its absorbance maximum from 465 nm to 595 when protein binding occurs. 990 µl of protein solution was mixed with 10 µl of dye solution (Sigma). After incubation for 5 minutes at RT, the absorbance at 595 was measured against a blank. A standard curve was determined using known concentrations of BSA. Protein concentration was read from the standard curve.

3.3.2 Preparation of protein extracts of *Saccharomyces cerevisiae* for SDS polyacrylamide electrophoresis.

Cells from a fresh liquid culture were pelleted by centrifugation at 5000xg for 5 minutes. The supernatant was discarded. The pellet was resuspended in 100 µl of lysis buffer per 1 OD_{600} unit and incubated on ice for 10 minutes. The proteins were precipitated by 1/10 volume of 100% (w/v) TCA. After 10 minutes of incubation on ice, proteins were pelleted by centrifugation in a bench centrifuge (10 min at 14 000 rpm). Protein pellets were washed briefly with larger amounts of a 1M Tris solution. After washing, the pellets were resuspended in 10 µl per 1 OD_{600} unit of Laemmli loading buffer and heated for 5 minutes to 95°C. Thus prepared samples were either loaded onto SDS gels or stored at -20°C until use.

Lysis buffer:

> 2M NaOH
>
> 5% β-mercaptoethanol

TCA solution:

> 100% (w/v) trichloroacetic acid

Tris solution:

> 1M Tris base

2x Laemmli loading buffer:

> 0.1 M Tris-HCl pH 6.8
>
> 2% SDS
>
> 2% β-mercaptoethanol
>
> 20% glycerol
>
> 0.002% (w/v) Bromphenol blue

3.3.3 SDS polyacrylamide electrophoresis according to Laemmli (1970) (SDS PAGE)

The samples were heated to 95°C for 5 minutes to denature the proteins by SDS binding and to disrupt the disulfide bonds by their reduction with β-Mercaptoethanol. Protein-SDS complexes possess a strong negative netcharge so that original charges of non-denatured proteins can be neglected. The charge density of all SDS complexes is approximately identical, so that the proteins are separated mainly according to their mobility through gel matrix when an electrical field is applied.

SDS PAGE was performed discontinuously, with stacking and separating gels. In the stacking gel, the glycine present in the running and loading buffers is not charged due to pH of the stacking gel. Therefore, the protein-SDS complexes move at the front and concentrate there. In the separating gel, glycine becomes negatively charged due to a change in the pH. It becomes a frontal ion and protein-SDS complexes separate behind it according to their size. The mobility of the protein is inversely proportional to the logarithm of its molecular mass. For the separation of larger proteins lower polyacrylamide concentrations in the separating gel were used and, *vica versa,* for smaller proteins, a higher percentage of the gel matrix was applied. Electrophoresis was run at 25V/cm until the bromphenol blue tracking dye reached the bottom of the separating gel. The gels were either stained with staining solution or electroblotted onto a nitrocellulose membrane for subsequent immunoblotting.

5x-Electrophoresis buffer:	0.125 M	Tris base
	0.96 M	glycine
	0.5 % (w/v)	SDS

5x-Laemmli loading buffer:	6.25 M	Tris-HCl, pH6.8
	2 % (w/v)	SDS
	10 % (v/v)	glycerol
	5 % (v/v)	ß-mercaptoethanol
	0.001 % (w/v)	bromphenol blue

Staining solution:	50 % (v/v)	methanol
	10 % (v/v)	acetic acid
	0.1 % (w/v)	Coomassie Blue G-250

Destaining solution:	10 % (v/v)	acetic acid

Preparation of gels

Gels were prepared in vertical arrangement between two glass plates separated by spacers. Separating gels of the required acrylamide percentage were poured immediately after polymerization was induced. The gel was overlayed by isopropanol and left to polymerize for 30-60 minutes. Isopropanol was removed and separating gels were overlayed with stacking gels. The comb was inserted immediately (before the solution starts to polymerize). After polymerization for 30 minutes, the gels were used or stored for further usage at 4°C. For analytical purposes, a Protean Minigel apparatus (BioRad), for preparative purposes a self-made apparatus was used.

4 % Stacking gel (10 ml):	1.3 ml	30 % bis-acrylamide-stock solution
	5.0 ml	0.25 M Tris-HCl, pH 6.8 + 0.2% SDS
	3.6 ml	H_2O
	75 µl	APS
	8 µl	TEMED

10 % Separation gel (10 ml):	3.3 ml	30 % bis-acrylamide-stock solution
	5.0 ml	0.75 M Tris-HCl, pH 8.8 + 0.2% SDS
	1.7 ml	H_2O
	100 µl	10 % APS
	3 µl	TEMED

12 % Separation gel (10 ml):	3.98 ml	30 % bis-acrylamide-stock solution
	5 ml	0.75 M Tris-HCl, pH 8.8 + 0.2 % SDS
	1.05 ml	H_2O
	100 µl	10 % APS
	3 µl	TEMED

14 % Separation gel (10 ml):	4.65 ml	30 % bis-acrylamide-stock solution
	5 ml	0.75 M Tris-HCl, pH 8.8 + 0.2 % SDS
	400 µl	H_2O
	100 µl	10 % APS
	3 µl	TEMED

3.3.4 Transfer of proteins from gels onto nitrocellulose filters, Western blotting

The gel with the separated proteins was washed with transfer buffer and put on soaked Whatmann paper. The gel was overlayed with nitrocellulose filter. Attention was paid not to introduce air bubbles. The whole sandwich was covered with two Whatmann papers, clipped in the holder and transferred to a chamber filled with transfer buffer. The cellulose filter aimed at the anode. The transfer was performed for 1 hour at a constant voltage of 100 V in the chilled chamber, or at 15 V overnight.

The transfer of the proteins was controlled by staining the nitrocellulose membranes with Ponceau-red which stains the proteins reversibly. The membrane was incubated briefly with Ponceau solution and washed with water to destain.

Transfer buffer:	20 mM	Tris-base
	150 mM	glycine
	20 % (v/v)	methanol

Ponceau solution:	40% (v/v)	methanol
	15%(v/v)	acetic acid
	2.5 g/l	Ponceau-red

filtered after Ponceau-red addition

3.3.5 Immunological detection of the proteins on the nitrocellulose filters

The nitrocellulose filter after Western blotting was incubated with 5% skim milk in TBST for 60 minutes to saturate the protein binding sites on the membrane. Then the membrane was incubated for 1 hour with the primary antibody diluted in TBST or 5% skim milk in TBST.

The filter was washed for 3 x 10 minutes in TBST. Bound antibodies were labelled by a 30 minutes incubation with a horse-radish peroxidase-coupled secondary antibody diluted 1:5 000. The filter was washed again as described above. The immobilized peroxidase was visualized by chemiluminiscence using the ECL System (Amersham) according to manufacturer's instructions. The chemiluminiscence was documented on ECL detection film (Amersham).

TBST buffer:	10mM	Tris-HCl pH7.5
	0.9% (w/v)	NaCl

0.05% (v/v)   Tween 20

3.3.6 Subcellular fractionation of yeast proteins by velocity sedimentation on sucrose density gradients

Membrane fractionation on 20-35 % sucrose gradients were done as described previously (Schroder et al., 1995). Cells were spheroblasted by treating with Lyticase in spheroblasting bufer at 30º C for 1 hour. Formation of spheroblasts was controlled trough osmolisis in H_2O (10µl per 990µl) by spectrometry on 600 nm. The spheroblasts were lysed trough 30 passages by glass homogenisator in lysic buffer plus protease inhibitors then ceared twice for 5 min at 500 g in 2-ml reaction tubes. 1 ml of supernatant was loaded onto an 11-ml sucrose gradient made up from 1-ml steps of 18, 22, 26, 30, 34, 38, 42, 46, 50, 54, and 60% (wt/vol) sucrose. The gradients were spun for 3 hours at 4ºC in SW-Ti rotor (Beckman) at 170,000 g. The gradient was then carefully collected into 12 equal fractions. Proteins were precipitated through incubation of probes with ice cold acetone in proportion 1:1 at -20ºC for two hours and following centrifugation on 14.000 g. The pellets were washed and resuspended in Laemmli loading buffer, resolved by SDS-PAGE and transferred to nitrocellulose and probed with antibodies.

Spheroblasting buffer:	0.05 M	NaH_2PO_7, pH 7.5
	1.4 M	Sorbitol
	0.01 M	NaN_3
	0.08 M	β-mercaptoethanol
Lysic buffer:	0.01 M	Triethanolamin-hydrosulfat, pH 7.5
	0.08 M	Sorbitol
	0.001 M	EDTA
	0.002 M	$MgCl_2$

3.3.7 Protein purification

3.3.7.1 Purification of humans recombinant His-tagged B-Raf proteins from *Saccharomyces cerevisiae*

Recombinant proteins containing a 6xHistidine-tag can be purified by Ni-NTA (nickel-nitrilotriacetic acid) chromatography which is based on the interaction between a transition Ni^{2+} ion immobilized on a matrix and the histidine side chains. Following washing of the matrix 6xHistidine-tag fusion proteins can be eluted by adding free imidazole or EDTA or by reducing the pH.

B-raf or their 14-3-3 binding mutants were cloned into an yeast expression vector pYES2 (Invitrogen) under the control of the *GAL1* promoter. To purify B-RAF or their 14-3-3 binding mutants, the plasmids were transformed into the strain cI3 ABYS. The yeast cells were grown overnight in 500 ml SC-(ura-) medium by shaking at 30ºC. The expression was induced by growth in galactose-containing medium for 24 hours. For this the cells were harvested, washed with and resuspended in SGal (ura-) medium. After induction overnight cells were harvested and washed with lysic buffer. The pellets were taken to purification or frozen at 80ºC.

For purification the cells were resuspended in 30 ml lysic buffer plus protease inhibitors. After disruption using a French pressure cell and removal of cell debris by centrifugation at 10000 g at 4ºC, the supernatant was added to 500 µl pre-washed Ni-NTA Sepharose (Amersham Biotechnology).

The probes were incubated by rotary for 2 hours at 4ºC, washed three times with 20 ml lysic buffer for 20 min by rotary. Protein was eluted in 300µl with 200-500 mM imidazole gradient.

Lysic buffer, pH 7.4

25 mM	Na_2PO_4
25 mM	NaH_2PO_4
150 mM	NaCl
10 mM	$Na_4P_2O_7$
25 mM	β-glycerophosphate disodium salt
10%	glycerol

Protease inhibitors:

Leupeptin 10 µg/ml (20 mg/ml : 5 µl per 10 ml)

Aprotinin 10 µg/ml (5 mg/ml : 20 µl per 10 ml)

Pepstatin 1,4 µg/ml (0,7 mg/ml : 20 µl per 10ml)

PMSF 1mM (200mM : 50 µl per 10ml)

3.3.7.2 Purification of human recombinant GST-tagged C-Raf protein from *Saccharomyces cerevisiae*

The GST•Bind purification systems are based on the widely recognized affinity of glutathione-S-transferase (GST•Tag) fusion proteins for immobilized glutathione. Proteins are quickly and easily purified to near homogeneity in a single chromatographic step. Glutathione-resin based purifications require that the GST domain is soluble and properly folded. The gentle elution condition (10 mM reduced glutathione) avoids target protein denaturation.

The *C-raf* was cloned an yeast expression vector pEG-KT under the control of the *GAL1* promoter. The plasmids were transformed into the strain yeast strain cI3 ABYS. The yeast cells were grown overnight in 500 ml SC-(ura-) medium by shaking at 30ºC. The expression was induced by growth in galactose-containing medium for 24 hours. For this the cells were harvested, washed with and resuspended in SGal (ura-) medium. After induction overnight cells were harvested and washed with lysic buffer. The pellets were taken to purification or frozen at 80ºC.

For purification the cells were resuspended in 30 ml lysic buffer + protease inhibitors. After disruption using a French pressure cell and removal of cell debris by centrifugation at 10000 g at 4ºC, the supernatant was added to 250 µl pre-washed GST- Sepharose (Qiagen).

The probes were incubated by rotary for 2 hours at 4ºC, washed three times with 20 ml kinase buffer for 20 min by rotary. Protein was eluted in 300 µl with 20 mM Glutathione in kinase buffer.

Lysic buffer

50 mM	Tris, pH 7.4
150 mM	NaCl
10 mM	$Na_4P_2O_7$
25 mM	β-glycerophosphate disodium salt
10%	glycerol

Kinase buffer

25 mM	Hepes, pH 8.0
150 mM	NaCl
10 mM	$Na_4P_2O_7$
25 mM	β-glycerophosphate disodium salt
10%	glycerol

Protease inhibitors:

Leupeptin 10 µg/ml (20 mg/ml : 5 µl per 10 ml)

Aprotinin 10 µg/ml (5 mg/ml : 20 µl per 10 ml)

Pepstatin 1,4 µg/ml (0,7 mg/ml : 20 µl per 10ml)

PMSF 1mM (200mM : 50 µl per 10ml)

3.3.7.3 Purification of human recombinant GGA3 protein from Escherichia coli

The GST purification system is based on the affinity of glutathione-S-transferase (GST•Tag) fusion proteins for immobilized glutathione. After washing steps of the matrix GST-tag fusion proteins can be eluted by adding free glutathione.

The BL21 E. coli cells were transformed with pGST-GGA3 plasmid, then inoculated in 50 ml LB medium and grown overnight at 37ºC by shaking. On the next morning this culture was diluted in proportion 1:20 in 900 ml LB medium and cultivated for 90 min at 37ºC by shaking. The expression was induced by incubation with 0.1 mM IPTG for 3 hours at 37ºC by shaking.

After that the cells were harvested, washed once with lysic buffer without TritonX-100 (TX-100) and resuspended in 8 ml lysic buffer. The cell suspension was sonicated 3 times for 15 sec and clarified by centrifugation at 10000g at 4ºC. To the collected supernatant 1.5 ml Glutationsepharose (Qiagen) was added and incubated by rotary at 4ºC for 2 or more hours.

Then the beads were washed 2 times with buffer A and 2 times with buffer B. after that the beads were resuspended well with 3.7 ml buffer B plus 0.3 ml glycerol and store at 4ºC.

About 20-50 µl of beads were run on the gel and quantify by Coomassie. Approximately 20 µg GST-GGA3 protein was used per pull down experiment.

> **Lysic buffer:**
> 1· PBS
> 10 mM EDTA
> 1% TX-100
> 1mM DTT
>
> **Protease inhibitors:**
> Leupeptin 10 µg/ml (20 mg/ml : 5 µl per 10 ml)
> Aprotinin 10 µg/ml (5 mg/ml : 20 µl per 10 ml)
> Pepstatin 1,4 µg/ml (0,7 mg/ml : 20 µl per 10ml)
> PMSF 1mM (200mM : 50 µl per 10ml
>
> **Wash buffer A**
> 1· PBS
> 300mM NaCl
> 0,5% TX-100
> 1mM DTT
> + protease inhibitors: see above

Wash bufer: B

PBS

0,5% TX-100

2mM $MgCl_2$

1mM DTT

+ protease inhibitors: see above

3.3.8 GGA3 pulldown assay

Activated ARF6•GTP was monitored by binding to its effector GGA3 as described previously (Martinu et al., 2004). Briefly, COS7 cells were co-transfected with HA-ARF6 plus indicated plasmids using jetPEI and grown for 24 h. EGF stimulation was performed after 24 h starvation in 0.03% serum with 100 ng/ml EGF (Cell System Biotechnologie Vertrieb) for 10 min at 37°C. Clarified lysates were incubated with 25 µg of GST-GGA3 immobilized on glutathione-Sepharose beads for 2 h at 4°C. The beads were washed three times with PBS, resuspended in SDS PAGE loading buffer and boiled. Bound proteins were size-fractionated by SDS-PAGE and detected by immunoblotting.

3.3.9 Immunoprecipitation of GFP-AR149 and ARF6

COS7 cells were transfected with GFP-AR149 and HA-ARF6wt, HA-ARF6(Q67L) or HA-ARF6(T27N) respectively with jetPEI (Biomol). After 24 h, cells were lysed in ARF6 lysis buffer (50mM Tris-HCl pH 7.0, 2mM $MgCl_2$, 100mM NaCl, 10% Glycerol, 0.75% NP-40) containing protease inhibitors. To avoid high signal from heavy and light chains of antibodies on the Western blot we used Mouse IgG TruhBlot Set (NatuTec) including beads and secondary HRP-conjugated antibody. The clarified lysates were divided into two equilibrated parts, each of them was incubated for 2 h at 4°C with anti-GFP or anti-HA antibody respectively (Santa Cruz Biotechnology, USA). Next, the probes were precipitated with mouse-TruhBlot agarose (NatuTec) for 1h at 4°C. Beads were washed three times in the lysis buffer with 0.2% NP-40 and protease inhibitors.

3.3.10 *In vitro* kinase activity assay

The kinase activity of an enzyme can be measured *in vitro* by the binding of phosphor from ATP by its substrate, so called phosphorylation reaction. In this work it was used the method for RAF proteins kinase activity detection based on following phosphorylation of recombinant MEK1 and Erk2, detected using an activation-specific Erk antibody that recognizes Erk only when specifically phosphorylated by RAF on Y202 and Y204.

The purified recombinant RAF kinases are stored at -80ºC, shawed directly for application and stored for short time on the ice. For reaction the following master mix was prepared:

5 µl 10 x kinase buffer --------	250 mM	Hepes, pH 8.0
0,5 µl MgCl$_2$ (1 M)	1,5 M	NaCl
1 µl DTT (100 mM)	250 mM	β-glycerophosphate disodium salt
3 µl MEK (1 mg/ml)	100 mM	Na$_4$P$_2$O$_7$
3 µl Erk (1 mg/ml)		

_ _ _ _ _

12.5 µl per sample

To this mix was added:

dd H$_2$O to hole volume of reaction 50 µl

3 µg RAF protein

5 µl ATP (10 mM) to induce the kinase reaction

The mixture was immediately incubated at 30°C for 30 min by shaking at 1200 rpm. The reaction is then stopped by adding of 20 µl 4 x SDS-loading buffer and incubated at 95°C for 5 min. The proteins are separated by SDS-PAGE and then blotted onto nitrocellulose membranes. Western blot is performed using phospho-specific pERK antibodies. Equal loading of the purified kinase is subsequently controlled by immunoblotting with specific antibodies.

3.4 Fluorescence Microscopy

Fluorescence microscopy was done with an Openlab software (Improvision, UK) controlled inverted DMIRBE microscope (Leica, Germany) with Leica oil immersion objective. All images were captured and stored as Openlab LIF files. Images were subsequently processed using Photoshop software.

3.4.1 Yeast cell imaging

3.4.1.1 Yeast live cell imaging

Yeast cells were transferred into a self-made chamber slide for imaging.

Yeast vital visualising of vacuoles and endocytic compartments with FM4-64 dye.

This method allows visualisation of vacuoles and endocytic compartments in yeast with FM4-64, N-(3-triethylammoniumpropyl)-4- (p-diethylaminophenyl-hexatrienyl) pyridinium dibromide, a lipophilic styryl dye, that is taken up by yeast cells via the endocytic pathway. Endocytosis of FM4-64 was modified from the protocol descriebed by Vida and Emr (1995).

Yeast strains were grown in SD-medium to an optical density OD_{600} of 0.5. Cells were harvested and resuspended at 3-5 OD U/ml. FM4-64 (16 mM in DMSO) was added to the cells at a final concentration of 40 µM. Cells were then incubated in the presence of the dye for 5 min on ice. After this internalisation step, the yeast cells were washed three times in ice-cold medium to remove surface-bound dye. The cells were resuspended in SC-medium and incubated for various times at 30ºC. Stained cells were placed on slides and visualised using optics (see above)

3.4.1.2 Fixed yeast cells imaging

Cells were fixed in 3.7% paraformaldehyde in PBS, washed and subsequently digested for 1 hour with lyticase (Sigma). After washing and mounting, samples were either stored at 4°C or processed for imaging.

3.4.2 Mammalian cells imaging

Cells were grown on cover slips, treated with growth factors or serum as indicated and subsequently fixed in 3.7% paraformaldehyde, permeabilized with 0.1% Triton X-100. Stainings were performed with specific antibodies and fluorescently labeled secondary antibodies.

3.4.2.1 Indirect immunofluorescence after cytosol depletion

HeLa cells were grown on coverslips overnight. After two washes with PBS cells were treated with 0,05% digitonin in isotonic sucrose buffer for 4 min on ice (Galmiche et al., 2008). After digitonin

treatment, cells were fixed with 3.7% paraformaldehyde in microtubule-stabilizing buffer (MSB; 0.1 M PIPES, pH 6.9, 2 mM $MgCl_2$, 2 mM EGTA), washed and subsequently permeabilized with 0,1% w/v Saponin in MSB with 0.5% BSA for 10 min. To stain non-cytosolic A-RAF, cells were incubated with anti-A-RAF antibodies (Santa Cruz, USA) in combination with anti β-Tubulin antibodies (Chemicon International) at concentration of 20 µg/ml in MSB buffer with 0,5% BSA and 0,1% Saponin at room temperature for 2 h. Unbound antibodies were removed by 3 washes with the same buffer. The coverslips were incubated with appropriate secondary antibody (conjugated to TRITC or CY5) diluted 1:200 for 1 h. After three washes with MSB and brief wash with deionized water the coverslips were mounted using MOWIOL (Calbiochem, USA).

3.4.2.2 Transferrin internalization

HeLa cells were grown on coverslips overnight, transfected with either GFP or GFP-fused AR149, ARF6(Q67L), ARF6(T27N) respectively for 48 h.
The cells were pre-incubated in serum-free medium for 1h 37°C. For continuous Tfn uptake, the cells were incubated in internalization medium (HBSS medium plus 1% BSA) containing 5 µg/ml Alexa Fluor 546-conjugated human Tfn (Invitrogen) at 37°C for indicated time. After Tfn internalization the cells were extensively washed three times with ice-cold PBS and fixed with 3.7% PFA.

3.4.2.3 siRNA-mediated depletion of human A-RAF.

For generation of A-RAF specific siRNA we used a self-producing approach using the "X-tremeGENE siRNA Dicer Kit" (Roche). Using this method we prepare first double-stranded RNA from T7-flanked target sequence. In our case it was 3'- end located A-RAF coding region from "Human easyRNA resourse" (German Resource Center for Genome). Next we digested the product with Dicer enzyme and purified approximately 20 µg siRNA as a set of about 15 different siRNA for A-RAF. To note as a big advantage, this procedure could be repeated as and when required.

Scramble siRNA was from QIAGEN. Transfection was carried out using 2 µg of siRNA mixture and 10 µl of "X-tremeGENE siRNA Transfection Reagent" (Roche) for 6-well culture plates, according to the instructions provided by the manufacturer.

4. Results

4.1 RAF protein properties in *Saccharomyces cerevisiae.*

4.1.1 RAF proteins purified from *Saccharomyces cerevisiae* in the active, phosphorylated state associate functionally with both hetero- and homodimeric forms of 14-3-3 proteins.

To study the RAF proteins in yeast system, we prepared several vectors for galactose- or methionine-inducible expression of tagged or intact RAF proteins in *Saccharomyces cerevisiae* (controlled by GAL1 and MET-25P promoters respectively). These vectors were transformed into different strains of S. cerevisiae and the expression levels of RAF proteins were tested by immunoblotting. Unfortunately only strains depleted of key vacuolar proteases pep-4 and prb-1, could produce decent levels of RAF proteins. In other strains RAF proteins were not detectable most possibly due to degradation. Therefore all our experiments were performed in two yeast strains: cl3-ABYS-86 and BJ5459 and their derivates.

Next, we purified GST-tagged RAFs from cI3-ABYS-86 strain and analysed them by SDS-PAGE and immunoblotting. Surprisingly, despite good expression, no GST-B-RAF was purified by affinity purification on glutathione beads, whereas A- and C-RAF could be purified under the same conditions. Therefore, B-RAF was expressed as N-terminally His-tagged protein and purified using metal chelating Ni-NTA agarose.

Purified GST-C-RAF and GST-A-RAF co-purified with a protein doublet of 33 and 35 kDa. The proteins of this doublet were identified by immunoblotting as yeast 14-3-3 homologues, Bmh1p and Bmh2p (Fig.4-1A). Importantly, budding yeast S. cerevisiae contains only these two 14-3-3 homologues in its genome, which is significantly less than mammalian and plant cells that express 7-14 isoforms of 14-3-3. It is known that 14-3-3 proteins function as dimers and most of mammalian isoforms preferentially associate with other isoforms to form heterodimers. With its two 14-3-3 isoforms, yeast provide a simple model system for functional studies of 14-3-3 interactions with RAF kinases. The fact that yeast cells express higher levels of Bmh1p than Bmh2p let us presume that Bmh1p exists at least partially as a homodimer in vivo.

To test whether RAF kinases associate functionally *in vivo* with both homo - and heterodimeric forms of 14-3-3 proteins we used cl3-ABYS-86 yeast and a *BMH2* gene-depleted cl3-ABYS-86, Δbmh2 strain (prepared by S. Albert, this laboratory). After purification of B-RAF protein from wild type and *BMH2*-deficient yeast strains, the kinase activity of the isolated proteins as well as their association with 14-3-3 proteins were investigated. In this experiment, B-RAF variants mutated at single 14-3-3 binding sites (B-RAF S365A and S729A), as well double mutant (B-RAF-S365/S729), were included as controls. Data presented in Fig. 4-1B document that wild type B-RAF

associates effectively with both hetero- and homodimeric forms of yeast 14-3-3 proteins. In case of *BMH2*-deficient strain, only wild type B-RAF, but none of its 14-3-3 binding mutants, was able to form a complex with Bmh1p homodimer. It can be concluded that both 14-3-3 binding sites of B-RAF are required for its association with 14-3-3 homodimer (Fig 4-1B), whereas the C-terminal 14-3-3 binding site suffices for binding of heterodimers.

   Kinase activities of B-RAF 14-3-3 binding mutants were comparable with that of wild type protein regardless whether only Bmh1p or Bmh1p/Bmh2p complex was present. Substitution of serines in the internal or C-terminal binding domain did not influence the activity of B-RAF considerably; only double mutant showed decreased kinase activity (Fig 4-1B). Consistently, both 14-3-3 binding serines of B-RAF were phosphorylated in yeast unless substituted with alanine (Fig 4-1B).
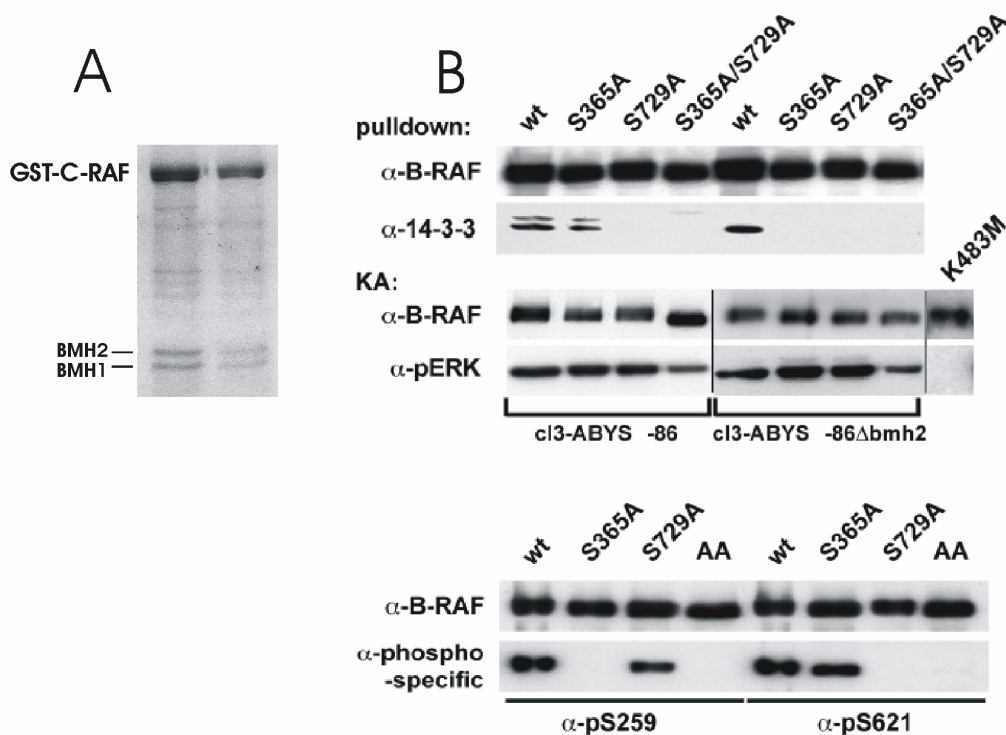

Figure 4-1. *RAF kinases associate in vivo with both homo- and heterodimers of 14-3-3 in S. cerevisiae.*

A. *GST-C-RAF associates with both 14-3-3 isoforms, BMH1 and BMH2.*
The GST-tagged C-RAF kinase isolated from protease-deficient *S. cerevisiae* strain cI3-ABYS-86 by glutathione-Sepharose affinity chromatography was resolved by SDS-RAGE and visualized by Coomassie staining.

B. *B-RAF binds to homo and heterodimers of 14-3-3 proteins.**
 BMH2 gene was knocked-out by homologous recombination in protease-deficient *S. cerevisiae* strain cI3-ABYS-86. Both, wild type and Δbmh2 strains were transformed with pYES2-B-RAF and its variants that were mutated at the single 14-3-3 binding sites (substitution of serine 365 and 729 by alanine) or B-RAF mutant impaired in both 14-3-3 coupling domains. His-tagged B-RAFs were purified by Ni-NTA chromatography. Expression level of the B-RAF proteins and their phosphorylation status were determined by immunoblotting using B-RAF antibodies and corresponding RAF phosphospecific antibodies as indicated. Kinase activities were measured by a coupled kinase assay (KA) in the presence of recombinant MEK and ERK proteins as described in Methods. The kinase dead variant of B-RAF (B-RAF-K483M) served as negative control and did not reveal any catalytic activity in yeast. These experiments were repeated three times and performed in cooperation with PhD S. Albert (University of Wuerzburg).

4.1.2 Localization of human RAF proteins in Saccharomyces cerevisiae

The initial aim of this work was to investigate in vivo the membrane assotiation of RAF isoforms. To this end, RAF proteins A-, B- and C-RAF fused to GFP were expressed under the control of the inducible *MET25* promotor. The distribution of overexpressed RAF proteins in S. cerevisiae was analyzed by fluorescent microscopy. GFP-B- and GFP-C-RAF, as well as the GFP protein alone, showed homogenous distribution in the cytosol. Only GFP-A-RAF decorated punctuate structures in the periplasmatic area (Fig.4-2, upper panel). In addition, GFP-A-RAF was enriched on bud necks during cell division and on shmoo tips after pheromone stimulation (Fig. 4-2, lower panel). Subcellular fractionation experiments corroborated the imaging data. Using sucrose density gradient proteins were separated into three fractions: cytosol/vacuole, light membrane, such as Golgi and endoplasmic reticulum, and heavy membrane, such as plasma membrane. GFP protein alone was found exclusively in cytosolic/vacuolar fraction, GFP-C-RAF was predominantly enriched in light fractions, while GFP-A-RAF was concentrated in heavy membrane fraction (Fig. 4-3). This observation indicated that of the three human RAF isoforms only A-RAF localized to specific sites of plasma membrane in S. cerevisiae, which are polarized during cell division and mating reaction.
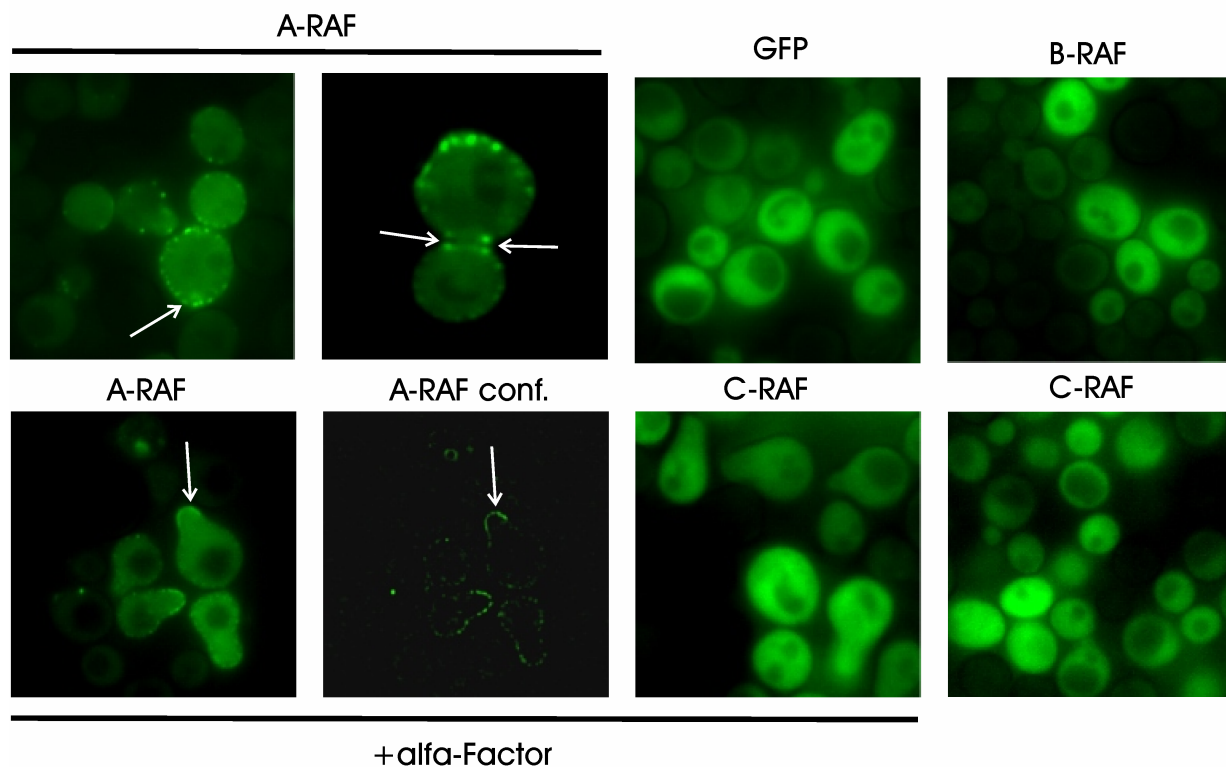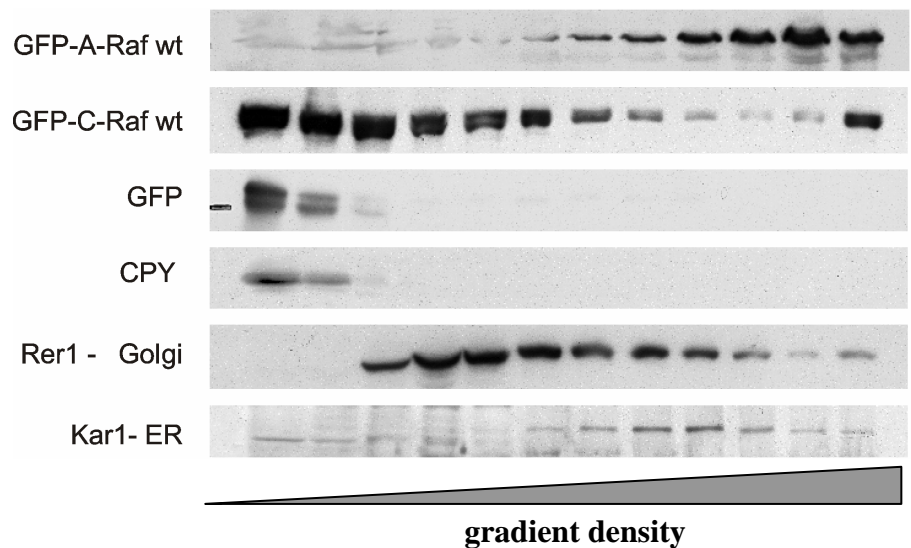

Figure 4-2. *Localization of RAF isoforms in yeast.* ******
RAF isoforms were expressed as GFP fusions in yeast. The cells were grown, fixed and imaged as descriebed in Chapter 3.4.1. Only GFP-A-RAF localizes to small dots in the cell cortex, which accumulate to the tips of small buds and to the necks of larger buds (upper row, left). Induced polarization of yeast by α-factor leads to relocation of GFP-A-RAF to the tip of mating projections called shmoos (lower row, left). Arrows indicate localization of GFP-A-RAF to the punctuate membrane sructures, which are enriched on the bud neck and at the shmoo tips. These experiments were performed in cooperation with PhD S. Albert (University of Wuerzburg) and PhD M. Becker (University of Wuerzburg).
conf.= confocal

Figure 4-3. *A-RAF is enriched in the heavy membrane fractions of yeast lysates.* **

Cell lysates from yeast, overexpressing GFP, GFP-A-RAF or GFP-C-RAF, were loaded on the top of sucrose gradient and centrifuged at 100.000xg. Fractionated lysates were subjected to protein precipitation and resuspended in Laemli loading buffer. Equivalent volumes of each fraction were loaded on SDS PAGE and immunoblotted. Proteins were visualized with specific antibodies as indicated on the left A-RAF is the only RAF protein, which segregates into heavymembrane/particle fractions. GFP alone fused C-RAF segregated into cytosolic/vacuolar fractions. Distribution of yeast membrane markers is shown in the lower rows. This experiment was performed in cooperation with PhD S. Albert (University of Wuerzburg)

gradient density

4.1.3 Two lipid binding domains in A-RAF mediate specific membrane association in Saccharomyces cerevisiae

To identify the A-RAF domains responsible for membrane association a mutational analysis was performed. To first narrow down the involvement of specyfic A-RAF domains GFP tagged C- and N-terminal deletions mutants were generated. The mutants overlapped to various degrees in the central region of the protein. In a second step GFP fused A-RAF point mutants were generated. The correct size and expression level of deletion mutants was monitored by Western blot analysis (Fig.4-5B). The subcellular distribution was analysed by epifluorescence microscopy. For schematic overview of all mutants used in this study and their subcellular localization please see Fig. 4-4. The analysis of the deletion mutants revealed that neither the N-terminal or C-terminal deletion mutants of A-RAF showed wild type localization. The N-terminal mutants, including the CR1 and CR2, but not CR3 domains, were homogenously distributed on the plasma membrane (Fig.4-5A, bottom panel). In contrast, the C-terminal mutants, including CR3 and CR2domains, showed predominantly homogenous cytosolic distribution with rare single spots (Fig.4-5A, upper panel). Only two deletion mutants, C-88-606 and N-1-388, which both contained a part of the CR1
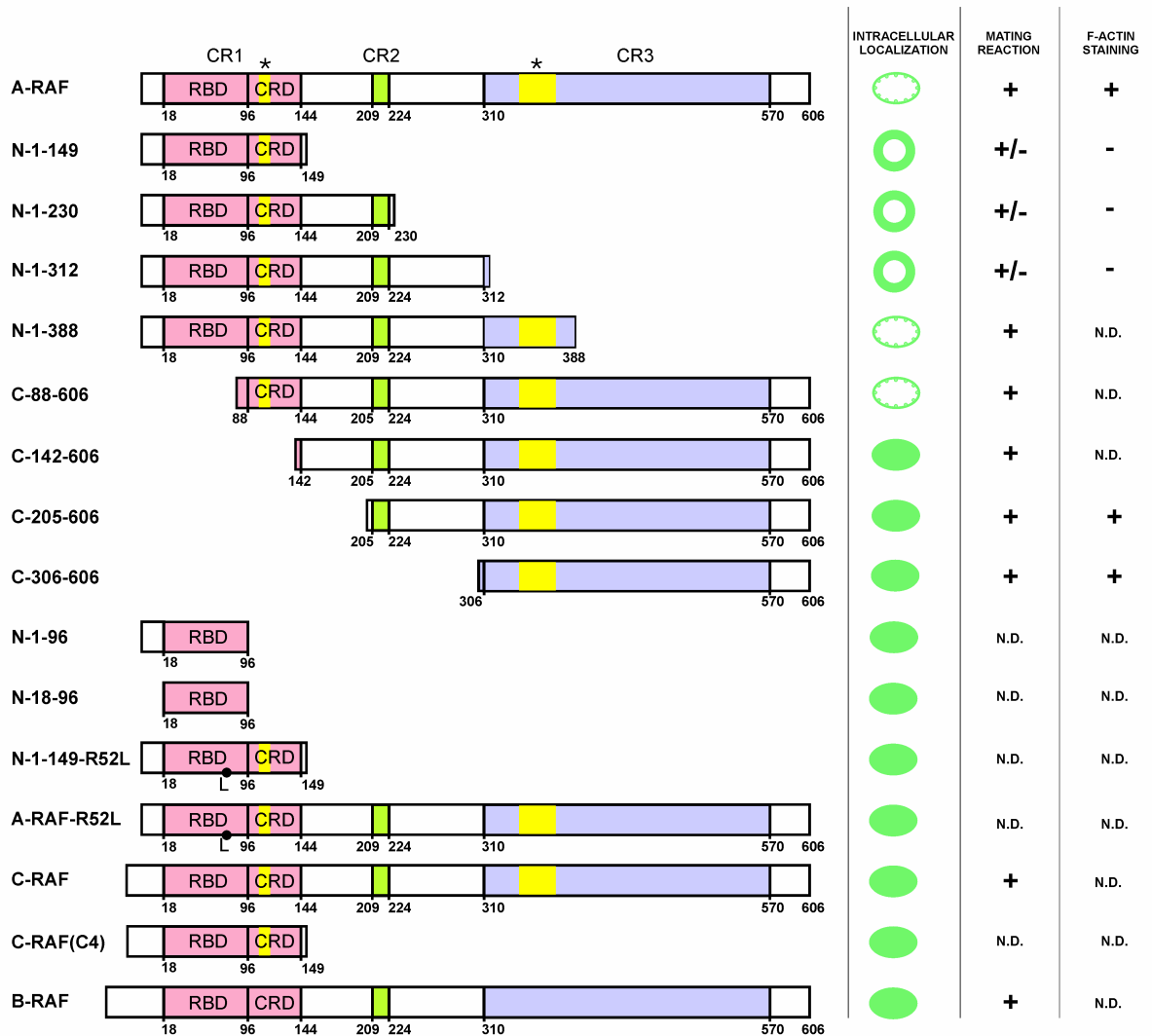
Construct	INTRACELLULAR LOCALIZATION	MATING REACTION	F-ACTIN STAINING
A-RAF		+	+
N-1-149		+/-	-
N-1-230		+/-	-
N-1-312		+/-	-
N-1-388		+	N.D.
C-88-606		+	N.D.
C-142-606		+	N.D.
C-205-606		+	+
C-306-606		+	+
N-1-96		N.D.	N.D.
N-18-96		N.D.	N.D.
N-1-149-R52L		N.D.	N.D.
A-RAF-R52L		N.D.	N.D.
C-RAF		+	N.D.
C-RAF(C4)		N.D.	N.D.
B-RAF		+	N.D.

Figure 4-4. *Schematic presentation of analysed wild type and mutant RAF isotypes in yeast.* **

N- and C-terminal deletions or point mutations were expressed as GFP fusions in yeast. Staining patterns of mutants are shown on the right. The largest C- and N-terminal deletions showing the "wild type" localisation are 1-388 and 88-606. Lipid binding domains (see also Fig.4-6), are indicated by yellow boxes.

domain, corresponding to so the called CRD, and a part of the CR3 domain, corresponding to the PA binding site in C-RAF, showed the punctuate plasma membrane distribution similar to A-RAF wild type (Fig.4-5A, right panel). The previously published work by Johnson et al. 2005, showed that CR1 region (RBD + CRD) was specifically required for binding to PtdIns(4,5)P_2. Thus, the deletion analysis reveals that two A-RAF domains were crucial for wild type localisation. The first one is the CRD domain on the N-terminus, participated in binding to the RAS protein and to PS/ PtdIns(4,5)P_2 rich membrane. The second one exhibit a part of the CR3 domain, corresponding to PA binding domain in the C-RAF. The identified sites in A-RAF are conserved among of three RAF isoforms; therefore we based our point mutation analysis on the published data for C-RAF.
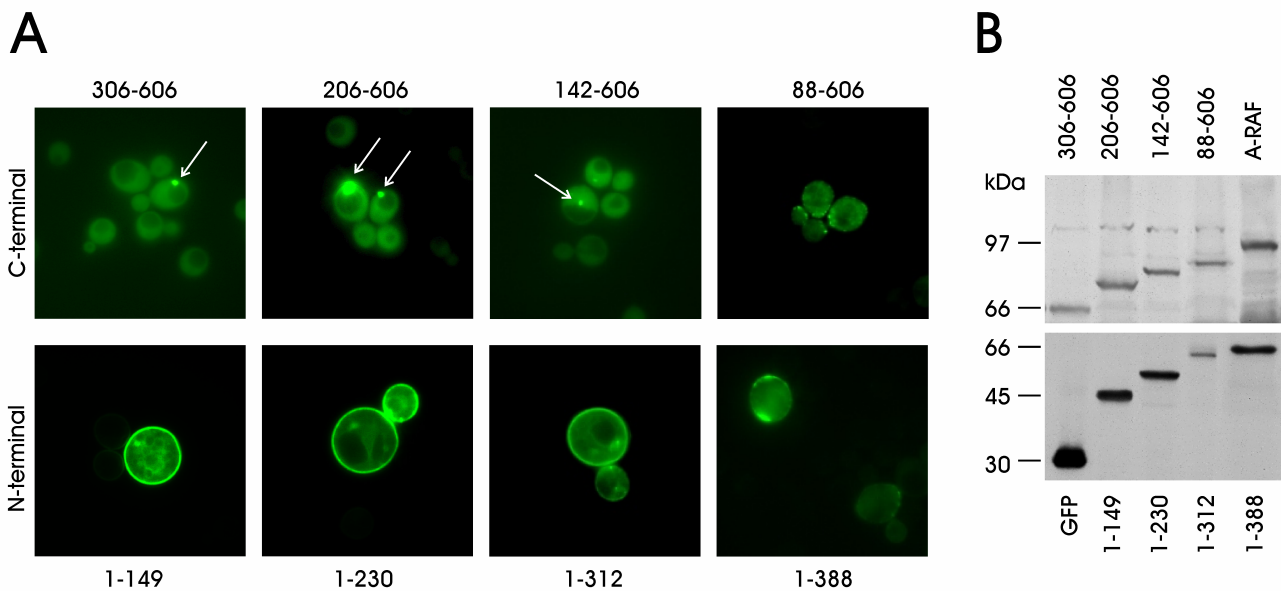
Figure 4-5. *Localization patterns of C- and N-terminal deletion mutants.* ******
A. Cells expressing A-RAF deletion mutants were grown and fixed as descriebed in Chapter 3.4.1. The smallest N-terminal deletion (88-606) and smallest C-terminal deletion (1-388) retain wild type distribution. C-terminal deletions that lost the presumptive PA binding motif, while retaining the PtdIns(4,5)P_2 binding motif in CRD (see the scheme above) are homogenously distributed to the plasma membrane. N-terminal deletions which possess only the PA-binding domain showed homogenous distribution with rare single spots (indicated by arrows). Magnification 100×.
B. *Immunoblot analysis of GFP-A-RAF deletion mutants*
Yeast cell lysates expressing indicated GFP-A-RAF constructs were subjected to protein extraction, as described in Chapter 3.3.2, loaded on SDS PAGE and analyzed by Western blot with antibodies against GFP.

Two lipid binding domains were demonstrated to be crucial for C-RAF association with plasma membrane (marked with yellow color, see Fig.4-4). One of them in CRD domain was required for binding to phosphatidylserin (PS) (Hekman et al., 2002; Improta-Brears et al., 1999), the other one was crucial for binding to phosphatidic acid (PA) in CR3 (Hekman et al., 2002) (Rizzo et al., 2000). We generated the A-RAF point mutants in the sites, corresponding to PS and PA binding in C-RAF. Previously published data by Fabian at all, 1994, showed that conserved R89 located in RBD of all RAF isoforms was crucial for the binding of C-RAF to RAS on the plasma membrane. Since the membrane localization pattern of A-RAF, as well as of its minimal N-terminal mutant AR149, may be mediated by protein-protein interactions with yeast RAS protein family members, a point mutation converting R to L at position 52 in A-RAF was introduced. The microscopy examination of cells expressing this mutant showed, that in both A-RAF_R52L and AR149_R52L the membrane association was destroyed (Fig.4-6A).

Figure 4-6. *Effect of specific point mutations on RAF membrane localization.* **

A. *A point mutation in the RAS binding domain, which is crusial for RAS-RAF interaction, disturb the membrane assotiation of AR149 and A-RAF.*
Basic residue in the RAS binding domain (R52) was replaced with leucine and subcellular distribution of mutant GFP fusion protein was inspected by microscopy. Arginine at position 52 (R52) has replaced by leucine, and the subcellular didtribution of the mutant GFP fusion proteins was inspected. R52L mutation, dislocated AR149 and A-RAF to the cytosol, with rare punctuate spots (indicated by arrow) in the case of full length A-RAF.

B. *Mutations in two presumable lipid binding domains mimic the distribution of the C- and N- terminal deletion mutants.*
Replacement of R359 and K360 with alanine in the C-terminal lipid binding domain (corresponding to the phosphatidic acid binding domain of C-RAF) results in a subcellular distribution that recembles the distribution of the deletion mutants, which lost this domain (for ex. AR149) (left). Mutation of R103 and K104 in CRD (corresponding to PS binding domain of C-RAF) fully dislocated the protein into the cytosol with typical rare punctuate spots, indicated by arrows.
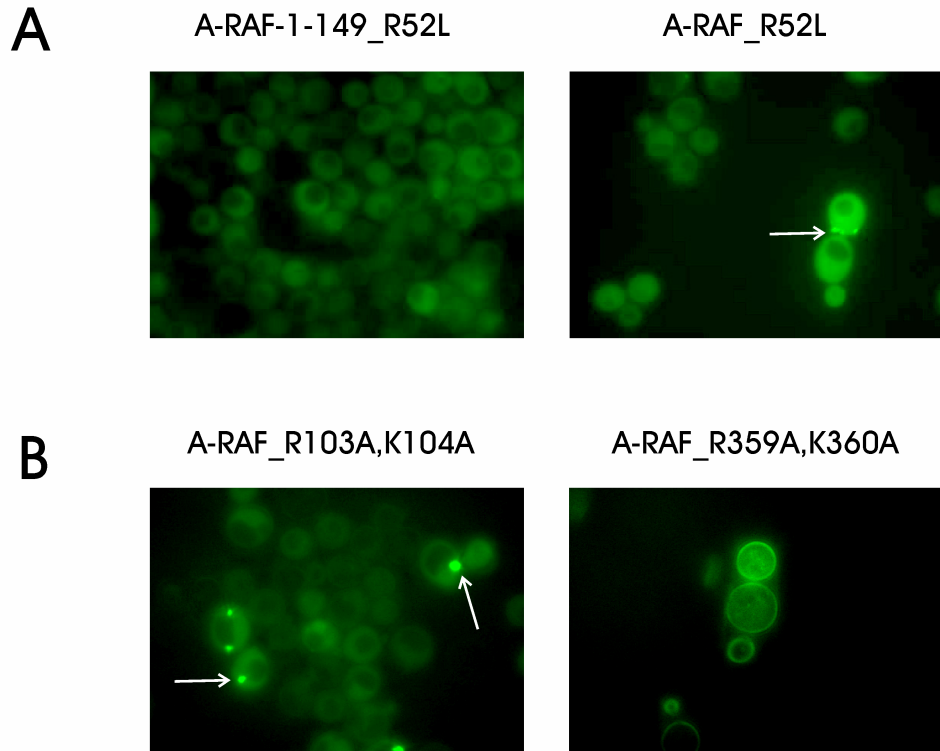
The substitution of the key basic residues of these lipid binding sites to alanine mimics the deletion of the C- or N-terminus respectively. Thus, A-RAF with a mutated PS binding site showed homogenously cytosolic distribution with some rare spots. Correspondingly, A-RAF with mutated PA lipid binding sites, showed homogenous distribution on the plasma membrane (Fig.4-6B). Taken together, two lipid binding sites, PS/ PtdIns(4,5)P$_2$ and PA, were responsible for the GFP-A-RAF punctuate pattern in S. cerevisiae.

4.1.4 AR149 expression inhibits yeast cell polarisation, actin polymerisation, cell growth and endocytosis

During the analysis of the A-RAF deletion mutants we noticed, that expression of several C-terminally truncated mutants changed the cell shape from oval to round and about 20% of the cells expressing AR149 became bigger in size. We focused our attention on the minimal N-terminal deletion mutant, called AR149, and analyzed the effects of its expression in S. cerevisiae.

The changing of the cell shape by yeast, so called cellular polarisation, is a fundamental process during the life cycle of yeast. Polarisation is associated with actin polymerisation and the subsequent pronounced change in cell morphology. Actin polymerization/depolymerisation events are essential for cell division, mating reaction and membrane trafficking. The polymerized actin, so called cortical actin, can be visualized by incorporation of rodamine labelled phalloidin.

The staining of cortical actin in the yeast cells which expressed A-RAF or AR149 brought two significant findings:

a) A-RAF containing patches did not co-localize with cortical actin (Fig. 4-7A, left)

b) the fraction of big round cells, that expressed high levels of GFP-AR149, was not stained by rodamin-phalloidin (Fig. 4-7A, right), which indicates that these cells did not contain polymerised actin.

Next, we asked whether other actin-dependent processes are affected in AR149 expressing cells too. The pheromone induced mating reaction, expressed in so called schmoo formation, is a process in yeast that depends on actin polymerisation. Schmoo formation is characterized by the transition from oval cell shape to pear-shaped cell. The big round GFP-AR149 expressing cells did not show a mating reaction after α- factor stimulation, like control cells (Fig.4-7B).

The actin dynamic is known to be essential for membrane invagination, endosome formation and following vesicle transport and vacuole fusion in yeast (Girao et al., 2008). Therefore, we proposed to test the endocytosis in the cells expressing AR149. For this aim the FM4-64 uptake assay was employed. FM4-64 is a lipophilic styryl dye, which is taken up by yeast cells via the endocytic pathway. In this assay it is possible to follow endocytotic processes from the plasma membrane to the vacuolar membrane, a process which is completed within 20min. The non transformed cells and cells, expressing GFP-A-RAF and GFP-AR149, were incubated with FM4-64 for 5 min on the ice to internalize the dye into the plasma membrane. Then, the cells were washed, resuspended in the medium and incubated at 30ºC for indicated time. The microscopy examination of the control cells and cells expressing GFP-A-RAF showed the standard distribution of visualized vesicles stepwise at 2 min to the plasma membrane (Fig. 4-7D, upper panel), at 6 min to internalized endosomes (Fig. 4-7D, middle panel), and at 20 min at the vacuolar membrane (Fig. 4-7D, bottom panel). In the cells, expressing GFP-AR149, FM4-64 visualized the few conglomerated spots. The huge round cell on 20 min depicted no FM4-64 fluorescent signal whereas its neighbouring small round cell contained only one big conglomerate of enocytosed FM4-64 (Fig. 4-7, middle column). These results suggested that yeast expressing GFP-AR149, but not GFP-A-RAF, were affected in endocytosis.
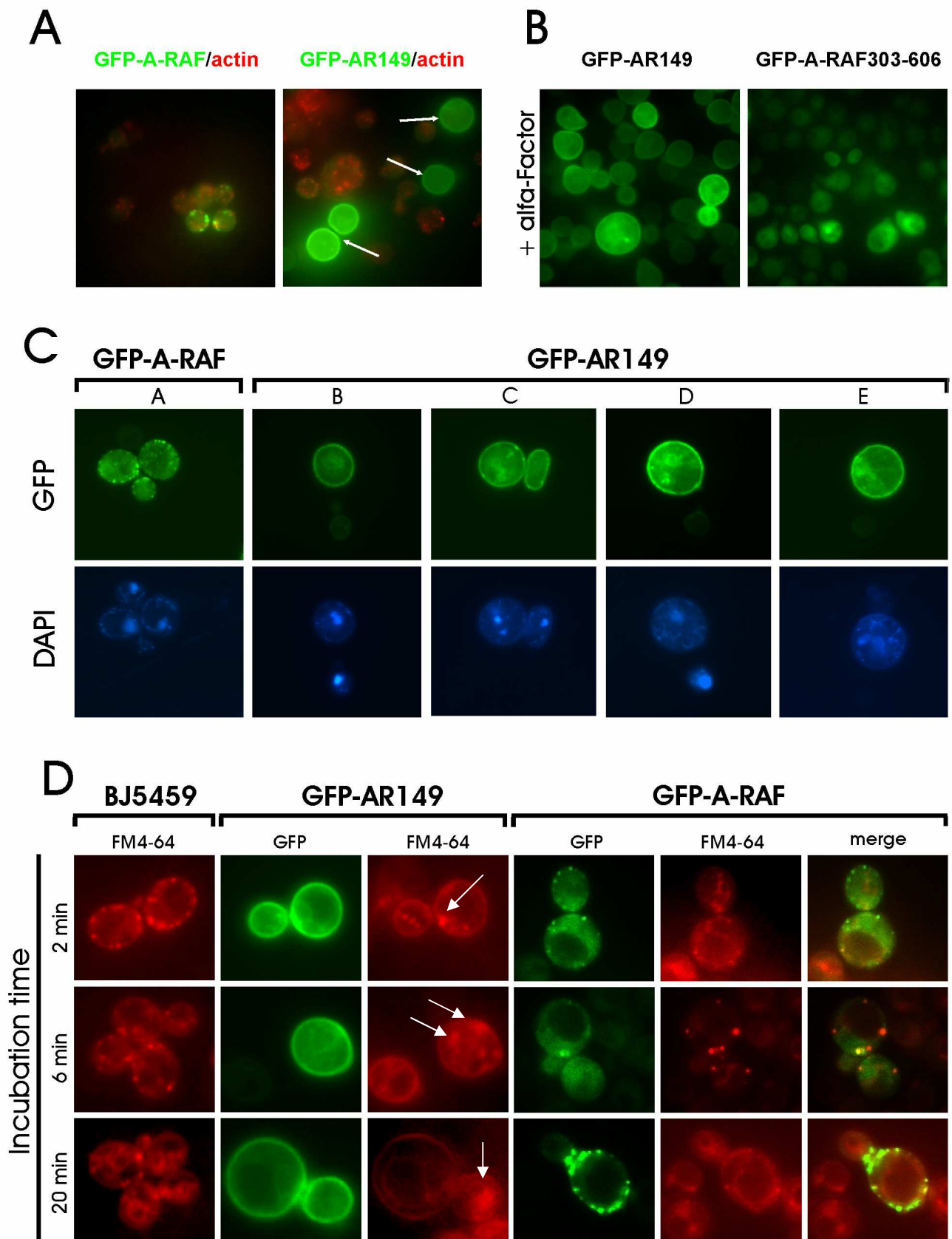
Figure 4-7. *AR149 expression causes defects in yeast physiology.* **

A. *Cells expressing high amounts of GFP-AR149 do not form cortical actin.*
Cells expressing GFP-A-RAF or GFP-AR149 were grown and fixed as described in Chapter 3.4.1. Polymerized actin was visualized by Alexa Fluor 546-conjugated Phalloidin. Note that cells expressing

higher levels of GFP-AR149 but not of full length A-RAF (bright green cells marked with arrows) lost cortical actin pathes.

B. *GFP-AR149 expression inhibits ∝-factor induced shmoo formation.*
Cells transformed with pUG36-AR149 (right) or A-RAF(303-606) (left) were treated with ∝-factor for 2h. Note increased overall size and absence of shmoos in cells expressing GFP-AR149

C. *GFP-AR149 expressing cells have nuclear abnormalities.*
DNA of the nucleus and mitochondria was stained with DAPI. Morphology of nuclei of AR149 expressors varied from fragmented (b) to completely dispersed (e).

D. *FM-4-64 uptake is affected in AR149-expressing yeast.*
Yeast transformed with pUG36-AR149, pUG36-A-RAF and an untransformed control were incubated with lipophilic styryl dye FM4-64 for 5 min on ice, washed, resuspended in medium and incubated by 30ºC for indicated periods. Then the cells were immediately subjected to life cell imaging. Transition of the red fluorescence from periplasmic endocytic sites to vacuoles is clearly visible at 20 minutes in control untranformed cells as well as in cells expressing GFP-A-RAF. In contrast, GFP-AR149 expressing cells show foulty endocytosis. At each time point the FM4-64 dye labels conglomerated membrane structures. (indicated by arrows).

The analysis of nuclear morphology by DAPI staining in the fraction of large apolar cells showed a number of changes which ranged from fragmented nuclei (Fig.4-7C, b) to fully dispersed DNA (Fig.4-7C, e). The viability test showed that about 20% of the cells did not survive after induction of GFP-AR149 under *MET25* promoter (mild conditions). This is in agreement with the number of large apolar cells. To analyse the effect of AR149 expression on cell cycle progression cells were first incubated under promoter repression condition (SD(ura-) medium). After dilution to the same optic density, protein production was induced by culturing the cells in medium lacking metheonine, SD (ura-met-) medium. Cell growth was monitored by determination of optic density at different time points after culture media replacement. The cells expressing GFP-AR149 grew slower compared to cells that expressed GFP or GFP-A-RAF (difference in duplication time about 28 min) (Fig.4-8A). In conclusion, AR149 expression caused sustained cell growth inhibition in yeast. Next we asked whether higher expression levels of the AR149 mutant would lead to a more severe phenotype. For this aim we expressed proteins as GST fusions under control of the strongly inducible *GAL1* promoter. As demonstrated in Fig. 4- 8B, cells transformed with either GST, GST-A-RAF or GST-AR149, grew expressing constructs well on repressive medium (with glucose as hydrogen sores). After induction of protein production (with galactose as hydrogen sores) GST-AR149 expressing yeast cells did not grow (Fig.4- 8B).

In summary, these experiments identified the minimal N-terminal A-RAF mutant (AR149), which localised homogenously to the plasma membrane in S. cerevisiae. The following analysis of AR149 expression showed that AR149, but not A-RAF, blocks yeast cell polarisation, actin polymerisation and endocytosis, which lead to cell growth inhibition.

An independent work from Yokoyama et al. (2007) discovered two C-terminal truncated splicing isoforms for A-RAF, called DA-RAF1 and DA-RAF2 in mammalian cells. One of them, DA-RAF 2, was nearly identical to our minimal N-terminal A-RAF mutant, AR149.

**Figure 4-8.** *AR149 causes lethal phenotype in yeasts.* **

A. *Growth inhibition of AR149 expressing cells.*

Cells transformed with pUG36, pUG36-A-RAF or pUG36-AR149 were grown under selective conditions in fresh selective medium. Cell proliferation was monitored by spectrophotometry.

B. *Lethality of GST-AR149.*

S.cerevisiae strain BJ 5459 was transformed with pEG-KT vehicle, pEG-A-RAF and pEG-AR149. Obtained colonies were streaked on uracil-dropout medium with glucose or galactose. Induction of protein production by galactose was lethal for GST-AR149 expressing cells, but not for these expressing either empty vehicle or full-length A-RAF.

Both experiments were performed in cooperation with PhD S. Albert (University of Wuerzburg).
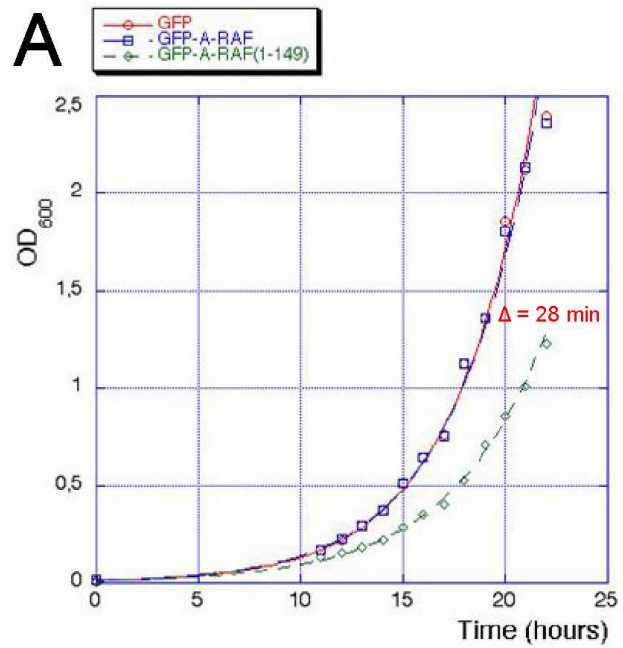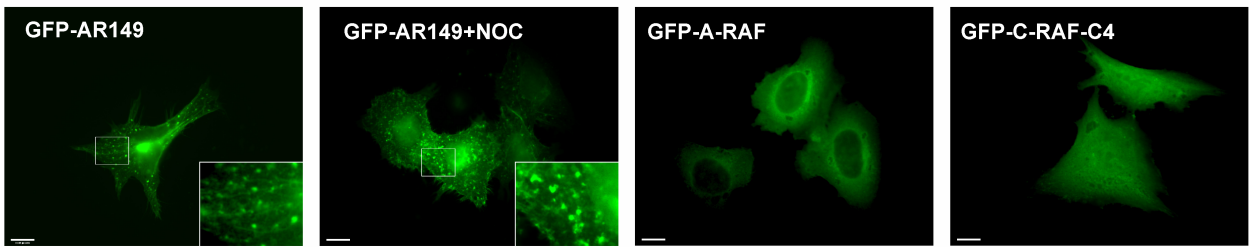
4.2 Study of A-RAF isoforms properties in mammalian cell lines

4.2.1 AR149 and A-RAF intracellular distribution in mammalian cells

The intrinsic strong phenotype of AR149 expressed yeast cells inspired to analyze the role of AR149 in membrane associated processes in mammalian cells. The first logical step was to investigate the subcellular localization of AR149 and A-RAF. HeLa cells were transiently transfected with GFP-AR149 and GFP-A-RAF encoding mammalian expression vectors. As controls GFP alone and a C-RAF N-terminal mutant, called RAF-C4 (Bruder et al., 1992), that corresponds to AR149, were used. As expected from yeast experiments, only GFP-AR149 was localized to the plasma membrane. Surprisingly, GFP-AR149 decorated also intracellular membrane structures, stretching through the cell body from the pericentriolar area to the plasma membrane. These structures were defined as "beads on a string" (Fischer et al., 2009) (Fig.4-11A). After nocodazole treatment, which caused depolymerisation of microtubules, these organised structures were destroyed (Fig.4-9A). In contrast to AR149, GFP-A-RAF and GFP-C-RAF-C4 showed nearly homogenous distribution in the cytoplasm (Fig.4-9A). The observed subcellular distribution of GFP-AR149 was not cell type specific since similar distribution was observed in the mouse fibroblast cell line NIH 3T3, albeit without the pronounced tubular "beads on a string" structures (Fig. 4-10). These vesicular tubular structures most likely represented the recycling endosome compartment, which is known to be extended in HeLa cells (Robertson et al., 2006). One of the established markers for recycling endosomes is the ARF6 GTPase. Previous work by D'Souza-Schorey et al., 1995, showed, that ARF6 localizes to plasma membrane in its active state (GTP-bound) and to recycling endosomes in the inactive state (GDP-bound). During the changes in its state through regulatory proteins, GAPs or GEFs, ARF6 move from the plasma membrane to the recycling compartment and back thereby regulating membrane trafficking (see (D'Souza-Schorey and Chavrier, 2006) for review). The overexpression of ARF6 GTP-locked (Q67L), GDP-locked (T27N) or nucleotide-free (N121I) mutant forms different effects on the endocytic process (Robertson et al., 2006).

Based on these data we hypothesized, that AR149 could be localized to ARF6-positive recycling compartments. To test this hypothesis co localization experiments were performed. To this end AR149 and A-RAF were fused to RFP. Microscopic analysis of HeLa cells overexpressing RFP-AR149 confirmed the GFP-AR149 distribution. The full length RFP-tagged A-RAF could not be detected under these conditions, possibly because of aberrant folding of the fusion protein. The same phenomenon was observed when we tried to express mCherry tagged A-RAF in yeast.Therefore, we used indirect immunfluorescence technique for detection of overexpressed Myc-tagged A-RAF.
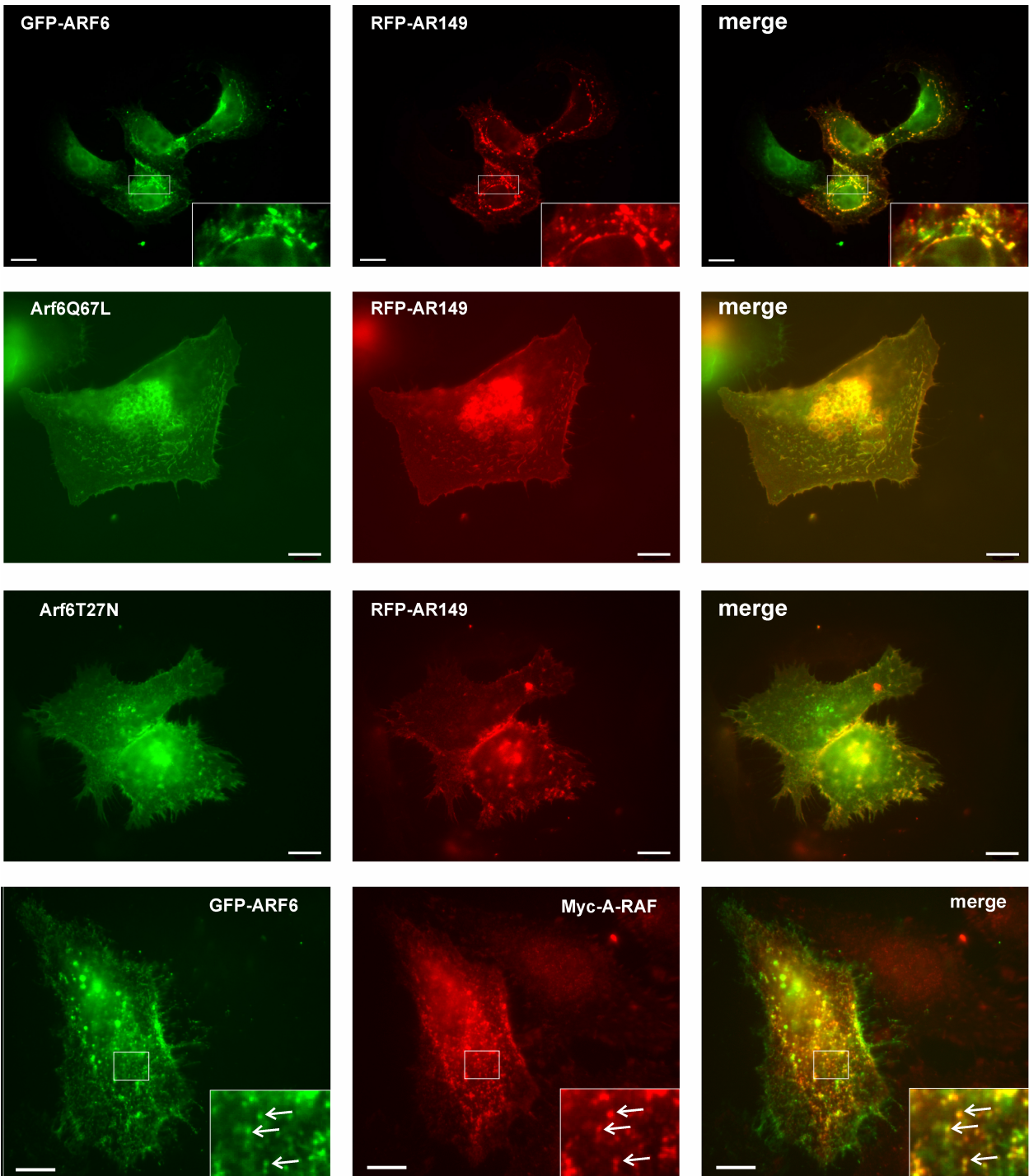
A

GFP-AR149

GFP-AR149+NOC

GFP-A-RAF

GFP-C-RAF-C4

B

GFP-ARF6

RFP-AR149

merge

Arf6Q67L

RFP-AR149

merge

Arf6T27N

RFP-AR149

merge

GFP-ARF6

Myc-A-RAF

merge

Figure 4-9. *Localization of GFP-A-RAF and GFP-AR149 in mammalian cells. ***

A. *AR149 localizes to the tubular vesicular endosomes.* HeLa cells were transiently transfected with pEGFP bearing the indicated genes for 2 days. GFP fusion proteins were detected by fluorescence microscopy. GFP-A-RAF is present throughout the cytoplasm and accumulates around the nucleus. In contrast, GFP-AR149 labels punctate structures often aligned on strings. Strings were disassembled by treatment with Nocodazole. A C-RAF fragment orthologous to AR149 is GFP-C-RAF(C4).

B. *AR149 and A-RAF colocalizes with ARF6 independently from its GTP·GDP- loading state·in HeLa cells.* HeLa cells were cotransfected with RFP-AR149 and GFP-ARF6 as described above. RFP and GFP fluorescences were recorded separately. RFP-AR149 was cotransfected with GFP-ARF6, dominant active GFP-ARF6(Q67L) or dominant negative GFP-ARF6(T27N) and inspected by fluorescent microscopy. High degree of colocalization with both ARF6 mutants is documented in overlay figures.

A large fraction of exogenously expressed A-RAF distributed homogenously in the cytoplasm. To visualize the membrane associated fraction of A-RAF, depletion of the cytosol was achieved through digitonin permeabilisation as previously described by Galmiche et al., 2008 . Colocalization experiments with GFP-ARF6 and RFP-AR149 showed that both proteins were localized to the same tubular vesicular compartment. A small portion of proteins was localized to the plasma membrane (Fig. 4-9B, upper panel). This pattern led us to propose that AR149 could be able to shift ARF6 from plasma membrane (GTP-loaded state) to recycling endosomes (GDP-loaded state). We hypothesized that AR149 has a dominant negative effect on ARF6 activity.

Two ARF6 nucleotide loading mutants GFP-ARF6_Q67L and GFP-ARF6_T27N (see above) were generated and included in the colocalization analysis. As demonstrated in Fig.4-9B, middle panels, RFP-AR149 colocalized with both GFP-ARF6_Q67L and GFP-ARF6_T27N on different subcellular compartments. The active GFP-ARF6_Q67L mutant localized to the plasma membrane. Typically, microvilli formation and macropinocytotic vesicles were observed under these conditions. In the case of GDP-locked ARF6 mutant (T27N), RFP-AR149 colocalized with ARF6_T27N on intracellular vesicles. In conclusion, RFP-AR149 was found to localize into the ARF6-positive membrane compartments, independent from ARF6 nucleotide loading state.

Analysis of the Myc-A-RAF distribution pattern showed that membrane-bound Myc-A-RAF colocalized with ARF6 on the plasma membrane and intracellular vesicles (Fig.4-9B, lower pannel).

In summary, AR149 and A-RAF localized to ARF6-positive membrane compartments, such as the tubular vesicular endosomes and the plasma membrane.

4.2.2. Reduction of stress fiber formation by AR149 in NIH3T3 cells

One of the dramatic effects of high AR149 expression on yeast cell morphology was the fully depolymerised actin. To investigate this effect of AR149 on actin polymerisation in mammalian cells the mouse fibroblast cell line NIH 3T3 which shows well-developed actin stress fibers was employed.

In this cell line overexpressed GFP-AR149 caused reduction of stress fibers labelled with Alexa-546 tagged phalloidin (Fig.4-10). This result is in agreement with results obtained by Yokoyama et al. (2007).
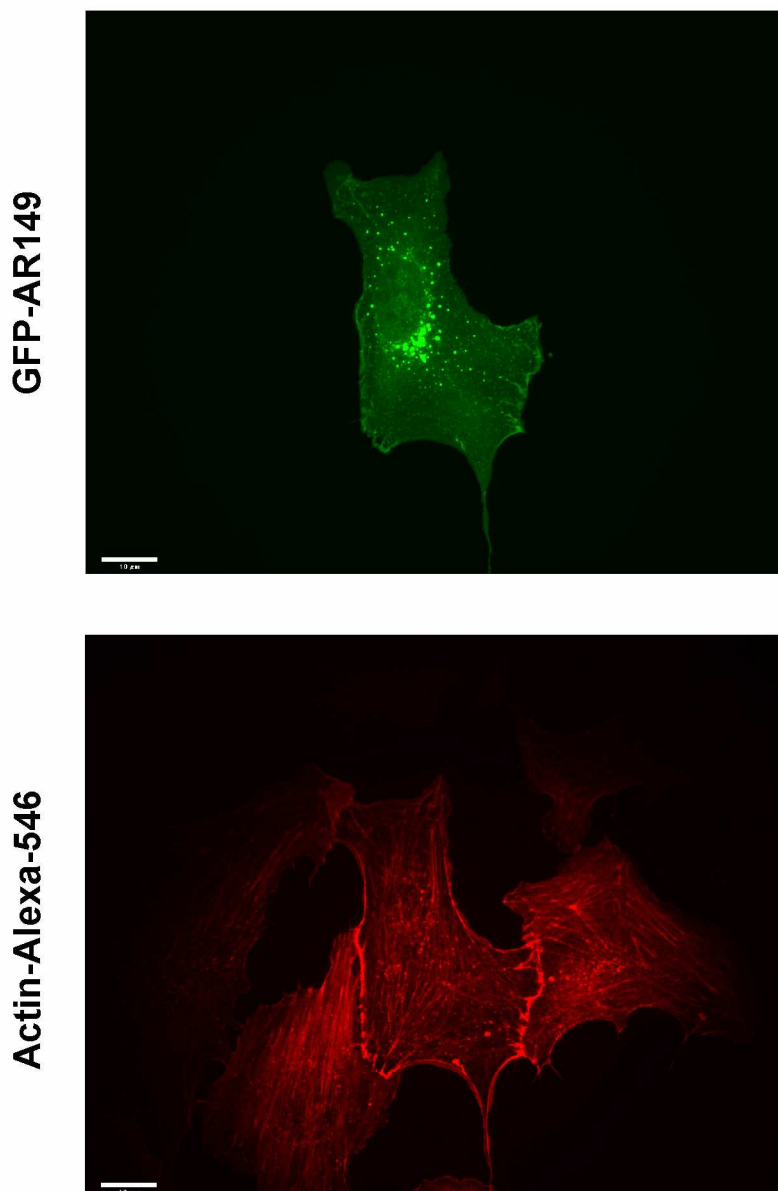

Figure 4-10. *AR149 expression reduses stress fibers formation in NIH 3T3 cells.* ******
NIH 3T3 cells were transfected with GFP-AR149 for 24 hours. After fixation, the polymerized actin was visualized with Alexa-546 conjugated phalloidin. Note the remarkable regression of actin stress fibers in the transfected cell.

4.2.3   Localization of endogenous membrane-bound A-RAF to microtubule-associated vesicles
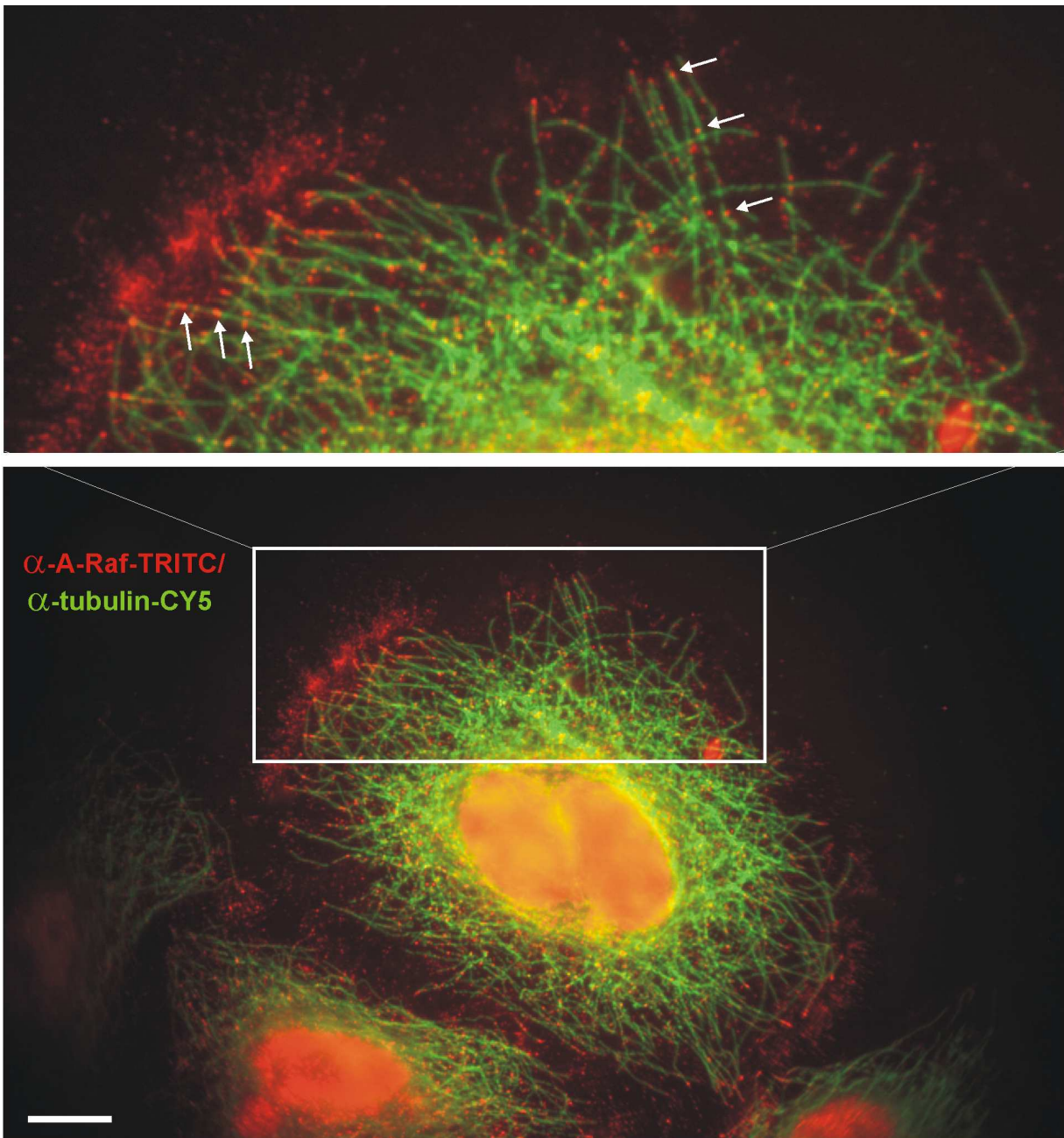
Apart from new data about cellular distribution of overexpressed A-RAF isoforms (Chapter 4.2.1), we proposed that at least a part of endogenous A-RAF should be localized to endosomes. To detect this we developed a new protocol for A-RAF labelling with α-A-RAF rabbit antibody (SantaCruz). Three optimizing factors were induced into standard protocol:

1)   digitonin extraction of cytosol fraction of A-RAF, allowed to detect only membrane-bound A-RAF;

2)   cell permeabilization with mild detergent – saponin, instead of TX-100, which permitted to preserve sensitive lipid structures like endosomes;

3)   all steps, except digitonin extraction, were carried out in microtubule-stabilizing buffer, which allowed to label unaffected microtubule network.

Due to this special protocol we were able to detect endogenous A-RAF on vesicular structures, which were found to associate with the microtubule network. As demonstrated in Fig.4-11A, A-RAF-positive vesicles localized to the cell periphery of the periplasmic area and to nearly each plus end of microtubule. Additionaly, these vesicles were lining microtubules to the perinuclear area. To confirm the specificity of the A-RAF antibody, the following controls were performed. First, cells with siRNA mediated abrogation of A-RAF were subjected to the staining conditions used to detect A-RAF-positive vesicles. Second, unspecific normal rabbit antibody, instead of the A-RAF antibody, was used in the analysis. Both approaches resulted in the loss of the punctuate/ vesicular staining while nuclear staining could still observed (Fig.15C). Therefore, we concluded that labelling of nuclei by A-RAF antibody was unspecific.

The fluorescent microscopy data were supported by biochemical fractionation. Thus, a big portion of GFP-AR149 and GFP-A-RAF was found in the cytoskeleton fraction (Fig.4-11B).

Taken together, endogenous A-RAF localises to endosomal vesicles, associated with the cytoskeleton.

α-A-Raf-TRITC/
α-tubulin-CY5

A

B

	cytosol	pl.membrane	nucleus	cytoskeleton
GFP-AR149				
GFP-A-RAF				
α-2MPK				
α-KDEL				
α-PARP				
α-vimentin				

Figure 4-11. *A-RAF associates with the cytoskeleton.* **

A. *Endogenous A-RAF localizes to vesicles along microtubules.* HeLa cells were treated with digitonin to extract cytosol. After fixation and washing, immunofluorescence microscopy with antibodies against A-RAF and β-tubulin was carried out. Small A-RAF positive vesicles are located at the periphery and line microtubules (indicated by arrows).
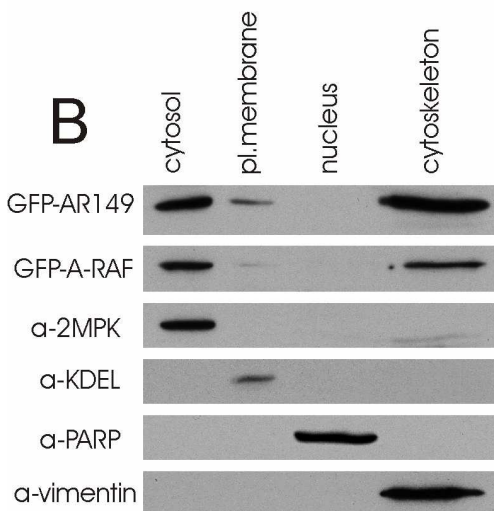
B. *AR149 and A-RAF are enriched in the cytoskeleton fraction.* Cells were fractionated using "ProteoExtract Subcellular Proteome Extraction Kit" (Calbiochem) and analyzed by immunoblotting. Antibodies against following proteins were used as compartmental markers: vimentin as cytoskeletal marker, PARP as nuclear marker, 2MPK as cytosolic marker. Both A-RAF and AR149 are co-fractionating predominantly with cytoskeleton and cytosol. A small portion of AR149 was also found in plasma membrane fraction.

4.2.4 Overexpression of AR149 in HeLa cells inhibits transferrin trafficking on the level of recycling compartments.

The data so far pointed to a possible role of AR149 in endocytosis in mammalian cells. To address this question transferrin (Tfn) uptake as an assay for endocytosis was performed. The Tfn uptake assay was chose due to the following advantages:

1)   it is well established

2)   it is considered as classical model for the study of clathrin-dependent endocytosis;

3)   Tfn trafficking is known to be accomplished by an ARF6-dependent mechanism.

Tfn is an iron binding protein participating in iron homeostasis, which is internalized upon binding to its receptor via a clathrin-dependent pathway. Subsequently, Tfn is transmitted to the recycling compartments in the pericentriolar area and is recycled back to the plasma membrane.

First, uptake and recycling of Transferrin (Tfn) was analysed. To this end, Hela cells were transfected with GFP alone, as a control, and GFP-AR149. After 1 hour under starvation conditions, the cells were incubated in medium, contaning Alexa546-tagged Tfn, for the indicated periods (Fig.4-12).

In concordance with published data, Tfn accumulated in the pericentriolar area after 30 min in control cells (Fig. 4-12, upper panel). On the contrary, enrichment of internalized Tfn in the pericentriolar area was vastly delayed in AR149 expressing cells (Fig.4-12, bottom panel), though Tfn internalisation was not impaired. This resulted in cells that were crowded with Tfn, which was distributed through out the cytoplasm and was strongly colocalized with AR149 positive vesicles. In conclusion, internalized Tfn was trapped in AR149 containing endosomes. To better understand in which endosomal compartment Tfn trafficking is blocked, we performed a triple colocalization experiment with early (EEA1) and recycling (ARF6 and RAB11) endosomal markers. Thus, we observed significant signal overlap of RFP-A149, Alexa647-Tfn and GFP-ARF6 as well as GFP-RAB11 at different time points (Fig. 4-13). In contrast, under the same conditions no significant colocalization was detected with GFP-EEA1 (Fig. 4-14).

In summary, AR149 expressing cells did not show defects in Tfn internalization and assignment to tubular vesicular recycling endosomes. At this level the transfer of Tfn to the TGN- associated recycling compartment was significantly blocked.
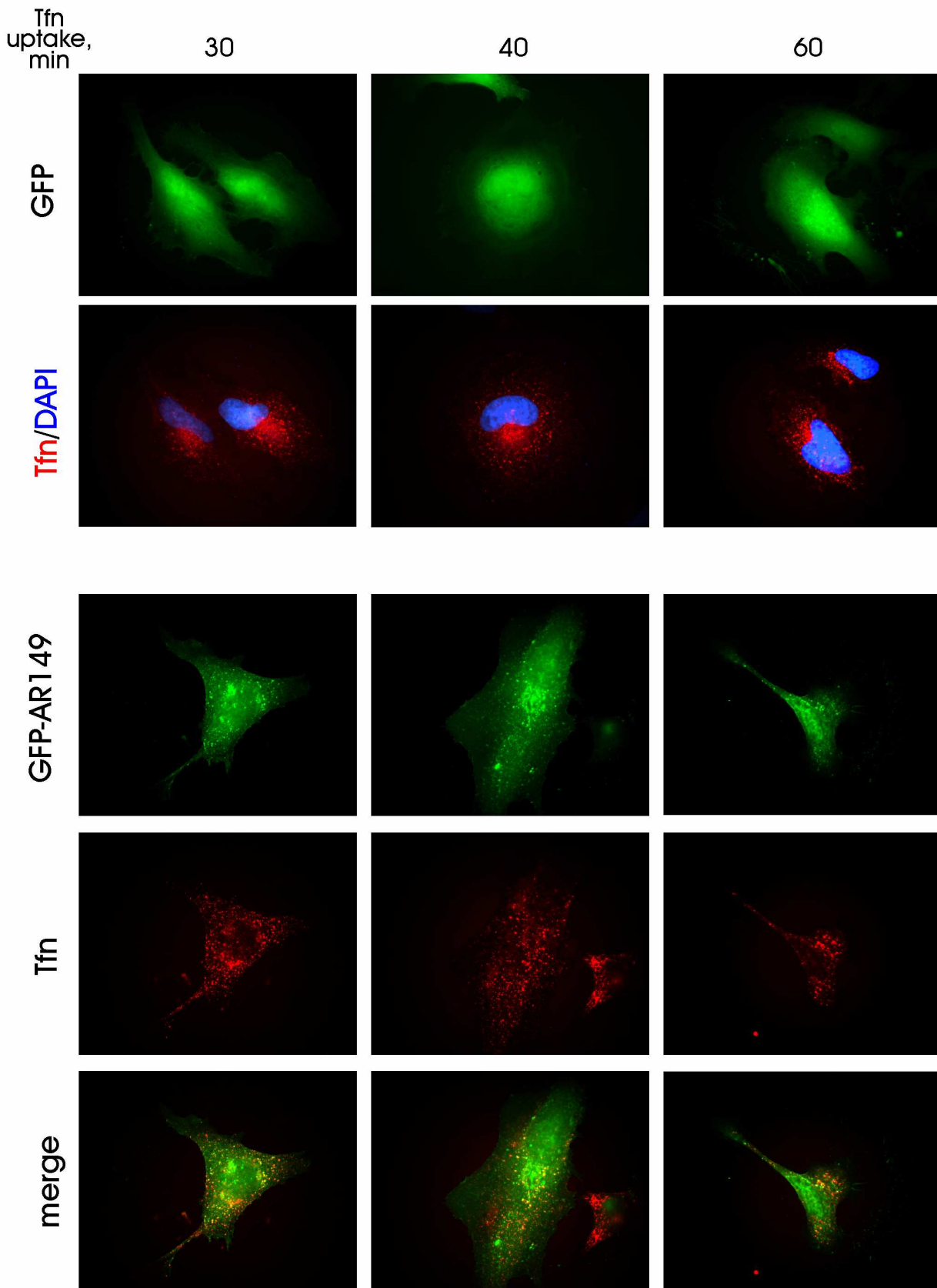
Figure 4-12. *Expression of GFP-AR149 blocks trafficking of Tfn to the pericentriolar endosome compartment.* **

GFP-AR149-transfected and control (GFP-transfected) cells were incubated with fluorescent Tfn for indicated times. Tfn containing vesicles accumulate in the pericentriolar area of control cells, but remain in the GFP-AR149 positive vesicles scattered throughout the cytosol of GFP-AR149 transfected cells.
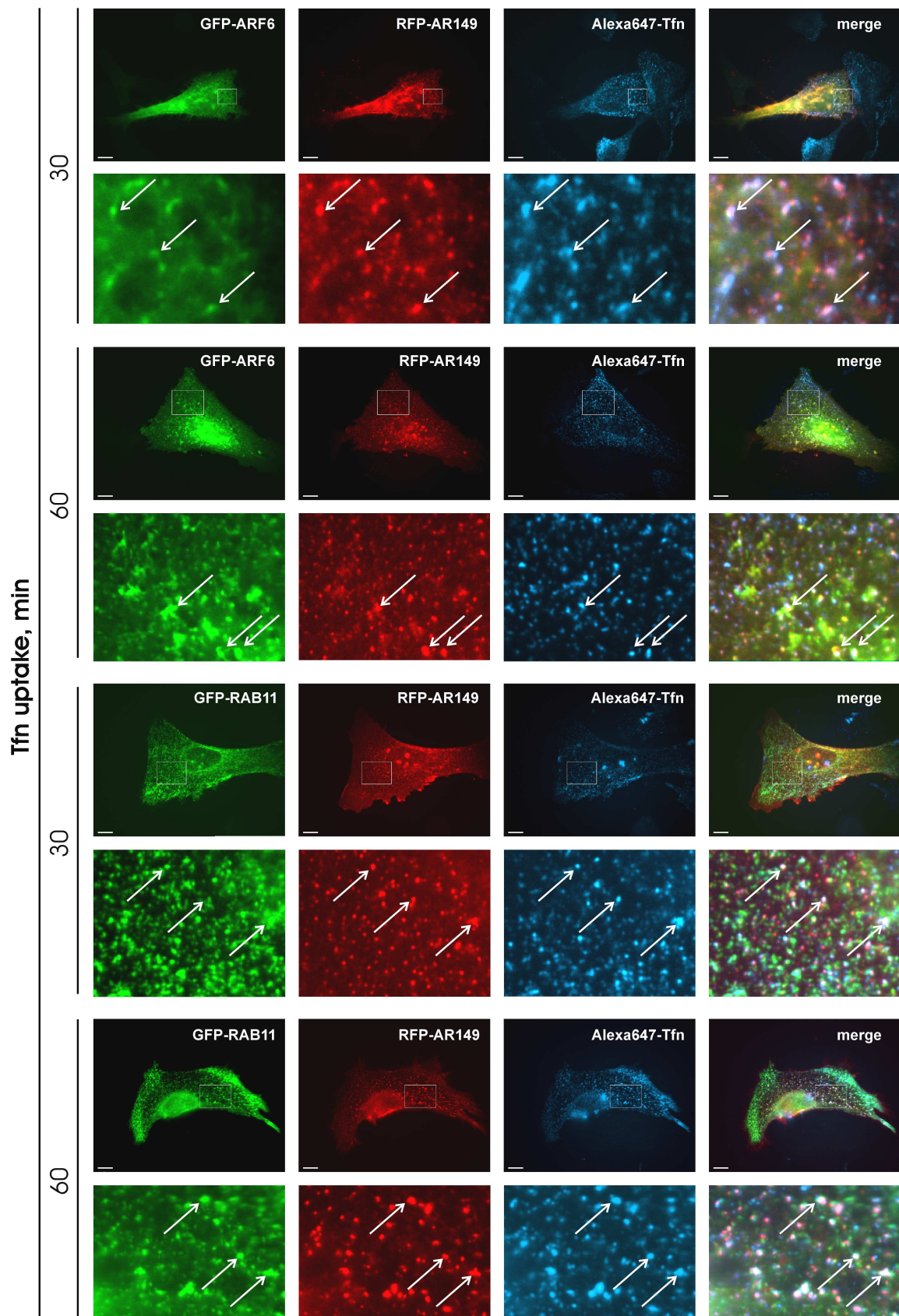
Figure 4-13. *AR149 causes accumulation of inernalized transferrin in ARF6 and RAB11 positive endosomes.* **

HeLa cells were transfected with RFP-AR149 and either GFP-ARF6 or RAB11 as indicated. Uptake of fluorescent Tfn was examined after 30 and 60 minutes. Representative images show that Tfn is trapped by AR149 in GFP-ARF6 positive and in GFP-RAB11 positive vesicles. Enlarged areas are marked by boxes. Arrows indicate co-localization. Scale bar = 10 µm.
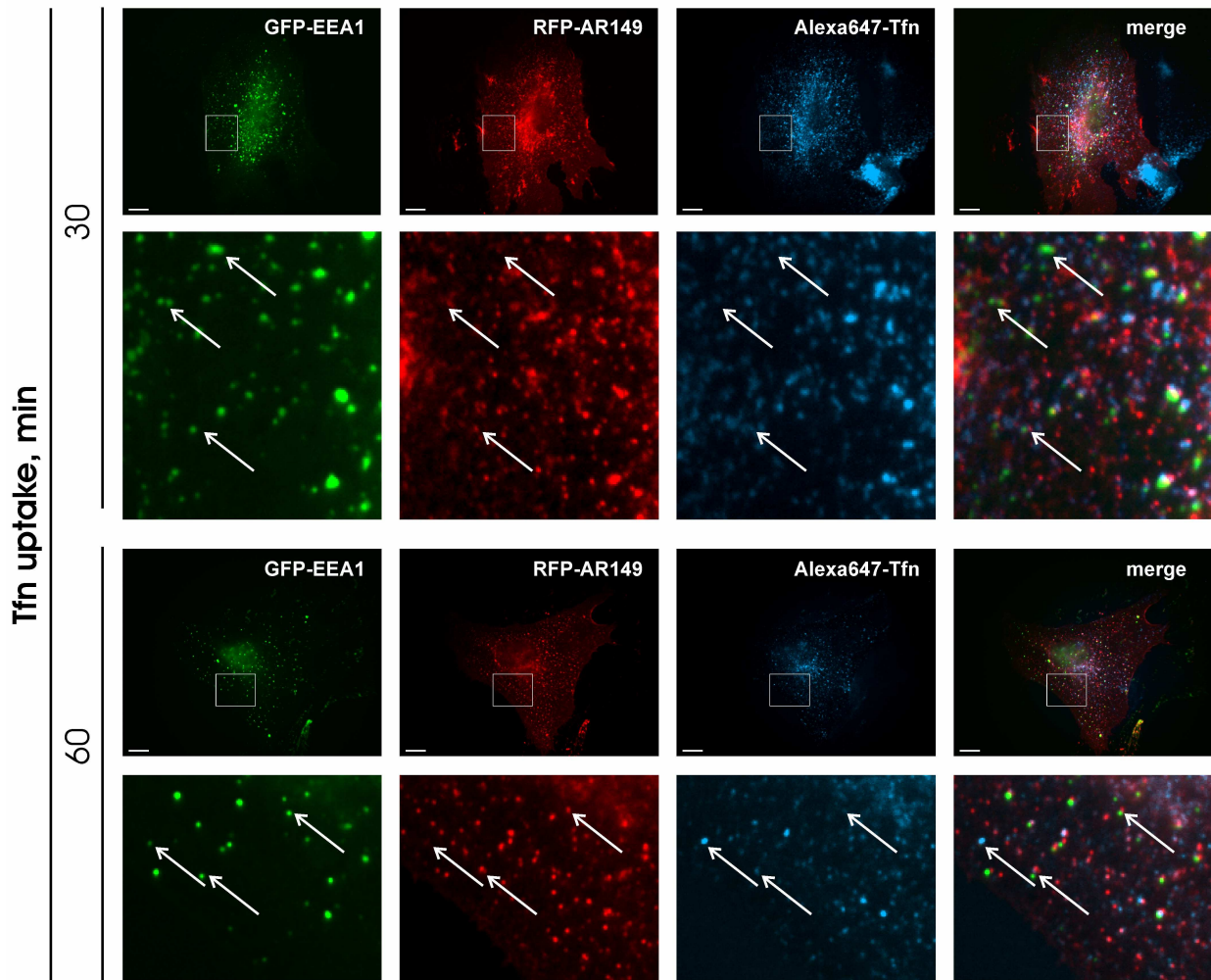
Figure 4-14. *Tfn does not accumulate in EEA1 positive early endosomes in AR149 expressing cells.* **
HeLa cells were transfected as indicated and used for Tfn uptake assays. Note that fluorescence of Tfn and
EEA1 do not mark identical vesicles. Enlarged areas are marked by boxes. Arrows indicate co-localization.
Scale bar = 10 µm.

4.2.5 A-RAF knock down and downstream cascade inhibition phenocopy the effect of AR149 expression on Tfn recycling

A dominant negative effect of the N-terminal part of RAF, such as C-RAF-C4(Bruder et al., 1992) or DA-RAF(Yokoyama et al., 2007), on ERK signalling has previously been described. Since AR149 was identical to DA-RAF2 isoform, we expected that AR149 also exerted a dominant negative effect on the mitogenic cascade. Therefore siRNA mediated depletion of A-RAF was expected to have the same effect as AR149 overexpression. Towards this end HeLa cells were transfected with this A-RAF siRNA and scrambled siRNA as control. The effectivity of A-Raf depletion was first analyzed by Western blot analysis of cell lysates. As documented on Fig. 4-15A, the amount of A-RAF protein was significantly reduced in A-RAF siRNA-treated cells. The expression of C- and B-RAF proteins was not affected.


Figure 4-15. *Specific depletion of A-RAF protein and mRNA by siRNA. ***

A. HeLa cells were treated with A-RAF specific or scrambled siRNA and subjected to Western blot analysis with antibodies against actin (loading control) and three RAF isoforms. A-RAF is the only RAF isoform the amount of which decreased after siRNA treatment.

B. HeLa cells were first treated with two different batches of A-RAF-specific or scrambled siRNA. Afterwards, the RNA was reverse transcribed and used as a template for quantitative PCR with primers specific for A-RAF, DA-RAF2 and Actin mRNAs. The ratio between the tested mRNA and actin mRNA was calculated from the qPCR data. From the diagram it can be concluded that A-RAF mRNA amount is decreasing significantly. DA-RAF2 mRNA was poorly expressed in these cells and its expression level did not change upon siRNA treatment. This experiment was performed in cooperation with PhD S. Albert (University of Wuerzburg)

C. *Controls of indirect immunofluorecent staining of endogenous A-RAF.* HeLa cells were incubated with normal rabbit serum (left panel) or with A-RAF specific antibodies after A-RAF knock-down with siRNA (right panel). In both cases periplasmic punctate structures (see Fig. 4-11A) disappeared, whereas nuclear staining remained.
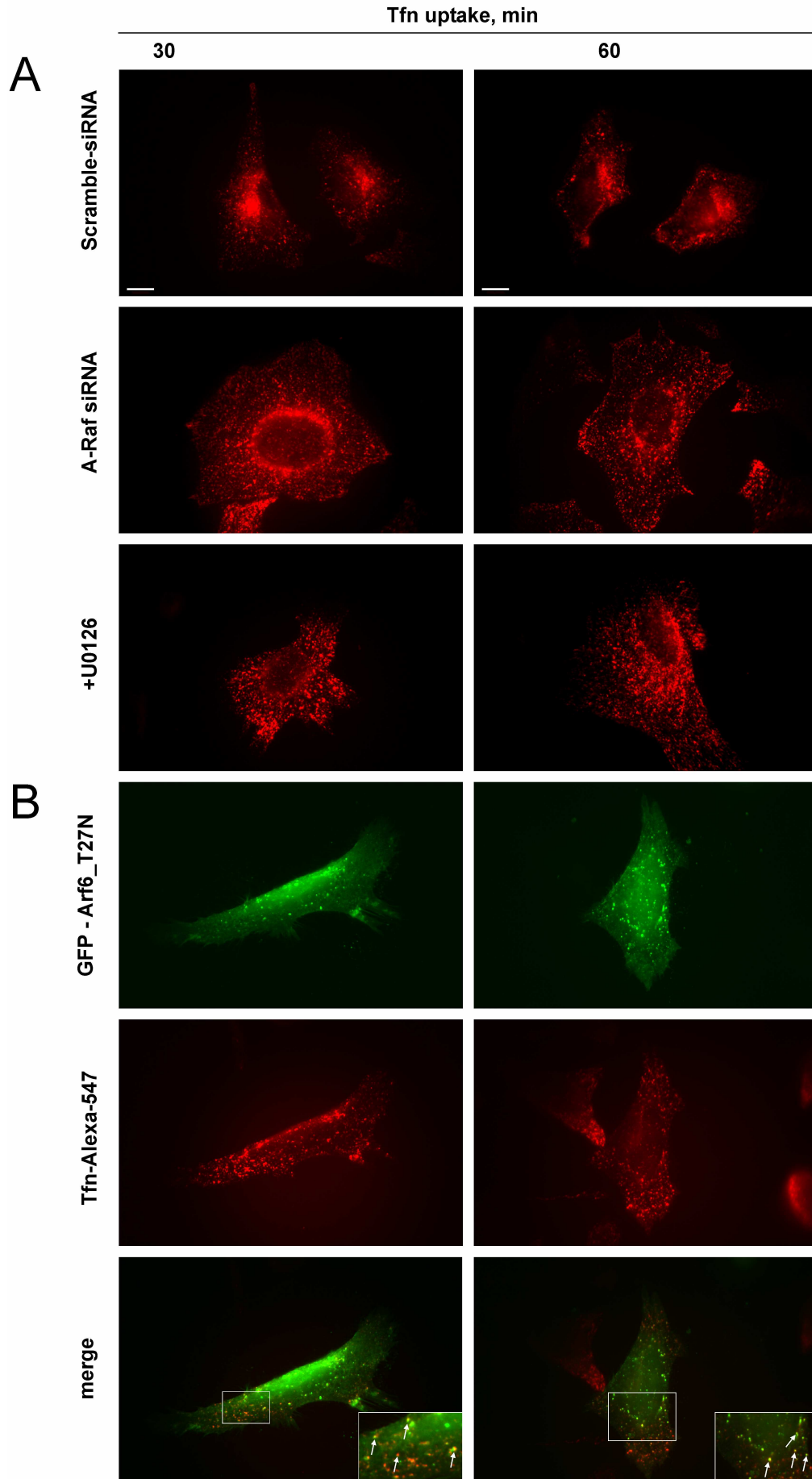
Tfn uptake, min
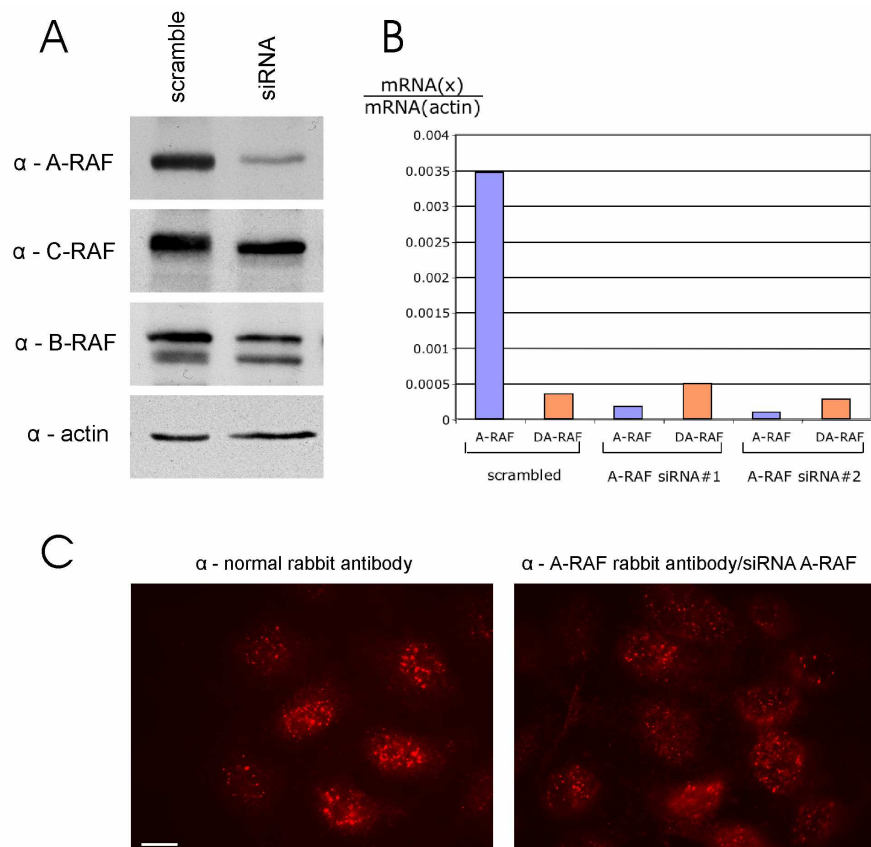
Figure 4-16. *siRNA mediated A-RAF depletion, MEK inhibition and expression of ARF6(T27N) also block accumulation of Tfn in the pericentriolar endosome compartment. ***
A. HeLa cells transfected with A-RAF siRNA, scrambled siRNA or treated with MEK inhibitor UO126 were subjected to Tfn uptake assay. Lack of accumulation of endocytosed Tfn in the pericentriolar compartment is similar to AR149-expressing cells (compare with Figure 4-12). Representative images are shown. Scale bar = 10 µm.
B. HeLa cells were transfected with ARF6(T27N) before assay for fluorescent Tfn uptake. ARF6(T27N) positive vesicles accumulate internalised Tfn. The pattern of distribution is similar to that in A-RAF siRNA and to U0126 treated cells.

Since the target sequences for siRNA silencing was located on the 3'-end of A-RAF and was therefore not present in the DA-RAF sequence, DA-RAF was also not affected as proven by semi-quantitative RT-PCR analysis. (Fig.4-15B). Therefore, with this approach, we achieved highly effective and specific depletion of A-RAF on both, the protein and mRNA level.

To test whether A-RAF silencing had any effect on endocytosis, HeLa cells, treated with A-RAF siRNA or with scrambled siRNA, as a control, were analyzed for Tfn uptake. The data clearly showed that A-RAF depletion resulted in redistribution of internalized Tfn similar to that caused by AR149 overexpression (Fig. 4-16). In conclusion, A-RAF kinase activity is required for normal Tfn trafficking. The chemical inhibition of the RAF down-stream effector – MEK by U0126, delayed the accumulation of Tfn in the pericentriolar area, which closely resembled the effect of siRNA mediated A-RAF silencing (Fig.4-16, middle panel). Of note, in both cases, the accumulated Tfn decorated tubular structures, reaching from the perinuclear area to the cell periphery.

To investigate in which compartment in A-RAF depleted cells is Tfn trapped, A-RAF siRNA treated HeLa cells were analysed for Tfn uptake and subsequently, colocalization of internalized Tfn and ARF-6 and RAB11-positives vesicles was examined (Fig. 4-16). In the case of the early endosome marker, EEA1, no significant overlap with Tfn was detected (Fig.4-18), while Tfn colocalized with ARF6- and RAB11- positive vesicles were detected (Fig. 4-17).

Due to the fact that the phenotypes of A-RAF knock down and inhibition of the mitogenic cascade overlapped, we conclude that localized ERK signalling, driven by A-RAF on the endosomes, is required for endosomal maturation. The splicing isoforms AR149/DA-RAF1,2 work as naturally occurring dominant negative inhibitors of A-RAF activity.

4.2.6 ARF6_T27N, like AR149, traps the internalized Tfn in the recycling compartment

The ARF6 GDP-locked mutant, ARF6_T27N, corresponds to the inactive state of ARF6 has previously been shown to localize to the recycling compartment (D'Souza-Schorey et al., 1998). The effect of ARF6_T27N expression has been described as re-distribution of Tfn receptor and inhibition of Tfn recycling to the plasma membrane (D'Souza-Schorey et al., 1995). If the hypothesis, that

AR149 has a dominant negative effect on ARF6 activity (see chapter 4.2.1) was correct, an effect of ARF6_T27N expression on Tfn trafficking would have been expected.To this end, HeLa cells, expressing GFP-ARF6_T27N, were subjected to the Tfn uptake assay. As documented in the Fig. 4-16B, Tfn accumulation in the pericentriolar area was affected in ARF6_T27N expressing cells. In addition, ARF6_T27N positive vesicles were colocalized with internalized Tfn.

In summary, expression of ARF6_T27N, AR149 and siRNA mediated negative regulation of A-RAF signalling, as well as MEK inhibition, exerted similar effects on Tfn trafficking.

Therefore, these data suggested that ARF6 and A-RAF are involved in the same regulatory step of endosome maturation. However, at this stage of the work, it was not clear, which epistatic relationship exists between A-RAF and ARF6.

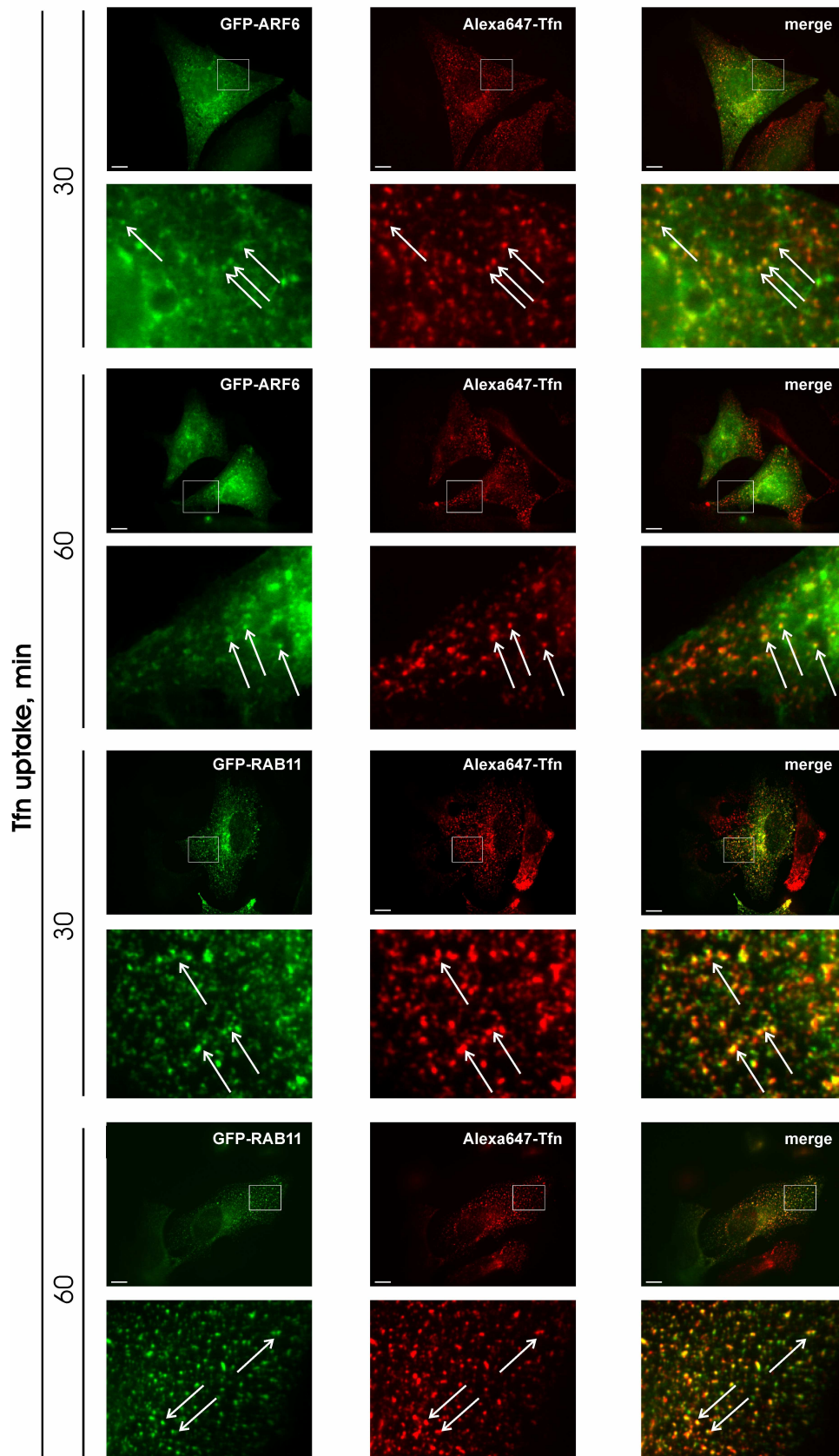**Figure 4-17.** *Tfn accumulates in ARF6 positives, RAB11 positives vesicles after siRNA silencing of A-RAF.* **

HeLa cells were cotransfected with either GFP-ARF6 or GFP-RAB11 and A-RAF siRNA. Tfn uptake was assayed as before. Tfn was found to co-localize with ARF6 or RAB11 as was observed in AR149 expressing cells. Enlarged areas are marked by boxes. Arrows indicate co-localization. Scale bar=10 µm.
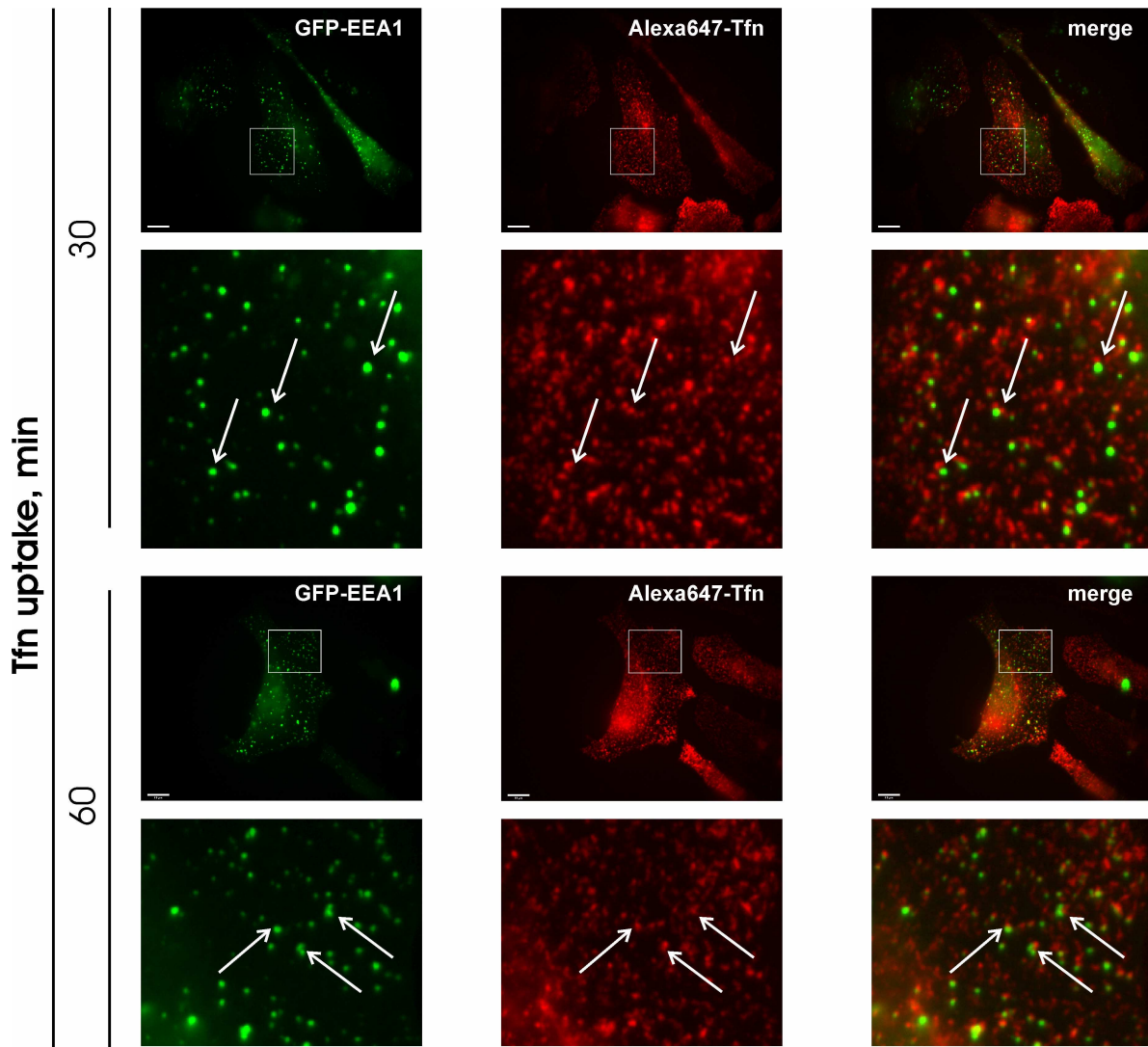
Figure 4-18. *Tfn trafficking is not blocked on the level of early endosomes in cells with abrogated A-RAF expression. ***

HeLa cells were transfected as indicated and used for Tfn uptake assays. Note that fluorescence of Tfn and EEA1 do not mark identical vesicles. Enlarged areas are marked by boxes. Arrows indicate co-localization. Scale bar = 10 µm.

4.2.7 AR149 is complexed with ARF6, independent of the ARF6 nucleotide status

The immunefluorescent experiments, described above (Chapter 4.2.1) showed colocalization of AR149 with ARF6 and its nucleotide locked mutants (Fig.4-9B). Moreover, AR149 had a dominant negative effect on ARF6 cargo trafficking (Fig.4-12). As independent means to verify complex formation of AR149 and ARF6 an immunoprecipitation approach was used. To isolate the putative complex, GFP-AR149 was co-expressed with HA-ARF6, or HA-ARF6_Q67L, or HA-ARF6T27N in COS7 cells respectively. After cell lysis, the cell lysates were divided into two parts and immunoprecipitation was performed in two directions: AR149 was precipitated by α-GFP antibody and co-isolated ARF6 was detected by WB. In parallel, ARF6 was isolated by α -HA antibody precipitation and AR149 was detected by WB. To control the specificity of immunoprecipitation, combinations of the individual expression vectors were performed (Fig.19A, bottom). As shown in Fig. 4-19A, in both direction, AR149 and ARF6 was isolated in one protein complex. As expected from colocalisation experiment, this binding occurred with ARF6 as well as with its GTP- and GDP-locked mutants, ARF6_Q67L and ARF6_T27N respectively. Thus, independent of its nucleotide status, ARF6 was biochemicaly show to be in one protein complex with AR149.

4.2.8 Activation of ARF6 is controlled by opposing function of A-RAF and AR149

Our interpretation of the results described above (4.2.2 and 4.2.4) was that AR149 could have a dominant negative effect on ARF6 activity. To monitore ARF6 activity we made used of the specific interaction of GGA3 (an effector of ARF6) with the active, GTP-loaded, form of ARF6. Based on this property it was possible to use purified GST-tagged GGA3 as bait to pull down ARF6·GTP from cell lysates. First, method was standardized with control probes (Fig.4-19B). Immobilized on GSH-sepharose GST-GGA3 protein was incubated with cell lysates of COS7 cells with ectopical expression of either wild type (wt) ARF6, dominant active ARF6_Q67L or dominant negative ARF6_T27N. WB analysis of the pulled down material showed in Fig. 4-19B. As expected, the dominant active form, ARF6_Q67L, pulled most efficiently, wt ARF6 was pulled less efficiently. The dominant negative form was not pulled at all.

Next, we stimulated starved COS7 cells with EGF, an activator of the mitogenic cascade. Under this condition, an increased amount of ARF6 protein was pulled by GGA3, in comparison to non-stimulated cells (Fig. 4-19C). In contrast, coexpression of AR149 (Fig.4-19E) or A-RAF depletion by siRNA (Fig.4-19F) diminished the activation of ARF6 by mitogenic signalling.
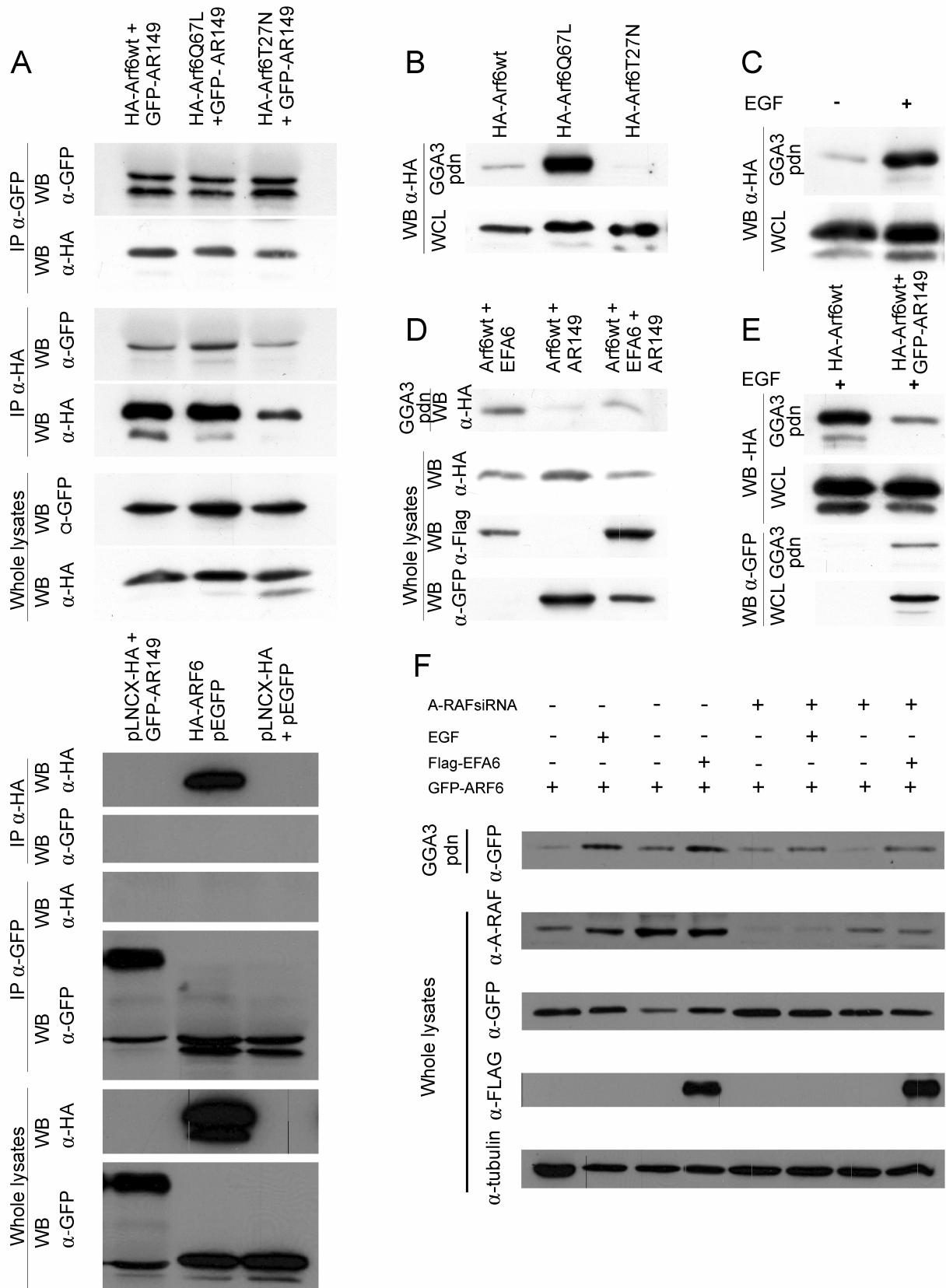
Figure 4-19. *Expression of AR149 or siRNA mediated depletion of A-RAF interferes with activation of ARF6.* **

A. *Interaction of AR149 and ARF6.*

COS7 cells were co-transfected with GFP-AR149 and either HA-tagged ARF6wt, GTP-locked [ARF6(Q67L)] or GDP-locked [ARF6(T27N)]. After immunoprecipitation with α-GFP antibodies, co-

precipitated ARF proteins were detected with α-HA antibodies. In the second experiment, precipitation and detection antibodies were exchanged.

Expression levels in whole cell lysates (WCL) is shown in two bottom panels. Empty vectors were used for control (bottom panel).

B. *GGA3 interacts with ARF6•GTP.* COS7 cells were transfected with wild type, GTP-locked (Q67L) or GDP-locked (T27N) HA-ARF6. Proteins pulled-down by incubation with GST-GGA3-Sepharose were detected with α-HA antibodies.

C.,E. *AR149 suppresses EGF-stimulated ARF6 activation.*

COS7 cells, transfected with either ARF6 alone or ARF6 + GFP-AR149, were treated with EGF for 10 min and subjected to GGA3 pull-down. Bound protein was analysed by immunoblotting. Note decrease in the amount of ARF•GTP by AR149 coexpression. AR149 remains in the pulled-down ARF6 complex confirming the immunoprecipitation data.

D. AR149 inhibits ARF6 activation by EFA6. COS7 cells were transfected with HA-ARF6 and either AR149, EFA6, or both. ARF6•GTP was pulled-down by GST-GGA3. AR149 decreases EFA6-stimulated ARF6 activation.

F. *ARF6 activation by EGF or EFA6 requires A-RAF.*

ARF6 activation was assessed by GGA3 pull-down. The amount of A-RAF and ARF6 protein were determed by Western blotting (WB). Treatment conditions are as indicated.

The fact, that precipitated ARF6·GTP was complexed with AR149 (Fig.4-19E) excluded competitive binding of AR149 and GGA3 to ARF6.

To gain further insight into the mechanism by which AR149 can inhibit ARF6 activity, the EFA6 protein, as ARF6 exchange factor and activator (Martinu et al., 2004), was included in the analysis. As documented in Fig.4-19D, coexpression of AR149, EFA6 and ARF6 attenuated the activating effect of EFA6 on ARF6. Similary, A-RAF depletion caused reduced activation of ARF6 by EGF stimulation, which can partially rescue by EFA6 coexpression (Fig.4-19F).

Together this data revealed a mechanism by which A-RAF as activator and AR149 as inhibitor of mitogenic signalling on endosomes can regulate ARF6 activity. Further this shows that the actual target of mitogenic cascade is ARF6 exchange factor EFA6.

5. Discussion

5.1 Saccharomyces cerevisiae as a simplified model for studies of RAF signalling

Budding yeast *S. cerevisiae* is an established eukaryotic model organism, which played a central role in the elucidation of basic cellular processes such as cell division (Nurse, 1985), intracellular trafficking (Novick et al., 1980) and signal transduction (Madhani and Fink, 1998). Despite the lack of RAF proteins, yeast has played an important role in RAF research, predominantly as a tool for the identification of interacting proteins by two-hybrid screening (Freed et al., 1994) (Hagemann and Rapp, 1999) (Yuryev and Wennogle, 2003, but also as genetic screens, where the absence of endogenous RAF kinases in yeast was successfully overcome, by a series of elegant genetic manipulations. Yeasts with deleted STE11 (MAPKKK) gene and bearing an activating STE7 (MAPKK) mutation were shown to depend on exogenous RAF kinase activity. Using this system, Irie et al. identified the yeast RAS protein and 14-3-3 homologues (Bmh1p, Bmh2p) as activators of mammalian RAF kinase {Irie, 1994 #16). Of note, budding yeast *S. cerevisiae* contains only two 14-3-3 homologues, BMH1 and BMH2, as compared with mammalian and plant cells that express 7-14 isoforms. Thus, *S. cerevisiae* provides a simple model system for functional studies of 14-3-3 interactions with other signalling molecules. 14-3-3 as adaptor proteins associate with phosphorylated RAF kinases through two highly conserved motifs, RSX**pS**XP, stabilize RAF conformation and participate in RAF activation. It was shown, that 14-3-3 isoforms form different homo- and hetero-dimers. These 14-3-3 dimer formation may have important role in RAF regulation. However, informations about 14-3-3 dimer specificity are very poor. Due to using of S. cerevisiae strain, containing only one 14-3-3 isoform, we were able to show in vivo, that BMH1 homodimer was sufficient to activate B-RAF. Mutational analysis of phosphorylated serines reveal that both 14-3-3 binding sites of B-RAF were required for association with 14-3-3 homodimers. These data contribute to a new model of RAF regulation by adaptor proteins (Fischer et al., 2009).

5.2 Unique properties of A-RAF kinase

In this work we disclosed an unexpected link between A-RAF and ARF6-dependent endocytosis. A-RAF has a set of differences, which distinguish it from C-and B-RAF. First, *A-raf* **gene** location and regulation is unique. *A-raf* gene is the only RAF gene located in X-chromosome and its promoter region contains glucocorticoid-response elements (Lee et al., 1996), which contribute to steroid-hormone regulation of A-RAF mRNA expression (Winer and Wolgemuth, 1995).

Next, A-RAF protein possess a number of features making it different from other RAF proteins. First, A-RAF has the lowest amplitude of kinase activity, due to amino acid substitution in the N-

region, located immediately upstream of kinase domain (Baljuls et al., 2007). Moreover, the profile of activation process is distinct from that of C- and B-RAF. Earlier work showed that 5 min after hormone stimulation, A-RAF has a short kinase activity pick, similar to C-RAF, but with lower amplitude. Then A-RAF activity reaches a plateau of prolonged kinase activity, similar to B-RAF, but much longer (Wixler et al., 1996). These data are clarified by recently published work focusing on A-RAF regulation by phosphorylation. It was shown, that feedback phosphorylation by RAF downstream effector, ERK, has a positive effect on A-RAF activity (Baljuls et al., 2008), whereas on C-RAF it has an inhibitory effect (Dougherty et al., 2005) (Hekman et al., 2005). This fact could explain the prolonged kinase activity of A-RAF after groth factor stimulation.

Pelkman et al. (2005) studied the role of human kinome with respect to different types of endocytosis. They found that knock down of A-RAF, but not B- or C-RAF, delayed the endocytosisof SV virus. In contrast, B- and C-RAF knock down accelerated it. These data are in agreement with the model of A-RAF acting in the regulation of endocytosis as presented in this work (see Chapter 5.8).

5.3 The role of lipid binding domains responsible for A-RAF/AR149 specific localization

The first evidence for A-RAF specific lipid binding domains was achieved from intrinsic localisation of A-RAF in S. cerevisiae. After ruling out the co-localization with cortical actin patches, A-Raf localization in yeast clearly resembled that of some proteins, participating in regulation of actin polymerisation and endocytosis, such as Abp1p, Pan1p, Sla1p and Sla2p(Gourlay et al., 2003; Sun et al., 2007).

Remarkably, all these proteins bind to $PtdIns(4,5)P_2$ -rich membranes, which could be labelled by expression of fluorescent sensor. Pleckstrin homology (PH) domain of PLCδ fused to GFP (GFP-PLCδPH) was described to visualize $PtdIns(4,5)P_2$ -rich membrane(Falasca et al., 1998). However, when expressed in S. cerevisiae, GFP-PLCδPH showed homogenous plasma membrane distribution instead of a patchlike one (Stefan et al., 2002). Another work identified a new sensor, which effectively labelled $PtdIns(4,5)P_2$ – rich membrane domains in yeast – so called AP180 N-terminally homology (ANTH) domain (Itoh et al., 2001).

Based on these data, we conclude that both A-RAF and AR149 bind to $PtdIns(4,5)P_2$ -rich membrane domains. The differences in localisation between A-RAF and AR149 could have two reasons. First, A-RAF possesses a second lipid binding domain on the C-terminus, which contributes to A-RAF membrane distribution. Second, GFP-AR149 binds the $PtdIns(4,5)P_2$ with higher affinity, which similar to GFP-PLCδPH, showed homogenously plasma membrane distribution, when highly expressed in yeast.

Our data are in concordance with biochemical data from Johnson et al. (2005), that showed that only A-RAF binds to immobilized PtdIns(4,5)P$_2$ in vitro. Mutation analysis of A-RAF revealed RAS binding domain as crucial for PtdIns(4,5)P$_2$ binding, which partially supports our data. In our experiments substitution of R52 to L in A-RAF or AR149, which is known to disrupt binding of C-RAF to RAS, disturbed its plasma membrane localisation. In contrast, our deletion analysis showed that CRD domain was sufficient for membrane localization of A-RAF and mutant lacking RBD domain (88-606) still bound the membranes.

Based on these facts we map the PtdIns(4,5)P$_2$ binding site in A-RAF to the CRD domain. The conflicting data with the R52L mutant we interpret as an indirect effect. We suppose that the R52L mutation in RBD could causes conformational changes in the CR1 conserved region. Given the known cooperation of RBD and CRD by binding to RAS (Drugan et al., 1996) it is conceivable, that the mutant RBD can prevent binding of CRD to PtdIns(4,5)P$_2$.

In this work we localized A-RAF/AR149 to ARF6-positive endosomal compartment. Interestingly, ARF6 GTPase, among other functions, regulates also metabolism of PtdIns(4,5)P$_2$. Thus, synergistic activation effect of ARF6 on PIP5K and PLD activity could lead to a large increase of the PtdIns(4,5)P$_2$ level at the cell periphery.

5.4   Possible mechanism of AR149 dominant negative effect in S. cerevisiae

On the stage of RAF investigation in yeast heterologous system we could not really define by which mechanism the dominant negative effect is provided. In general, there were two possibilities of AR149 working: strong association with **proteins** or with **lipids** and affecting their normal function. Apart from possible interference of AR149 with one of 6 yeast MAP pathways, proteins from two other signalling cascades were in the running: mating-pheromone response and filamentation-invasion pathways. The mating-pheromone pathway is more related to mitogenic cascade in mammals, but is not triggered by RAS protein. S. cerevisiae has two RAS isoform: Ras1p and Ras2p, which are involved in filamentation-invasion pathways. Double knock out of RAS genes is viable. Both cascades include the same MAP kinase module (Ste11p-Ste7p-MAP), except for MAP kinase. For the mitogen cascade Fus3p is an effector of transcription factor activation, wich initiates mating reaction. A second MAP kinase Kss1, on the other hand, is characterized by formation of so called pseudohyphae. The pseudohyphae are formed at the edge of colonies. They consist of filaments of extended and connected cells, that invade solid medium. This effect is induced under specific nitrogen starvation conditions by diploid yeast, but haploid strains can be also induced to invade solid medium (reviewed by (Gustin et al., 1998)). So, it is still an open question whether AR149 effect is mediated by affecting RAS function or wether some other unknown proteins become disregulated by AR149 expression.

On the other hand, AR149 can bind directly to the PtdIns(4,5)P$_2$ (s. chapter 5.3) and block the processes, regulated by this lipid messenger, such as actin polymerisation and endocytosis (Sun et al., 2007). Only the experiments in mammalian cells provided clear evidence, that ARF6-GTPase is target of AR149, which links the mitogenic cascade to regulation of PtdIns(4,5)P$_2$ production, actin polymerization and endocytosis.

In yeast the functional homolog of ARF6 is Arf3p, which was recently shown to regulate actin polymerisation (Lambert et al., 2007) and PtdIns(4,5)P$_2$ level at the plasma membrane (Smaczynska-de Rooij et al., 2008) and facilitate membrane trafficking. Thus, we conclude that dominant lethal phenotype of AR149 is most probably mediated by the interference with Arf3p function.

5.5   A-RAF and AR149 localize to endosomes

The striking localisation pattern of A-RAF isoform to punctuated structures in yeast resembled that in mammalian cells. In yeast, A-RAF localisation to cortical patches represents distribution of Sla1p and Sla2p, which binds to both activators of protein dynamics, Abp1, Las17p/WASP and Pan1, and to cargo proteins. Moreover, this complex includes Arf3p (homolog of ARF6) and localizes to PtdIns(4,5)P$_2$ –rich membrane domains (Costa and Ayscough, 2005). The AP180/Pan1p complex localizes to cortical actin patches and participates in early steps of endocytosis. These steps in endocytosis seem to be conserved among eukaryotes. Their homologues in mammals, so called E/ANTH proteins, such as HIP1/Sla2p and CALM/AP180, possess protein-protein and protein-lipid interaction domains, stabilizes clathrin coats and provide links between endocytic membranes and microtubules (Legendre-Guillemin et al., 2004). Localization of endogenous A-RAF on the tip of microtubules resembled that of cytoplasmic linker protein 170 (CLIP-170) (Akhmanova and Hoogenraad, 2005), a plus-end tracking protein, which together with regulation of microtubule dynamics, connects microtubule plus-end and specific sites of cortical actin and, what is most important for us, captures cargos for motor-dependent movement. According to the current view, CLIP-170 first recruits dynactin to the microtubuli plus-end. Dynactin is a large adaptor protein, which on the one hand associates with microtubules, on the other hand links the motor protein dynein to its membrane-based cargos. Through LIS1-dependent uncoupling of dynactin from CLIP-170 the movement of dynein-dynactin-vesicle complex towards the microtubule-organizing-centre (MTOS) begins (Wu et al., 2006). Interestingly, a connection between CLIP-170 and ERK was documented: IQGAP1 protein is found to interact with CLIP-170 (Fukata et al., 2002) and ERK2 (Roy et al., 2004).

Unfortunately, it is technically impossible to label endogenous A-RAF under live conditions to get eventually some time-lapse movies of A-RAF positives vesicles. Nevertheless, the unique particular distribution of membrane-bound A-RAF to the vesicles on the tip along microtubules let us speculate

on involvement of A-RAF-driven mitogen signalling in to cytoskeleton-associated motor-dependent vesicular trafficking.

The localization of AR149 to the tubular vesicular endosomes seems to be caused by tight interaction with PtdIns(4,5)P$_2$ and ARF6.Consistently, this localisation was sensitive to microtubule destabilization by Nocodazole. It is conceivable that AR149 localizes to recycling endosomes *per se*, whereas A-RAF localizes to endosomes in all stages of endosome maturation.

5.6   Involvement of A-RAF and AR149 in vesicular trafficking

The fact, that AR149 overexpression traps the internalized Tfn in ARF6- and RAB11-positive recycling compartment and mimics thereby the effect of dominant-negative mutant of ARF6 (T27N), required the clear definition of all steps of Tfn uptake. In our work we employed as a standard the definitions of (D'Souza-Schorey et al., 1998). According to this view, Tfn, bound to Tfn receptor at the plasma membrane is first internalized by clathrin-dependent mechanism and relocated into early endosomes. Following endosome maturation Tfn is led through tubulo-vesicular recycling endosomes to the pericentriolar TGN-associated recycling endosomes and, finally, is recycled back to the plasma membrane. All these steps are dependent on ARF6 GTPase activity. Dominant active mutant, ARF6_Q67L, prevents the internalisation of Tfn, whereas its dominant negative mutant, ARF6_T27N causes redistribution of internalized Tfn from pericentriolar recycling compartment (D'Souza-Schorey et al., 1995). In our work we demonstrated, that expression of AR149 or siRNA silencing of A-RAF resulted in the trapping of Tfn in to ARF6-positive endosomes similar to ARF6_T27N and prevented recycling of Tfn to the plasma membrane. AR149 and A-RAF were found in the complex with ARF6 (Fig. 4-7B and 4-17A), which indicates a possible mechanism for their effect on Tfn recycling.

The first suggestion for a role of A-RAF in endocytosis was obtained by screening work. A-RAF kinase was proposed as a potential regulator of caveolae-dependent endocytosis (Pelkmans et al., 2005). Further analysis of A-RAF contribution in caveolae-mediated endocytosis showed in siRNA silencing experiments that A-RAF stabilizes the structure of caveolae (Pelkmans and Zerial, 2005). Our data demonstrate for the first time A-RAF localization to the endosomes. Moreover, our finding suggests a requirement of A-RAF kinase activity in a descrete step of vesicular trafficking: transfer of cargo from tubular recycling endosomes to TGN-associated recycling compartment.

Our work postulates a broad role of A-RAF in regulation of endocytosis, including inhibitory effect of A-RAF splicing isoforms, DA-RAF1 and DA-RAF2 (Yokoyama et al., 2007), on vesicular trafficking. In fact, the unique localisation of DA-RAF2/AR149 to the tubular vesicular endosomes suggests local inhibition of mitogenic signalling, attached to endosomes by A-RAF, on the level of recycling compartment. This conclusion differ from a suggestion of general inhibitory effect of DA-RAF on mitogenic signalling (Yokoyama et al., 2007).

Based on intrinsic localisation of endogenous A-RAF (discussed in Chapter 5.5), we conclude that A-RAF functionally associates with endosomes shuttling from plasma membrane by short-distance (actin-dependent) trafficking to the tip of microtubule and then by the long-distance (microtubule-associated) vesicular trafficking to recycling compartment. At this level, the A-RAF kinase activity is essential for the transfer of Tfn-positives endosomes to TGN-associated recycling compartment and subsequent recycling to the plasma membrane.

5.7   A-RAF and AR149 regulate ARF6 activation

Cooperation of ARF6 and ERK was notified in some earlier reports. One work focused on ARF6-ERK epistasis, could not decide about direction of co-regulation of these proteins and proposed that ERK functions upstream and downstream of ARF6 (Robertson et al., 2006). Some other reports asserted that active ARF6 cause increased pERK level during epithelial tubule development (Tushir and D'Souza-Schorey, 2007) or glioma cell invasion (Li et al., 2006) and concluded that ARF6 functions upstream of ERK. Till now, the exact mechanism and epistasis of ARF6 and ERK is an unsolved question. Based on our results, we clearly define the epistatic direction of A-RAF-ARF6 cooperation and suggest the following sequence of event: A-RAF-driven ERK activation results in activation of ARF6. The reason for earlier obscurities seems to be involvement of ARF6 GTPase in mitogen receptor internalisation and its subsequent, indirect influence on receptor signalling. It is known that constitutively active (GTP-bound) ARF6 localizes to the plasma membrane and prevents the internalisation of activated receptors(D'Souza-Schorey et al., 1995), which can result in sustained signalling from mitogen receptor to ERK. However, the sole fact that increased level of active ERK could be detected in cells expressing constitutively active ARF6 does not established ERK as a downstream effector of ARF6. Our biochemical experiments reveal not only epistatic direction, but also the fine details of ARF6 regulation by ERK. ERK, regulating ARF6 activity, should be phosphorylated locally on recycling endosomes by A-RAF. Additionally, we identified a possible target of ERK activity, the GEF of ARF6, EFA6 (Fig.4-17D, F). The analysis of EFA6 sequence by NetPhos software reveals a number of potential ERK phosphorylation sites that suggest EFA6 could be a substrate for ERK. Moreover, we found a potential ERK binding site in EFA6A, amino acid sequence FXFP, which occurs in KSR and A-RAF too, but not in C-and B-RAF (Jacobs et al., 1999).

In general, crosstalk between signal transduction and endocytosis seems to be of physiological necessity (Polo and Di Fiore, 2006; Sorkin and Von Zastrow, 2002). There is some evidence that the MAP kinase signalling is on the one hand involved in endocytosis regulation and on the other hand is dependent on that. For example, it was shown, that activated RAS can facilitate mitogen

receptor internalisation by activation of RIN, a GEF factor for RAB5 (Huang et al., 2001). Another potential player in cross talk is ERK, which, curiously, was originally named microtubule-associated protein-2 kinase which phosphorylates microtubule-bound protein-2 in vitro (Ray and Sturgill, 1987). Nevertheless, no confirmation of ERK association with microtubule in proliferating cells has been published. Therefore this name was rejected by the scientific community as misleading. Only later, the ERK association with microtubule in vivo was documented (Reszka et al., 1995) and then, showed to control orientation of actin fibers and microtubule to the plasma membrane (Reszka et al., 1997). Indeed, at least part of mitogenic signalling is shown to take place on the endosomes. For example, MEK partner, MP1, which is associated with p14, a protein tightly associated with late endosomes/lysosomes, was shown to target MEK to late endosomes and to be crucial for ERK activation in response to EGF (Teis et al., 2006; Teis et al., 2002). In the nervous system ERK was shown to be essential for synaptic plasticity by regulation of endocytosis/exocytosis of NMDA and AMPA receptors (reviewed in (Samuels et al., 2009)). Interestingly, ARF6 was also found to regulate synaptic plasticity, where EFA6 is its main GEF-factor (rewieved in (Jaworski, 2007)). In summary, our data begin to bring these separated pieces of evidence together like fragments of a puzzle and propose a new link between mitogenic cascade and ARF6-dependent endocytosis.

5.8 Model of A-RAF function in vesicular trafficking

Discovery of A-RAF localisation on the endosomes, its specific interaction with ARF6 and regulation of ARF6 activity through EFA6, led us to propose a new model of A-RAF function shown in Fig. 5-1. Activation of growth factor receptor leads to conformational changes and subsequently to activation of RAS. In this activated state, RAS·GTP recruits RAF proteins at the plasma membrane, which triggers a number of phosphorylation events, activating RAF proteins and causing the formation of MAPK signalling module on the plasma membrane. All three RAF isoforms are activated successively and shift the mitogenic signalling to different intracellular compartments. A-RAF has prolonged kinase activity (Wixler et al., 1996) due to positive feedback phosphorylation by ERK (Baljuls et al., 2008), whereas C-RAF is readily inhibited by negative ERK feedback phosphorylation (Dougherty et al., 2005) (Hekman et al., 2005).

Because of its intrinsic interaction with membrane lipids (see chapter 5.3), A-RAF localizes to PtdIns(4,5)P$_2$-rich membrane domains on the plasma membrane and on the endosomes. Here A-RAF is in immediate proximity to ARF6 GTPase and, probably, to its GEF-factor - EFA6. A-RAF-driven mitogenic cascade on the endosomes is activated with delay to initial receptor stimulation, because it prior production of ERK and endocytosis of the activated receptors. The endosomally

located cascade activates ARF6. This activation is mediated by EFA6, which is activated by phosphorylation with ERK. The A-RAF inhibitory splicing isoform, DA-RAF/AR149, localizes to tubular recycling endosomes, where it blocks the ERK phosphorylation and, subsequent by the ERK effect on ARF6 activation.

Our findings on A-RAF regulation of endosome recycling pave the way for explaining the phenotype of A-RAF knock-out mice, which display a number of neurological defects: ataxia, muscle rigidity and megacolon (reminder on Hirschsprung's disease with aganglionic ethiology). This phenotype still awaits elucidation of molecular/cellular mechanisms underlying it. Excitingly, A-RAF, ARF6 and EFA6 are strongly expressed in the Purkinje cells of mouse cerebellum (Luckett et al., 2000) (Matsuya et al., 2005). Moreover, tissue distribution of A-RAF splicing isoforms DA-RAF1,2 shows a profile different from that of wild type A-RAF with strong expression in the mouse brain (Yokoyama et al., 2007). The meaning of these facts will be first clarified after physiological and/or ultrastructural analysis of synapses in knock-out mice. All in all, discovery of A-RAF function in vesicle recycling is compatible with a role of A-RAF in synaptic plasticity.
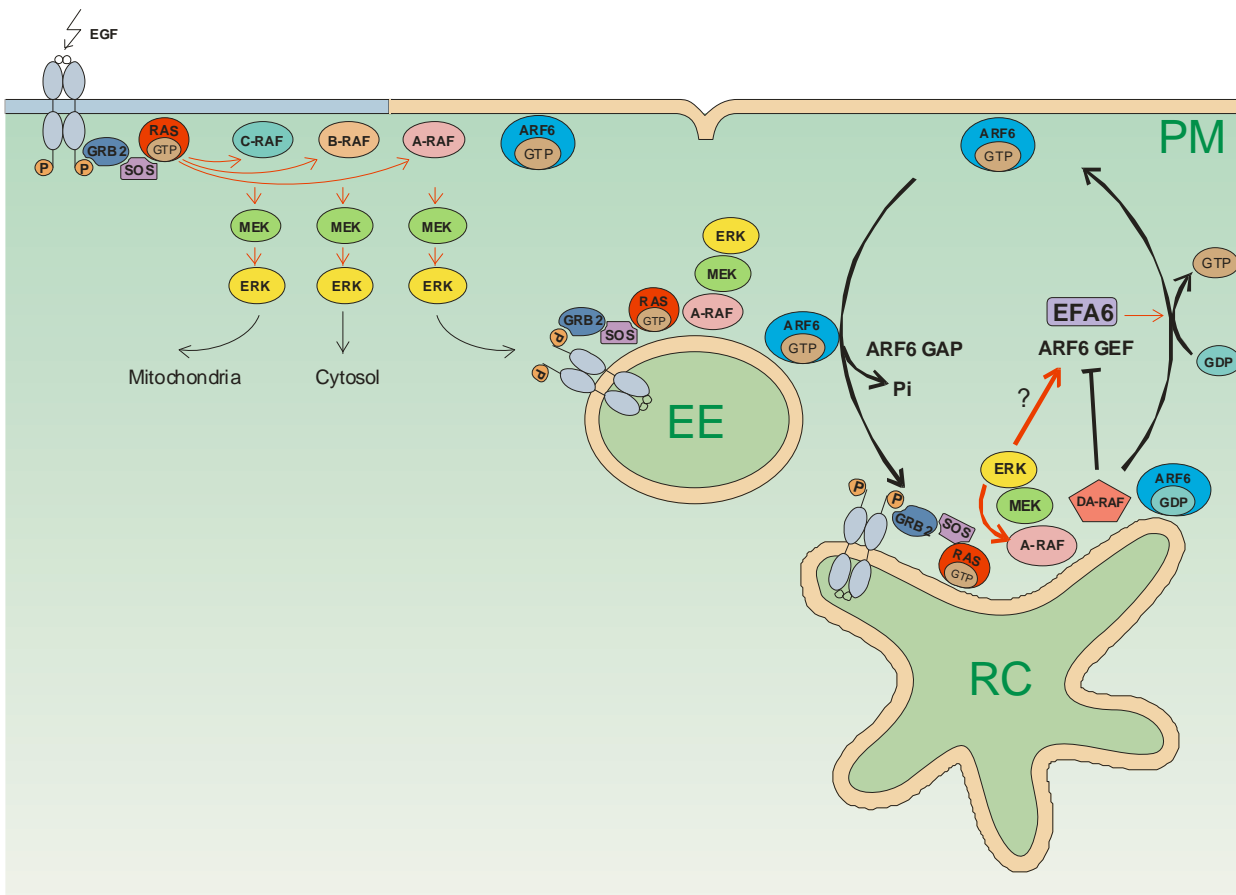
Figure 5-1. *Model of A-RAF and AR149/DA-RAF function in regulation of endocytosis.* **

Activation of growth factor receptor (here EGF receptor) leads to RAS-mediated activation of RAF kinases. RAF isoforms sort into different membrane microdomains, such as A-RAF into PtdIns(4,5)P$_2$ rich domains. Activated Erk has opposing effects on A-RAF and C-RAF. Whereas A-RAF is activated, C-RAF becomes inactivated by feedback phosphorylation. A-RAF bound to PtdIns(4,5)P$_2$ rich membranes continues to signal on endosomes leading to ARF6 activation. AR149/DA-RAF locates to recycling endosomes and blocks Erk activation in this compartment. See the main text for details

EE - early endosome, RC – recycling compartment, PM – plasma membrane. Red arrows indicate positive regulation of the process. Pale brown color indicates PtdIns(4,5)P$_2$ rich membrane microdomains.

References

Aitken, A. (2002). Functional specificity in 14-3-3 isoform interactions through dimer formation and phosphorylation. Chromosome location of mammalian isoforms and variants. Plant Mol Biol *50*, 993-1010.

Akhmanova, A., and Hoogenraad, C.C. (2005). Microtubule plus-end-tracking proteins: mechanisms and functions. Curr Opin Cell Biol *17*, 47-54.

Amiel, J., Sproat-Emison, E., Garcia-Barcelo, M., Lantieri, F., Burzynski, G., Borrego, S., Pelet, A., Arnold, S., Miao, X., Griseri, P.*, et al.* (2008). Hirschsprung disease, associated syndromes and genetics: a review. J Med Genet *45*, 1-14.

Ashery, U., Koch, H., Scheuss, V., Brose, N., and Rettig, J. (1999). A presynaptic role for the ADP ribosylation factor (ARF)-specific GDP/GTP exchange factor msec7-1. Proc Natl Acad Sci U S A *96*, 1094-1099.

Balan, V., Leicht, D.T., Zhu, J., Balan, K., Kaplun, A., Singh-Gupta, V., Qin, J., Ruan, H., Comb, M.J., and Tzivion, G. (2006). Identification of novel in vivo Raf-1 phosphorylation sites mediating positive feedback Raf-1 regulation by extracellular signal-regulated kinase. Mol Biol Cell *17*, 1141-1153.

Baljuls, A., Mueller, T., Drexler, H.C., Hekman, M., and Rapp, U.R. (2007). Unique N-region determines low basal activity and limited inducibility of A-RAF kinase: the role of N-region in the evolutionary divergence of RAF kinase function in vertebrates. J Biol Chem *282*, 26575-26590.

Baljuls, A., Schmitz, W., Mueller, T., Zahedi, R.P., Sickmann, A., Hekman, M., and Rapp, U.R. (2008). Positive regulation of A-RAF by phosphorylation of isoform-specific hinge segment and identification of novel phosphorylation sites. J Biol Chem.

Barnier, J.V., Papin, C., Eychene, A., Lecoq, O., and Calothy, G. (1995). The mouse B-raf gene encodes multiple protein isoforms with tissue-specific expression. J Biol Chem *270*, 23381-23389.

Blagosklonny, M.V. (2002). Hsp-90-associated oncoproteins: multiple targets of geldanamycin and its analogs. Leukemia *16*, 455-462.

Broek, D., Samiy, N., Fasano, O., Fujiyama, A., Tamanoi, F., Northup, J., and Wigler, M. (1985). Differential activation of yeast adenylate cyclase by wild-type and mutant RAS proteins. Cell *41*, 763-769.

Brose, M.S., Volpe, P., Feldman, M., Kumar, M., Rishi, I., Gerrero, R., Einhorn, E., Herlyn, M., Minna, J., Nicholson, A.*, et al.* (2002). BRAF and RAS mutations in human lung cancer and melanoma. Cancer Res *62*, 6997-7000.

Brown, D.A., and London, E. (1998). Functions of lipid rafts in biological membranes. Annu Rev Cell Dev Biol *14*, 111-136.

Brown, F.D., Rozelle, A.L., Yin, H.L., Balla, T., and Donaldson, J.G. (2001). Phosphatidylinositol 4,5-bisphosphate and Arf6-regulated membrane traffic. J Cell Biol *154*, 1007-1017.

Brown, H.A., Gutowski, S., Moomaw, C.R., Slaughter, C., and Sternweis, P.C. (1993). ADP-ribosylation factor, a small GTP-dependent regulatory protein, stimulates phospholipase D activity. Cell *75*, 1137-1144.

Bruder, J.T., Heidecker, G., and Rapp, U.R. (1992). Serum-, TPA-, and Ras-induced expression from Ap-1/Ets-driven promoters requires Raf-1 kinase. Genes Dev *6*, 545-556.

Bruder, J.T., Heidecker, G., Tan, T.H., Weske, J.C., Derse, D., and Rapp, U.R. (1993). Oncogene activation of HIV-LTR-driven expression via the NF-kappa B binding sites. Nucleic Acids Res *21*, 5229-5234.

Burke, P., Schooler, K., and Wiley, H.S. (2001). Regulation of epidermal growth factor receptor signaling by endocytosis and intracellular trafficking. Mol Biol Cell *12*, 1897-1910.

Camarero, G., Tyrsin, O.Y., Xiang, C., Pfeiffer, V., Pleiser, S., Wiese, S., Gotz, R., and Rapp, U.R. (2006). Cortical migration defects in mice expressing A-RAF from the B-RAF locus. Mol Cell Biol *26*, 7103-7115.

Chiu, V.K., Bivona, T., Hach, A., Sajous, J.B., Silletti, J., Wiener, H., Johnson, R.L., 2nd, Cox, A.D., and Philips, M.R. (2002). Ras signalling on the endoplasmic reticulum and the Golgi. Nat Cell Biol *4*, 343-350.

Claing, A., Chen, W., Miller, W.E., Vitale, N., Moss, J., Premont, R.T., and Lefkowitz, R.J. (2001). beta-Arrestin-mediated ADP-ribosylation factor 6 activation and beta 2-adrenergic receptor endocytosis. J Biol Chem *276*, 42509-42513.

Cockcroft, S., Thomas, G.M., Fensome, A., Geny, B., Cunningham, E., Gout, I., Hiles, I., Totty, N.F., Truong, O., and Hsuan, J.J. (1994). Phospholipase D: a downstream effector of ARF in granulocytes. Science *263*, 523-526.

Cohen, Y., Xing, M., Mambo, E., Guo, Z., Wu, G., Trink, B., Beller, U., Westra, W.H., Ladenson, P.W., and Sidransky, D. (2003). BRAF mutation in papillary thyroid carcinoma. J Natl Cancer Inst *95*, 625-627.

Conner, S.D., and Schmid, S.L. (2003). Regulated portals of entry into the cell. Nature *422*, 37-44.

Costa, R., and Ayscough, K.R. (2005). Interactions between Sla1p, Lsb5p and Arf3p in yeast endocytosis. Biochem Soc Trans *33*, 1273-1275.

D'Souza-Schorey, C., Boshans, R.L., McDonough, M., Stahl, P.D., and Van Aelst, L. (1997). A role for POR1, a Rac1-interacting protein, in ARF6-mediated cytoskeletal rearrangements. EMBO J *16*, 5445-5454.

D'Souza-Schorey, C., and Chavrier, P. (2006). ARF proteins: roles in membrane traffic and beyond. Nat Rev Mol Cell Biol *7*, 347-358.

D'Souza-Schorey, C., Li, G., Colombo, M.I., and Stahl, P.D. (1995). A regulatory role for ARF6 in receptor-mediated endocytosis. Science *267*, 1175-1178.

D'Souza-Schorey, C., van Donselaar, E., Hsu, V.W., Yang, C., Stahl, P.D., and Peters, P.J. (1998). ARF6 targets recycling vesicles to the plasma membrane: insights from an ultrastructural investigation. J Cell Biol *140*, 603-616.

Daum, G., Eisenmann-Tappe, I., Fries, H.W., Troppmair, J., and Rapp, U.R. (1994). The ins and outs of Raf kinases. Trends Biochem Sci *19*, 474-480.

Davies, H., Bignell, G.R., Cox, C., Stephens, P., Edkins, S., Clegg, S., Teague, J., Woffendin, H., Garnett, M.J., Bottomley, W.*, et al.* (2002). Mutations of the BRAF gene in human cancer. Nature *417*, 949-954.

Dell, K.R. (2003). Dynactin polices two-way organelle traffic. J Cell Biol *160*, 291-293.

Diaz, B., Barnard, D., Filson, A., MacDonald, S., King, A., and Marshall, M. (1997). Phosphorylation of Raf-1 serine 338-serine 339 is an essential regulatory event for Ras-dependent activation and biological signaling. Mol Cell Biol *17*, 4509-4516.

Dogan, T., Harms, G.S., Hekman, M., Karreman, C., Oberoi, T.K., Alnemri, E.S., Rapp, U.R., and Rajalingam, K. (2008). X-linked and cellular IAPs modulate the stability of C-RAF kinase and cell motility. Nat Cell Biol *10*, 1447-1455.

Donaldson, J.G. (2003). Multiple roles for Arf6: sorting, structuring, and signaling at the plasma membrane. J Biol Chem *278*, 41573-41576.

Dougherty, M.K., and Morrison, D.K. (2004). Unlocking the code of 14-3-3. J Cell Sci *117*, 1875-1884.

Dougherty, M.K., Muller, J., Ritt, D.A., Zhou, M., Zhou, X.Z., Copeland, T.D., Conrads, T.P., Veenstra, T.D., Lu, K.P., and Morrison, D.K. (2005). Regulation of Raf-1 by direct feedback phosphorylation. Mol Cell *17*, 215-224.

Drugan, J.K., Khosravi-Far, R., White, M.A., Der, C.J., Sung, Y.J., Hwang, Y.W., and Campbell, S.L. (1996). Ras interaction with two distinct binding domains in Raf-1 may be required for Ras transformation. J Biol Chem *271*, 233-237.

Dumaz, N., and Marais, R. (2003). Protein kinase A blocks Raf-1 activity by stimulating 14-3-3 binding and blocking Raf-1 interaction with Ras. J Biol Chem *278*, 29819-29823.

Falasca, M., Logan, S.K., Lehto, V.P., Baccante, G., Lemmon, M.A., and Schlessinger, J. (1998). Activation of phospholipase C gamma by PI 3-kinase-induced PH domain-mediated membrane targeting. EMBO J *17*, 414-422.

Fischer, A., Baljuls, A., Reinders, J., Nekhoroshkova, E., Sibilski, C., Metz, R., Albert, S., Rajalingam, K., Hekman, M., and Rapp, U.R. (2009). Regulation of RAF activity by 14-3-3 proteins: RAF kinases associate functionally with both homo- and heterodimeric forms of 14-3-3 proteins. J Biol Chem *284*, 3183-3194.

Fischer, A., Hekman, M., Kuhlmann, J., Rubio, I., Wiese, S., and Rapp, U.R. (2007). B- and C-RAF display essential differences in their binding to Ras: the isotype-specific N terminus of B-RAF facilitates Ras binding. J Biol Chem *282*, 26503-26516.

Franco, M., Peters, P.J., Boretto, J., van Donselaar, E., Neri, A., D'Souza-Schorey, C., and Chavrier, P. (1999). EFA6, a sec7 domain-containing exchange factor for ARF6, coordinates membrane recycling and actin cytoskeleton organization. EMBO J *18*, 1480-1491.

Freed, E., Symons, M., Macdonald, S.G., McCormick, F., and Ruggieri, R. (1994). Binding of 14-3-3 proteins to the protein kinase Raf and effects on its activation. Science *265*, 1713-1716.

Fujishiro, S.H., Tanimura, S., Mure, S., Kashimoto, Y., Watanabe, K., and Kohno, M. (2008). ERK1/2 phosphorylate GEF-H1 to enhance its guanine nucleotide exchange activity toward RhoA. Biochem Biophys Res Commun *368*, 162-167.

Fukata, M., Watanabe, T., Noritake, J., Nakagawa, M., Yamaga, M., Kuroda, S., Matsuura, Y., Iwamatsu, A., Perez, F., and Kaibuchi, K. (2002). Rac1 and Cdc42 capture microtubules through IQGAP1 and CLIP-170. Cell *109*, 873-885.

Galmiche, A., Fueller, J., Santel, A., Krohne, G., Wittig, I., Doye, A., Rolando, M., Flatau, G., Lemichez, E., and Rapp, U.R. (2008). Isoform-specific Interaction of C-RAF with Mitochondria. J Biol Chem *283*, 14857-14866.

Ghosh, S., Moore, S., Bell, R.M., and Dush, M. (2003). Functional analysis of a phosphatidic acid binding domain in human Raf-1 kinase: mutations in the phosphatidate binding domain lead to tail and trunk abnormalities in developing zebrafish embryos. J Biol Chem *278*, 45690-45696.

Girao, H., Geli, M.I., and Idrissi, F.Z. (2008). Actin in the endocytic pathway: from yeast to mammals. FEBS Lett *582*, 2112-2119.

Gourlay, C.W., Dewar, H., Warren, D.T., Costa, R., Satish, N., and Ayscough, K.R. (2003). An interaction between Sla1p and Sla2p plays a role in regulating actin dynamics and endocytosis in budding yeast. J Cell Sci *116*, 2551-2564.

Gruenberg, J. (2001). The endocytic pathway: a mosaic of domains. Nat Rev Mol Cell Biol *2*, 721-730.

Gustin, M.C., Albertyn, J., Alexander, M., and Davenport, K. (1998). MAP kinase pathways in the yeast Saccharomyces cerevisiae. Microbiol Mol Biol Rev *62*, 1264-1300.

Hagemann, C., and Rapp, U.R. (1999). Isotype-specific functions of Raf kinases. Exp Cell Res *253*, 34-46.

Hancock, J.F. (2003). Ras proteins: different signals from different locations. Nat Rev Mol Cell Biol *4*, 373-384.

Hannun, Y.A., Loomis, C.R., and Bell, R.M. (1986). Protein kinase C activation in mixed micelles. Mechanistic implications of phospholipid, diacylglycerol, and calcium interdependencies. J Biol Chem *261*, 7184-7190.

Hekman, M., Fischer, A., Wennogle, L.P., Wang, Y.K., Campbell, S.L., and Rapp, U.R. (2005). Novel C-Raf phosphorylation sites: serine 296 and 301 participate in Raf regulation. FEBS Lett *579*, 464-468.

Hekman, M., Hamm, H., Villar, A.V., Bader, B., Kuhlmann, J., Nickel, J., and Rapp, U.R. (2002). Associations of B- and C-Raf with cholesterol, phosphatidylserine, and lipid second messengers: preferential binding of Raf to artificial lipid rafts. J Biol Chem *277*, 24090-24102.

Hekman, M., Wiese, S., Metz, R., Albert, S., Troppmair, J., Nickel, J., Sendtner, M., and Rapp, U.R. (2004). Dynamic changes in C-Raf phosphorylation and 14-3-3 protein binding in response to

growth factor stimulation: differential roles of 14-3-3 protein binding sites. J Biol Chem *279*, 14074-14086.

Honda, A., Nogami, M., Yokozeki, T., Yamazaki, M., Nakamura, H., Watanabe, H., Kawamoto, K., Nakayama, K., Morris, A.J., Frohman, M.A.*, et al.* (1999). Phosphatidylinositol 4-phosphate 5-kinase alpha is a downstream effector of the small G protein ARF6 in membrane ruffle formation. Cell *99*, 521-532.

Huang, C.F., Liu, Y.W., Tung, L., Lin, C.H., and Lee, F.J. (2003). Role for Arf3p in development of polarity, but not endocytosis, in Saccharomyces cerevisiae. Mol Biol Cell *14*, 3834-3847.

Huang, C.L. (2007). Complex roles of PIP2 in the regulation of ion channels and transporters. Am J Physiol Renal Physiol *293*, F1761-1765.

Huang, M., Weissman, J.T., Beraud-Dufour, S., Luan, P., Wang, C., Chen, W., Aridor, M., Wilson, I.A., and Balch, W.E. (2001). Crystal structure of Sar1-GDP at 1.7 A resolution and the role of the NH2 terminus in ER export. J Cell Biol *155*, 937-948.

Ikeda, S., Ushio-Fukai, M., Zuo, L., Tojo, T., Dikalov, S., Patrushev, N.A., and Alexander, R.W. (2005). Novel role of ARF6 in vascular endothelial growth factor-induced signaling and angiogenesis. Circ Res *96*, 467-475.

Improta-Brears, T., Ghosh, S., and Bell, R.M. (1999). Mutational analysis of Raf-1 cysteine rich domain: requirement for a cluster of basic aminoacids for interaction with phosphatidylserine. Mol Cell Biochem *198*, 171-178.

Itoh, T., Koshiba, S., Kigawa, T., Kikuchi, A., Yokoyama, S., and Takenawa, T. (2001). Role of the ENTH domain in phosphatidylinositol-4,5-bisphosphate binding and endocytosis. Science *291*, 1047-1051.

Jacobs, D., Glossip, D., Xing, H., Muslin, A.J., and Kornfeld, K. (1999). Multiple docking sites on substrate proteins form a modular system that mediates recognition by ERK MAP kinase. Genes Dev *13*, 163-175.

Jansen, H.W., Lurz, R., Bister, K., Bonner, T.I., Mark, G.E., and Rapp, U.R. (1984). Homologous cell-derived oncogenes in avian carcinoma virus MH2 and murine sarcoma virus 3611. Nature *307*, 281-284.

Jaworski, J. (2007). ARF6 in the nervous system. Eur J Cell Biol *86*, 513-524.

Jiang, X., and Sorkin, A. (2002). Coordinated traffic of Grb2 and Ras during epidermal growth factor receptor endocytosis visualized in living cells. Mol Biol Cell *13*, 1522-1535.

Johnson, L.M., James, K.M., Chamberlain, M.D., and Anderson, D.H. (2005). Identification of key residues in the A-Raf kinase important for phosphoinositide lipid binding specificity. Biochemistry *44*, 3432-3440.

Kahn, R.A., and Gilman, A.G. (1986). The protein cofactor necessary for ADP-ribosylation of Gs by cholera toxin is itself a GTP binding protein. J Biol Chem *261*, 7906-7911.

Kerkhoff, E., Fedorov, L.M., Siefken, R., Walter, A.O., Papadopoulos, T., and Rapp, U.R. (2000). Lung-targeted expression of the c-Raf-1 kinase in transgenic mice exposes a novel oncogenic character of the wild-type protein. Cell Growth Differ *11*, 185-190.

Kinbara, K., Goldfinger, L.E., Hansen, M., Chou, F.L., and Ginsberg, M.H. (2003). Ras GTPases: integrins' friends or foes? Nat Rev Mol Cell Biol *4*, 767-776.

King, A.J., Wireman, R.S., Hamilton, M., and Marshall, M.S. (2001). Phosphorylation site specificity of the Pak-mediated regulation of Raf-1 and cooperativity with Src. FEBS Lett *497*, 6-14.

Kolch, W. (2005). Coordinating ERK/MAPK signalling through scaffolds and inhibitors. Nat Rev Mol Cell Biol *6*, 827-837.

Kolesnick, R., and Xing, H.R. (2004). Inflammatory bowel disease reveals the kinase activity of KSR1. J Clin Invest *114*, 1233-1237.

Krauss, M., Kinuta, M., Wenk, M.R., De Camilli, P., Takei, K., and Haucke, V. (2003). ARF6 stimulates clathrin/AP-2 recruitment to synaptic membranes by activating phosphatidylinositol phosphate kinase type Igamma. J Cell Biol *162*, 113-124.

Kuznetsov, A.V., Smigelskaite, J., Doblander, C., Janakiraman, M., Hermann, M., Wurm, M., Scheidl, S.F., Sucher, R., Deutschmann, A., and Troppmair, J. (2008). Survival signaling by C-RAF: mitochondrial reactive oxygen species and Ca2+ are critical targets. Mol Cell Biol *28*, 2304-2313.

Kyriakis, J.M., App, H., Zhang, X.F., Banerjee, P., Brautigan, D.L., Rapp, U.R., and Avruch, J. (1992). Raf-1 activates MAP kinase-kinase. Nature *358*, 417-421.

Lambert, A.A., Perron, M.P., Lavoie, E., and Pallotta, D. (2007). The Saccharomyces cerevisiae Arf3 protein is involved in actin cable and cortical patch formation. FEMS Yeast Res *7*, 782-795.

Lamberti, A., Longo, O., Marra, M., Tagliaferri, P., Bismuto, E., Fiengo, A., Viscomi, C., Budillon, A., Rapp, U.R., Wang, E.*, et al.* (2007). C-Raf antagonizes apoptosis induced by IFN-alpha in human lung cancer cells by phosphorylation and increase of the intracellular content of elongation factor 1A. Cell Death Differ *14*, 952-962.

Lee, J.E., Beck, T.W., Wojnowski, L., and Rapp, U.R. (1996). Regulation of A-raf expression. Oncogene *12*, 1669-1677.

Legendre-Guillemin, V., Wasiak, S., Hussain, N.K., Angers, A., and McPherson, P.S. (2004). ENTH/ANTH proteins and clathrin-mediated membrane budding. J Cell Sci *117*, 9-18.

Li, M., Ng, S.S., Wang, J., Lai, L., Leung, S.Y., Franco, M., Peng, Y., He, M.L., Kung, H.F., and Lin, M.C. (2006). EFA6A enhances glioma cell invasion through ADP ribosylation factor 6/extracellular signal-regulated kinase signaling. Cancer Res *66*, 1583-1590.

Liu, P., Rudick, M., and Anderson, R.G. (2002). Multiple functions of caveolin-1. J Biol Chem *277*, 41295-41298.

Luckett, J.C., Huser, M.B., Giagtzoglou, N., Brown, J.E., and Pritchard, C.A. (2000). Expression of the A-raf proto-oncogene in the normal adult and embryonic mouse. Cell Growth Differ *11*, 163-171.

Madhani, H.D., and Fink, G.R. (1998). The riddle of MAP kinase signaling specificity. Trends Genet *14*, 151-155.

Marais, R., Light, Y., Paterson, H.F., and Marshall, C.J. (1995). Ras recruits Raf-1 to the plasma membrane for activation by tyrosine phosphorylation. EMBO J *14*, 3136-3145.

Marais, R., Light, Y., Paterson, H.F., Mason, C.S., and Marshall, C.J. (1997). Differential regulation of Raf-1, A-Raf, and B-Raf by oncogenic ras and tyrosine kinases. J Biol Chem *272*, 4378-4383.

Mark, G.E., and Rapp, U.R. (1984). Primary structure of v-raf: relatedness to the src family of oncogenes. Science *224*, 285-289.

Martin, T.F. (2001). PI(4,5)P(2) regulation of surface membrane traffic. Curr Opin Cell Biol *13*, 493-499.

Martinu, L., Masuda-Robens, J.M., Robertson, S.E., Santy, L.C., Casanova, J.E., and Chou, M.M. (2004). The TBC (Tre-2/Bub2/Cdc16) domain protein TRE17 regulates plasma membrane-endosomal trafficking through activation of Arf6. Mol Cell Biol *24*, 9752-9762.

Matsuya, S., Sakagami, H., Tohgo, A., Owada, Y., Shin, H.W., Takeshima, H., Nakayama, K., Kokubun, S., and Kondo, H. (2005). Cellular and subcellular localization of EFA6C, a third member of the EFA6 family, in adult mouse Purkinje cells. J Neurochem *93*, 674-685.

Maxfield, F.R., and McGraw, T.E. (2004). Endocytic recycling. Nat Rev Mol Cell Biol *5*, 121-132.

Mazurek, S., Drexler, H.C., Troppmair, J., Eigenbrodt, E., and Rapp, U.R. (2007). Regulation of pyruvate kinase type M2 by A-Raf: a possible glycolytic stop or go mechanism. Anticancer Res *27*, 3963-3971.

McGrath, J.L. (2005). Dynein motility: four heads are better than two. Curr Biol *15*, R970-972.

Mikula, M., Schreiber, M., Husak, Z., Kucerova, L., Ruth, J., Wieser, R., Zatloukal, K., Beug, H., Wagner, E.F., and Baccarini, M. (2001). Embryonic lethality and fetal liver apoptosis in mice lacking the c-raf-1 gene. EMBO J *20*, 1952-1962.

Mischak, H., Seitz, T., Janosch, P., Eulitz, M., Steen, H., Schellerer, M., Philipp, A., and Kolch, W. (1996). Negative regulation of Raf-1 by phosphorylation of serine 621. Mol Cell Biol *16*, 5409-5418.

Moelling, K., Heimann, B., Beimling, P., Rapp, U.R., and Sander, T. (1984). Serine- and threonine-specific protein kinase activities of purified gag-mil and gag-raf proteins. Nature *312*, 558-561.

Morrison, D.K., Heidecker, G., Rapp, U.R., and Copeland, T.D. (1993). Identification of the major phosphorylation sites of the Raf-1 kinase. J Biol Chem *268*, 17309-17316.

Mosior, M., Golini, E.S., and Epand, R.M. (1996). Chemical specificity and physical properties of the lipid bilayer in the regulation of protein kinase C by anionic phospholipids: evidence for the lack of a specific binding site for phosphatidylserine. Proc Natl Acad Sci U S A *93*, 1907-1912.

Mott, H.R., Carpenter, J.W., Zhong, S., Ghosh, S., Bell, R.M., and Campbell, S.L. (1996). The solution structure of the Raf-1 cysteine-rich domain: a novel ras and phospholipid binding site. Proc Natl Acad Sci U S A *93*, 8312-8317.

Mukherjee, S., Gurevich, V.V., Jones, J.C., Casanova, J.E., Frank, S.R., Maizels, E.T., Bader, M.F., Kahn, R.A., Palczewski, K., Aktories, K.*, et al.* (2000). The ADP ribosylation factor nucleotide exchange factor ARNO promotes beta-arrestin release necessary for luteinizing hormone/choriogonadotropin receptor desensitization. Proc Natl Acad Sci U S A *97*, 5901-5906.

Murray, J.W., and Wolkoff, A.W. (2003). Roles of the cytoskeleton and motor proteins in endocytic sorting. Adv Drug Deliv Rev *55*, 1385-1403.

Nekhoroshkova, E., Albert, S., Becker, M., and Rapp, U.R. (2009). A-RAF kinase functions in ARF6 regulated endocytic membrane traffic. PLoS ONE *4*, e4647.

Nichols, B. (2003). Caveosomes and endocytosis of lipid rafts. J Cell Sci *116*, 4707-4714.

Novick, P., Field, C., and Schekman, R. (1980). Identification of 23 complementation groups required for post-translational events in the yeast secretory pathway. Cell *21*, 205-215.

Nurse, P. (1985). Cell cycle control genes in yeast. Trends in Genetics *1*, 51-55.

Ory, S., Zhou, M., Conrads, T.P., Veenstra, T.D., and Morrison, D.K. (2003). Protein phosphatase 2A positively regulates Ras signaling by dephosphorylating KSR1 and Raf-1 on critical 14-3-3 binding sites. Curr Biol *13*, 1356-1364.

Oude Weernink, P.A., Lopez de Jesus, M., and Schmidt, M. (2007). Phospholipase D signaling: orchestration by PIP2 and small GTPases. Naunyn Schmiedebergs Arch Pharmacol *374*, 399-411.

Palacios, F., Schweitzer, J.K., Boshans, R.L., and D'Souza-Schorey, C. (2002). ARF6-GTP recruits Nm23-H1 to facilitate dynamin-mediated endocytosis during adherens junctions disassembly. Nat Cell Biol *4*, 929-936.

Paleotti, O., Macia, E., Luton, F., Klein, S., Partisani, M., Chardin, P., Kirchhausen, T., and Franco, M. (2005). The small G-protein Arf6GTP recruits the AP-2 adaptor complex to membranes. J Biol Chem *280*, 21661-21666.

Payne, D.M., Rossomando, A.J., Martino, P., Erickson, A.K., Her, J.H., Shabanowitz, J., Hunt, D.F., Weber, M.J., and Sturgill, T.W. (1991). Identification of the regulatory phosphorylation sites in pp42/mitogen-activated protein kinase (MAP kinase). EMBO J *10*, 885-892.

Pelkmans, L., Fava, E., Grabner, H., Hannus, M., Habermann, B., Krausz, E., and Zerial, M. (2005). Genome-wide analysis of human kinases in clathrin- and caveolae/raft-mediated endocytosis. Nature *436*, 78-86.

Pelkmans, L., and Helenius, A. (2002). Endocytosis via caveolae. Traffic *3*, 311-320.

Pelkmans, L., and Zerial, M. (2005). Kinase-regulated quantal assemblies and kiss-and-run recycling of caveolae. Nature *436*, 128-133.

Pike, L.J., and Casey, L. (1996). Localization and turnover of phosphatidylinositol 4,5-bisphosphate in caveolin-enriched membrane domains. J Biol Chem *271*, 26453-26456.

Polo, S., and Di Fiore, P.P. (2006). Endocytosis conducts the cell signaling orchestra. Cell *124*, 897-900.

Powelka, A.M., Sun, J., Li, J., Gao, M., Shaw, L.M., Sonnenberg, A., and Hsu, V.W. (2004). Stimulation-dependent recycling of integrin beta1 regulated by ARF6 and Rab11. Traffic *5*, 20-36.

Prior, I.A., Harding, A., Yan, J., Sluimer, J., Parton, R.G., and Hancock, J.F. (2001). GTP-dependent segregation of H-ras from lipid rafts is required for biological activity. Nat Cell Biol *3*, 368-375.

Pritchard, C.A., Bolin, L., Slattery, R., Murray, R., and McMahon, M. (1996). Post-natal lethality and neurological and gastrointestinal defects in mice with targeted disruption of the A-Raf protein kinase gene. Curr Biol *6*, 614-617.

Radhakrishna, H., and Donaldson, J.G. (1997). ADP-ribosylation factor 6 regulates a novel plasma membrane recycling pathway. J Cell Biol *139*, 49-61.

Rajagopalan, H., Bardelli, A., Lengauer, C., Kinzler, K.W., Vogelstein, B., and Velculescu, V.E. (2002). Tumorigenesis: RAF/RAS oncogenes and mismatch-repair status. Nature *418*, 934.

Rajalingam, K., Wunder, C., Brinkmann, V., Churin, Y., Hekman, M., Sievers, C., Rapp, U.R., and Rudel, T. (2005). Prohibitin is required for Ras-induced Raf-MEK-ERK activation and epithelial cell migration. Nat Cell Biol *7*, 837-843.

Rapp, U.R., Goldsborough, M.D., Mark, G.E., Bonner, T.I., Groffen, J., Reynolds, F.H., Jr., and Stephenson, J.R. (1983). Structure and biological activity of v-raf, a unique oncogene transduced by a retrovirus. Proc Natl Acad Sci U S A *80*, 4218-4222.

Rapp, U.R., Gotz, R., and Albert, S. (2006). BuCy RAFs drive cells into MEK addiction. Cancer Cell *9*, 9-12.

Ray, L.B., and Sturgill, T.W. (1987). Rapid stimulation by insulin of a serine/threonine kinase in 3T3-L1 adipocytes that phosphorylates microtubule-associated protein 2 in vitro. Proc Natl Acad Sci U S A *84*, 1502-1506.

Reszka, A.A., Bulinski, J.C., Krebs, E.G., and Fischer, E.H. (1997). Mitogen-activated protein kinase/extracellular signal-regulated kinase 2 regulates cytoskeletal organization and chemotaxis via catalytic and microtubule-specific interactions. Mol Biol Cell *8*, 1219-1232.

Reszka, A.A., Seger, R., Diltz, C.D., Krebs, E.G., and Fischer, E.H. (1995). Association of mitogen-activated protein kinase with the microtubule cytoskeleton. Proc Natl Acad Sci U S A *92*, 8881-8885.

Rizzo, M.A., Kraft, C.A., Watkins, S.C., Levitan, E.S., and Romero, G. (2001). Agonist-dependent traffic of raft-associated Ras and Raf-1 is required for activation of the mitogen-activated protein kinase cascade. J Biol Chem *276*, 34928-34933.

Rizzo, M.A., Shome, K., Vasudevan, C., Stolz, D.B., Sung, T.C., Frohman, M.A., Watkins, S.C., and Romero, G. (1999). Phospholipase D and its product, phosphatidic acid, mediate agonist-dependent raf-1 translocation to the plasma membrane and the activation of the mitogen-activated protein kinase pathway. J Biol Chem *274*, 1131-1139.

Rizzo, M.A., Shome, K., Watkins, S.C., and Romero, G. (2000). The recruitment of Raf-1 to membranes is mediated by direct interaction with phosphatidic acid and is independent of association with Ras. J Biol Chem *275*, 23911-23918.

Robbins, D.J., Zhen, E., Owaki, H., Vanderbilt, C.A., Ebert, D., Geppert, T.D., and Cobb, M.H. (1993). Regulation and properties of extracellular signal-regulated protein kinases 1 and 2 in vitro. J Biol Chem *268*, 5097-5106.

Robertson, S.E., Setty, S.R., Sitaram, A., Marks, M.S., Lewis, R.E., and Chou, M.M. (2006). Extracellular signal-regulated kinase regulates clathrin-independent endosomal trafficking. Mol Biol Cell *17*, 645-657.

Rocks, O., Peyker, A., Kahms, M., Verveer, P.J., Koerner, C., Lumbierres, M., Kuhlmann, J., Waldmann, H., Wittinghofer, A., and Bastiaens, P.I. (2005). An acylation cycle regulates localization and activity of palmitoylated Ras isoforms. Science *307*, 1746-1752.

Roy, M., Li, Z., and Sacks, D.B. (2004). IQGAP1 binds ERK2 and modulates its activity. J Biol Chem *279*, 17329-17337.

Roy, S., Luetterforst, R., Harding, A., Apolloni, A., Etheridge, M., Stang, E., Rolls, B., Hancock, J.F., and Parton, R.G. (1999). Dominant-negative caveolin inhibits H-Ras function by disrupting cholesterol-rich plasma membrane domains. Nat Cell Biol *1*, 98-105.

Samuels, I.S., Saitta, S.C., and Landreth, G.E. (2009). MAP'ing CNS development and cognition: an ERKsome process. Neuron *61*, 160-167.

Santy, L.C., Ravichandran, K.S., and Casanova, J.E. (2005). The DOCK180/Elmo complex couples ARNO-mediated Arf6 activation to the downstream activation of Rac1. Curr Biol *15*, 1749-1754.

Schaeffer, H.J., Catling, A.D., Eblen, S.T., Collier, L.S., Krauss, A., and Weber, M.J. (1998). MP1: a MEK binding partner that enhances enzymatic activation of the MAP kinase cascade. Science *281*, 1668-1671.

Schroder, S., Schimmoller, F., Singer-Kruger, B., and Riezman, H. (1995). The Golgi-localization of yeast Emp47p depends on its di-lysine motif but is not affected by the ret1-1 mutation in alpha-COP. J Cell Biol *131*, 895-912.

Simons, K., and Toomre, D. (2000). Lipid rafts and signal transduction. Nat Rev Mol Cell Biol *1*, 31-39.

Simons, K., and Vaz, W.L. (2004). Model systems, lipid rafts, and cell membranes. Annu Rev Biophys Biomol Struct *33*, 269-295.

Singer, G., Oldt, R., 3rd, Cohen, Y., Wang, B.G., Sidransky, D., Kurman, R.J., and Shih Ie, M. (2003). Mutations in BRAF and KRAS characterize the development of low-grade ovarian serous carcinoma. J Natl Cancer Inst *95*, 484-486.

Smaczynska-de Rooij, I., Costa, R., and Ayscough, K.R. (2008). Yeast Arf3p modulates plasma membrane PtdIns(4,5)P2 levels to facilitate endocytosis. Traffic *9*, 559-573.

Smart, E.J., Graf, G.A., McNiven, M.A., Sessa, W.C., Engelman, J.A., Scherer, P.E., Okamoto, T., and Lisanti, M.P. (1999). Caveolins, liquid-ordered domains, and signal transduction. Mol Cell Biol *19*, 7289-7304.

Smythe, E., and Ayscough, K.R. (2006). Actin regulation in endocytosis. J Cell Sci *119*, 4589-4598.

Soldati, T., and Schliwa, M. (2006). Powering membrane traffic in endocytosis and recycling. Nat Rev Mol Cell Biol *7*, 897-908.

Sorkin, A., and Von Zastrow, M. (2002). Signal transduction and endocytosis: close encounters of many kinds. Nat Rev Mol Cell Biol *3*, 600-614.

Stefan, C.J., Audhya, A., and Emr, S.D. (2002). The yeast synaptojanin-like proteins control the cellular distribution of phosphatidylinositol (4,5)-bisphosphate. Mol Biol Cell *13*, 542-557.

Stefan, C.J., Padilla, S.M., Audhya, A., and Emr, S.D. (2005). The phosphoinositide phosphatase Sjl2 is recruited to cortical actin patches in the control of vesicle formation and fission during endocytosis. Mol Cell Biol *25*, 2910-2923.

Storm, S.M., Cleveland, J.L., and Rapp, U.R. (1990). Expression of raf family proto-oncogenes in normal mouse tissues. Oncogene *5*, 345-351.

Sun, H., King, A.J., Diaz, H.B., and Marshall, M.S. (2000). Regulation of the protein kinase Raf-1 by oncogenic Ras through phosphatidylinositol 3-kinase, Cdc42/Rac and Pak. Curr Biol *10*, 281-284.

Sun, Y., Carroll, S., Kaksonen, M., Toshima, J.Y., and Drubin, D.G. (2007). PtdIns(4,5)P2 turnover is required for multiple stages during clathrin- and actin-dependent endocytic internalization. J Cell Biol *177*, 355-367.

Sun, Y., Kaksonen, M., Madden, D.T., Schekman, R., and Drubin, D.G. (2005). Interaction of Sla2p's ANTH domain with PtdIns(4,5)P2 is important for actin-dependent endocytic internalization. Mol Biol Cell *16*, 717-730.

Tall, E.G., Spector, I., Pentyala, S.N., Bitter, I., and Rebecchi, M.J. (2000). Dynamics of phosphatidylinositol 4,5-bisphosphate in actin-rich structures. Curr Biol *10*, 743-746.

Teis, D., Taub, N., Kurzbauer, R., Hilber, D., de Araujo, M.E., Erlacher, M., Offterdinger, M., Villunger, A., Geley, S., Bohn, G.*, et al.* (2006). p14-MP1-MEK1 signaling regulates endosomal traffic and cellular proliferation during tissue homeostasis. J Cell Biol *175*, 861-868.

Teis, D., Wunderlich, W., and Huber, L.A. (2002). Localization of the MP1-MAPK scaffold complex to endosomes is mediated by p14 and required for signal transduction. Dev Cell *3*, 803-814.

Tian, S., Mewani, R.R., Kumar, D., Li, B., Danner, M.T., Ahmad, I., Rahman, A., Notario, V., Dritschilo, A., Kasid, U.N.*, et al.* (2006). Interaction and stabilization of X-linked inhibitor of apoptosis by Raf-1 protein kinase. Int J Oncol *29*, 861-867.

Tushir, J.S., and D'Souza-Schorey, C. (2007). ARF6-dependent activation of ERK and Rac1 modulates epithelial tubule development. Embo J *26*, 1806-1819.

Tzivion, G., Luo, Z., and Avruch, J. (1998). A dimeric 14-3-3 protein is an essential cofactor for Raf kinase activity. Nature *394*, 88-92.

Vale, R.D. (2003). The molecular motor toolbox for intracellular transport. Cell *112*, 467-480.

van Drogen, F., and Peter, M. (2001). MAP kinase dynamics in yeast. Biol Cell *93*, 63-70.

van Rheenen, J., Achame, E.M., Janssen, H., Calafat, J., and Jalink, K. (2005). PIP2 signaling in lipid domains: a critical re-evaluation. EMBO J *24*, 1664-1673.

Wan, P.T., Garnett, M.J., Roe, S.M., Lee, S., Niculescu-Duvaz, D., Good, V.M., Jones, C.M., Marshall, C.J., Springer, C.J., Barford, D.*, et al.* (2004). Mechanism of activation of the RAF-ERK signaling pathway by oncogenic mutations of B-RAF. Cell *116*, 855-867.

Weber, C.K., Slupsky, J.R., Herrmann, C., Schuler, M., Rapp, U.R., and Block, C. (2000). Mitogenic signaling of Ras is regulated by differential interaction with Raf isozymes. Oncogene *19*, 169-176.

Wiese, S., Digby, M.R., Gunnersen, J.M., Gotz, R., Pei, G., Holtmann, B., Lowenthal, J., and Sendtner, M. (1999). The anti-apoptotic protein ITA is essential for NGF-mediated survival of embryonic chick neurons. Nat Neurosci *2*, 978-983.

Wiese, S., Pei, G., Karch, C., Troppmair, J., Holtmann, B., Rapp, U.R., and Sendtner, M. (2001). Specific function of B-Raf in mediating survival of embryonic motoneurons and sensory neurons. Nat Neurosci *4*, 137-142.

Winer, M.A., and Wolgemuth, D.J. (1995). The segment-specific pattern of A-raf expression in the mouse epididymis is regulated by testicular factors. Endocrinology *136*, 2561-2572.

Wittinghofer, A., and Nassar, N. (1996). How Ras-related proteins talk to their effectors. Trends Biochem Sci *21*, 488-491.

Wixler, V., Smola, U., Schuler, M., and Rapp, U. (1996). Differential regulation of Raf isozymes by growth versus differentiation inducing factors in PC12 pheochromocytoma cells. FEBS Lett *385*, 131-137.

Wojnowski, L., Stancato, L.F., Larner, A.C., Rapp, U.R., and Zimmer, A. (2000). Overlapping and specific functions of Braf and Craf-1 proto-oncogenes during mouse embryogenesis. Mech Dev *91*, 97-104.

Wojnowski, L., Stancato, L.F., Zimmer, A.M., Hahn, H., Beck, T.W., Larner, A.C., Rapp, U.R., and Zimmer, A. (1998). Craf-1 protein kinase is essential for mouse development. Mech Dev *76*, 141-149.

Wojnowski, L., Zimmer, A.M., Beck, T.W., Hahn, H., Bernal, R., Rapp, U.R., and Zimmer, A. (1997). Endothelial apoptosis in Braf-deficient mice. Nat Genet *16*, 293-297.

Wu, J., Dent, P., Jelinek, T., Wolfman, A., Weber, M.J., and Sturgill, T.W. (1993). Inhibition of the EGF-activated MAP kinase signaling pathway by adenosine 3',5'-monophosphate. Science *262*, 1065-1069.

Wu, X., Xiang, X., and Hammer, J.A., 3rd (2006). Motor proteins at the microtubule plus-end. Trends Cell Biol *16*, 135-143.

Xu, L., Frankel, P., Jackson, D., Rotunda, T., Boshans, R.L., D'Souza-Schorey, C., and Foster, D.A. (2003). Elevated phospholipase D activity in H-Ras- but not K-Ras-transformed cells by the synergistic action of RalA and ARF6. Mol Cell Biol *23*, 645-654.

Yin, H.L., and Janmey, P.A. (2003). Phosphoinositide regulation of the actin cytoskeleton. Annu Rev Physiol *65*, 761-789.

Yip-Schneider, M.T., Miao, W., Lin, A., Barnard, D.S., Tzivion, G., and Marshall, M.S. (2000). Regulation of the Raf-1 kinase domain by phosphorylation and 14-3-3 association. Biochem J *351*, 151-159.

Yokoyama, T., Takano, K., Yoshida, A., Katada, F., Sun, P., Takenawa, T., Andoh, T., and Endo, T. (2007). DA-Raf1, a competent intrinsic dominant-negative antagonist of the Ras-ERK pathway, is required for myogenic differentiation. J Cell Biol *177*, 781-793.

Yoon, S., and Seger, R. (2006). The extracellular signal-regulated kinase: multiple substrates regulate diverse cellular functions. Growth Factors *24*, 21-44.

Yuryev, A., and Wennogle, L.P. (2003). Novel raf kinase protein-protein interactions found by an exhaustive yeast two-hybrid analysis. Genomics *81*, 112-125.

Zimmermann, S., and Moelling, K. (1999). Phosphorylation and regulation of Raf by Akt (protein kinase B). Science *286*, 1741-1744.

List of Abbreviations

aa	amino acids
ATP	adenosine 5'-triphosphate
ARF6	ADP-ribosylation factor 6
BSA	bovine serum albumin
C	cytosine, cysteine
CNK	conector enchancer of KSR
CME	clatrin-mediated endocytosis
CR1, 2, 3	conserved region 1, 2, 3
GRE-1,-2,-3	glucocorticoid response elements 1, -2,-3
CRD	cysteine rich domain
D	aspartate
Da	Dalton
DA-RAF1,2	deleted A-Raf
DMEM	dulbecco's modi_ed eagle medium
DMSO	dimethyl sulfoxide
DNA	deoxyribonucleic acid
DTT	dithiothreitol
E	glutamic acid
ECL	enhanced chemoluminiscence
E. coli	Escherichia coli
EDTA	ethylenediamine tetraacetic acid
EEA1	early endosome antigen 1
e.g.	for example; Lat.: *exempli gratia*
EGF	epidermal growth factor
EGFR	epidermal growth factor receptor
eEF-1a	eukaryotic elongation factor 1A
Elk1	Ets LiKe gene1
ERC	endosomal recycling compartment
ERK	extracellular signal-regulated kinase
etc.	and other things or and so on, Lat.: *et cetera*
EtOH	ethanol
FCS	fetal calf serum
GAP	GTPase activating protein, GTPase accelerating protein
GDP	guanosine diphosphate
GEF	guanine nucleotide exchange factor
GFP	green fluorescence protein
GS	glutathione sepharose
GST	glutathione S-transferase
GTP	guanosine triphosphate
HEK293	human embryonic kidney cells
Hepes	4-(2-hydroxyethyl)-1-piperazineethanesulfonic acid
KSR	kinase suppressor of Ras
L	leucine
LBPA	phospholipid lysobisphosphatidic acid
MAPK	mitogen-activated protein kinase
MAPKK	mitogen-activated protein kinase kinase
MAPKKK	mitogen-activated protein kinase kinase kinase
MEK	mitogen-activated protein kinase kinase
mRNA	messenger ribonucleic acid

M2PK	pyruvate kinase isoenzyme type M2
MP1	MEK partner 1
N	asparagine
Ni-NTA	nickel-nitrilotriacetic acid
NP40	nonidet 40
NR	n-region
NSCLC	non-small-cell lung cancer
PA	phosphatidic acid
PAGE	sodium dodecyl sulfate polyacrylamide gel electrophoresis
PBS	phosphate buffered saline
PLC	phospholipase C
PLD	phospholipase D
PM	plasma membrane
PS	phosphatidylserine
PtdIns(4,5)P$_2$	phosphatidylinositol-4,5-bisphosphate
Q	glutamine
R	arginine
RAB	Ras-related in brain
RAF	**ra**pidly growing **f**ibrosarcoma protein
RBD	ras binding domain
RFP	red fluorescence protein
RhoA	Ras homolog gene family, member A
RNA	ribonucleic acid
ROS	reactive oxygen species
RT	room temperature
RTK	receptor tyrosine kinase
SDS	sodium dodecyl sulfate
S	serine
siRNA	small interfering RNA
T	threonine
TBST	tris-bi-ered saline Tween-20
Tfn	Transferrin
TGN	trans-Golgi-network
wt	wild type
X-Gal	5-bromo-4-chloro-3-indoxyl-β-D-galactopyranoside
XIAP	X-linked Inhibitor of Apoptosis Protein
Y	tyrosine
*	published by (Fischer et al., 2009)
**	published by (Nekhoroshkova et al., 2009)

Acknowledgments

CURRICULUM VITAE

Personal data

Name:	Elena K. Nekhoroshkova (birth name Ruf)
Born:	December 9, 1974; Urdshar, Kazakhstan
Citizenship:	Russian
Adress:	Versbacherstrasse 225
	97078 Würzburg
	Germany
Marital status:	married with Sergey Nekhoroshkov, 2000
Children:	Dmitry Nekhoroshkov, born 2000

Education

1982-1992	High school Diploma with Honours degree, Nowokusnezk, Russia
1992-1998	Medical Doctor – Biophysics Diploma with Honours degree, Medical Biological Faculty, Siberian Medical University, Tomsk, Russia
1998-2000	Pre-doctoral experience in the laboratory of Biochemistry of Xenobiotics, head of lab. PhD A. Y. Grishanova, Institute of Molecular Biology and Biophysics (IMB&B), Nowosibirsk, Siberian Division of Russian Medical Academy, Russia.
2003 -2009	PhD fellow ship, Laboratory of Biochemistry, Institute for Medical Radiation and Cell Research, head of lab. Prof. Dr. U.R. Rapp, University of Würzburg, Germany

Professional Development

1998	**Diploma student**, Department for Clinical Immunology and Allergology, Siberian Medical University, Tomsk, Russia **Research area:** Immunological status by patients with a chronic mucosal inflammation.
1998-2000	**PhD student**, Laboratory of Biochemistry of Xenobiotics, head of lab. PhD A. Y. Grishanova. Institute of Molecular Biology and Biophysics (IMB&B), Nowosibirsk, Siberian Division of Russian Medical Academy, Russia **Research area**: Role of cytochromes P450 in formation of multi-drug resistanse.
2003-2009	**PhD student**, group leader PhD Stefan Albert, head of lab. Prof. MD U.R. Rapp, Institute for Medical Radiation and Cell Research, University of Würzburg, Germany **Research area:** Localisation and functional analysis of RAF kinases in heterologous and homologous system.

Publications

1. Kologrivova EN, **Ruf EK**, Bobkova NV, Lebedev MP. (2000) <u>Cellular content of mixed saliva sediment in patiens with chronic mucosa inflammation.</u> *Tsitologia 42 (5): 441-3   (in Russian)*

2. Grishanova AI, Kaledin VI, Zueva TV, **Nekhoroshkova EK**, Nikolin VP, Liachovich   VV (2003) <u>Activity and induction of CYP2B, CYP2C and CYP3A in tissues of cyclophosphane-sensetive   and resistant neoplasms and the liver of neoplasm-carrying mice.</u> *Biomed Khim. Jan-Feb;49(1):27-34 (in Russian)*

3. * Andreas Fischer, Angela Baljuls, Joerg Reinders, **Elena Nekhoroshkova**, Claudia Sibilski, Renate Metz, Stefan Albert, Mirko Hekman and Ulf R. Rapp. (2009) <u>Regulation of RAF Activity by 14-3-3 Proteins - RAF Kinases Associate Functionally   with both Homo- and Heterodimeric Forms of 14-3-3 Proteins.</u> *J Biol Chem. 2009   Jan30;284(5):3183-94.*

4. ** **Elena Nekhoroshkova**, Stefan Albert, Matthias Becker and Ulf R. Rapp. (2009) <u>A-RAF kinase functions in ARF6 regulated endocytic membrane traffic.</u> *PLoS ONE* 4(2): e4647. doi:10.1371/journal.pone.0004647

Poster presentations

1. **Elena K. Nekhoroshkova**, Stefan Albert, Matthias Becker, Ulf R. Rapp.
   <u>A-RAF kinase participates in regulation of endocytosis.</u> (2007) 27th Meeting of Cancer Research UK Society "Genes and Cancer", December 10-12, University of Warwick, UK

2. Andreas Fischer, Mirko Hekman, Jörg Reinders, **Elena Nekhoroshkova**, Stefan Albert, Angela Baljuls, Ulf R. Rapp. <u>Regulation of RAF Activity by 14-3-3 Proteins.</u> (2008) Gordon Research Conference "Biology of 14-3-3 Proteins", February 24-29, Ventura (CA), USA

3. **Elena K. Nekhoroshkova**, Stefan Albert, Matthias Becker and Ulf R. Rapp. <u>A-RAF kinase function in ARF6 regulated endocytosis.</u> (2008) EMBO workshop "Can epigenetics influence reprogramming & metastatic progression?", October 6-9, Bad Staffelstein, Germany

Affidavit

I hereby declare that my thesis entitled "A-RAF kinase functions in ARF6 regulated endocytic membrane traffic"
is the result of my own work. I did not receive any help or support from third parties, i.e. commercial consultants or others. All sources and / or materials applied are listed and specified in the thesis.

Furthermore, I verify that this thesis, neither in identical nor similar form, (please tick as applicable)

has not yet been submitted as part of another examination process   ☒

has already been submitted as part of another examination process   ☐

I confirm that the information which I have given in this application is complete and true.

Würzburg…………………………………………………………………………………
               Date   Signature